January 2015

Climate Driven Hillslope Degradation Of Mono Basin Moraine, Eastern Sierra Nevada, California, USA

Risa Madoff

CLIMATE DRIVEN HILLSLOPE DEGRADATION OF MONO BASIN MORAINE, EASTERN SIERRA NEVADA, CALIFORNIA, USA

by

Risa Madoff
Bachelor of Science, New Mexico State University, 1998
Master of Science, New Mexico State University, 2002

A Dissertation
Submitted to the Graduate Faculty

of the

University of North Dakota

in partial fulfillment of the requirements

for the degree of

Doctor of Philosophy

Grand Forks, North Dakota
May
2015

This dissertation, submitted by Risa Madoff in partial fulfillment of the requirements for the Degree of Doctor of Philosophy from the University of North Dakota, has been read by the Faculty Advisory Committee under whom the work has been done and is hereby approved.

Jaakko Putkonen

Joseph Hartman

Richard LeFever

Ronald Matheney

Matthew Gilmore

This dissertation is being submitted by the appointed advisory committee as having met all of the requirements of the School of Graduate Studies at the University of North Dakota and is hereby approved.

Wayne Swisher
Dean of the School of Graduate Studies

April 10, 2015
Date

PERMISSION

Title	Climate Driven Hillslope Degradation of Mono Basin Moraine, Eastern Sierra Nevada, California, USA
Department	Geology and Geological Engineering
Degree	Doctor of Philosophy

In presenting this dissertation in partial fulfillment of the requirements for a graduate degree from the University of North Dakota, I agree that the library of this University shall make it freely available for inspection. I further agree that permission for extensive copying for scholarly purposes may be granted by the professor who supervised my dissertation work or, in his absence, by the Chairperson of the department or the dean of the School of Graduate Studies. It is understood that any copying or publication or other use of this dissertation or part thereof for financial gain shall not be allowed without my written permission. It is also understood that due recognition shall be given to me and to the University of North Dakota in any scholarly use which may be made of any material in my dissertation.

Risa Madoff
April 7, 2015

TABLE OF CONTENTS

LIST OF FIGURES

LIST OF TABLES

ACKNOWLEDGEMENTS

I certainly could not have achieved what I did in the PhD journey without help through instruction, critical feedback, and financial support. For virtual around-the-clock and, for a couple of weeks, around-the-hemispheres, instruction and feedback thanks go to my PhD supervisor and committee chair, Dr. Jaakko Putkonen. Even when things looked low, his input would keep me motivated to follow through on the challenges.

In addition to GTAs the first few years, I am grateful for the School of Graduate Studies' financial assistance through a Summer Doctoral Fellowship (2010) and Neil C. MacDonald Scholarship (2014-2015), as well as travel grants to help with the travel costs related to presenting at AGU (2014) and GSA (2013). I also thank the School of Geology and Geological Engineering and the College of Engineering and Mines for support through Dr. Alan Cvancara research awards and travel assistance to conferences through the Student Experience Fund. Opportunities for teaching experiences and learning new skills that I would not have been given elsewhere were also greatly appreciated.

I was glad to have had the chance to make revisions to the dissertation text. Certainly far from perfect, or even publishable, a basic structure that expresses the reach of the study was eventually able to emerge. Thanks go to my committee for their critical feedback that helped to draw out that basic structure. I also have developed a deeper appreciation and fascination with the writing and thinking process in science.

The PhD is a rough road in so many ways, but mainly because of the solitude. In other words, the more it is what it's supposed be, the more unlike anything it is anyone can imagine. It certainly is not for the faint of heart or the very sensitive. The kind and friendly help of those who work in various capacities in the School of Geology and Geological Engineering and the College of Engineering and Mines was always much appreciated. For computer help over the years I thank Jeremy Malheim and Christal Mormann and their IT crew. For sage advice in the engineering machine shop, I thank Gary Dubuque and Jay Evanstad. For paper work handling with a smile and resilience for answering the same questions repeatedly, I thank Katie Sagstuen, Jolene Marsh, and Aeryk Weiser. For kind support and library assistance I thank Darin Buri. I thank Jin Zhang for kindness and generosity as an office neighbor and friend.

ABSTRACT

Regolith transport within the uppermost 30-50 cm of Earth's surface is responsive to shifts in climate. Rates of surface change affect accumulation rates of sediment and nutrients, thereby affecting ecology, surface stability, and the ability to date landform surfaces. However, little is known about the quantitative effects past climates have had on the long term evolution of the landscape. A space-for-time substitution method was used to study this knowledge gap. Known degradation rates from widely varying climates were used to generate a transfer function where published paleo-temperature records from the Death Valley sediment core (DV93-1) were applied to derive paleo-degradation rates at Mono Basin moraine, CA. Together with a published glacial chronology for Mono Basin, CA for the approximately last 100 kyrs, the method related past climates to varying rates of landform degradation.

In conventional applications, landscape evolution models use a diffusion equation, based on a transport law, to describe a linear relation between degradation and slope. In the transport equation, $q = \kappa (dz/dx)$, a topographic diffusivity coefficient, κ, expresses all the combined effects other than slope on landform degradation. However, as it has been used, κ does not express the diverse responses of surface processes to shifts in climate. This study used numerical modeling to vary the coefficient of topographic

diffusivity in accordance with documented variations in climate to model the cross-section profile of an 85 kyr old Mono Basin moraine.

Results from hillslope profile modeling with various scenarios - an optimized constant κ, time-varying κ, and a current-time κ – were compared. In comparison with the time-varying value, an optimized constant κ, overestimated the surface elevation by up to 10% during the first 60 kyrs and underestimated it by up to approximately the same amount during a 5 thousand year time span 20 to 15 kyrs ago. Application of the current κ value, assumed to reflect current interglacial climate, underestimated surface elevation by up to 32%. The results provide a first step in relating past climate shifts to variable erosion rates and surface processes through time, particularly with respect to the uppermost 1-2 meters of regolith mantling landforms.

CHAPTER I

INTRODUCTION

1.1 Motivation

Processes that erode and subsequently transport sediment across Earth's surface and degrade the landscape have long been thought to follow regular quantifiable patterns based on topographic structures (Gilbert, 1909; Culling, 1960). Even before attempts to quantify surface changes were made, patterns of landform degradation were recognized to result from the long term breakdown and removal of material associated with the natural aging of landscapes (Davis, 1902). Hence, since the earliest observations, landform structures and their evolution have been central to the field of geomorphology – the science of landforms and the evolution of Earth's surface.

Early analytical work made a first-order assumption that the volume of unconsolidated sediment, called regolith, blanketing landform surfaces, follows a transport rate linearly related to surface gradient. Culling (1960) provided an idealized model based on this assumption and applied it to hillslope-shaped landforms that characterized generalized stream valley and ridge systems. Macroscopic processes recognized by Culling (1965) contributing to regolith transport rates and degradation, such as rain splash, surface wash, and weathering rate, were incorporated into the model as mobility factors independent of surface gradient. Since this early work, the field of geomorphology has come to incorporate a framework where larger scale forces originating both from within the earth – endogenic, which include uplift and volcanism related to tectonism – and external to it – exogenic, which include climate – affect surface processes. In this framework, these larger scale inputs are recognized as providing energy that modifies regular patterns of degradation that are considered to have a slow and ongoing diffusive effect on eroding the landscape (Ritter et al., 2011). However, the effects of these inputs are not easily incorporated into the idealized quantitative models of landform degradation because the sources of energy act at different temporal and spatial scales.

The present study focuses on the exogenic sources occurring at a temporal scale of thousands to tens of thousands of years. It assesses the differences in modeling results generated from employing different assumptions about the rate of landform surface mobility through time. One modeling application assumes an optimized constant (time averaged) to represent the mobility. An alternative application assumes a time varying climatic parameter represent the variability in regolith transport. The third alternative assumes that the present rates of sediment transport on a landform surface are close enough to the rates over the lifespan of a landform and applies a current rate of surface mobility taken from a measurement of sediment flux from the landform being modeled.

The topic holds importance not simply as a modeling problem but as a problem in addressing erosion rates over time. This is a problem that is critical and at the foundation of analyses of past geologic and environmental processes and of their comparisons with processes in recent times. The present work does not address every place in the literature where erosion rates are relevant for a reconstruction of past events over geological time or for predicting the effects of current climate change on soil erosion, for example. Instead, the purpose of the present study is to examine landscape evolution by focusing on the intermediate spatial scale of the landform and occurring over thousands to tens of thousands of years instead of the landscape scale of change measured in kilometers and which occurs over hundreds of thousands to millions of years. It also does not investigate landform processes occurring on an anthropogenic time scale of decades to hundreds of years. The intermediate scale of sediment transport is an area where research has focused less but which is important for understanding the effects of climate shifts on the landscape.

This intermediate scale notably contrasts with the mountain range scale, occurring over the hundreds of thousands to millions of years during which mountain building processes are considered by geologists to occur. The landform scale also contrasts with the time scale in which agricultural plots are studied, where the human time scale of decades to hundreds of years is applied. Because the focus here is on the effects of past global climate fluctuations, which have occurred over thousands to tens of thousands of years, a single landform at a location where proxy records of past climate fluctuations provide evidence is taken as a case study in order to track the effects of past changes on sediment transport through time. The significance is that recognition of degradation processes and rates at the scale being considered may provide insight to physical relationships, such as with global climate, not considered before as having a significantly strong enough influence on the evolution of Earth's surface. This study does not deny the influences of exogenic forces occurring at the other spatial and temporal scales as contributors to landform evolution. The point stressed here is that a knowledge gap was recognized as relevant for a set of geologic events pertaining to global climate and a set of methods were employed to address it.

While published investigations have quantified erosion rates at the other scales mentioned, one set of methods is used here to initiate an advance of the problem of quantifying the effects of past climate fluctuations on regolith erosion rates. The methods focus on landform degradation in order to contribute to the general geomorphic topic of hillslope processes, under which the case study investigated falls. While other scales and purposes are important for understanding the relation of tectonics, for example, to the response of surface processes (Molnar and England, 1990; Molnar, 2009) or land management practices in response to recent and future climate change (Pruski and Nearing, 2002; Nearing et al., 2004), the present focus is on a gap in landscape evolution models. The purpose is to show that a relationship exists, in this case, between a natural hillslope - a glacial moraine ~85 kyrs old in the eastern Sierra Nevada, CA - and global climate changes known to have occurred during that time. Evidence for the climate change in Mono Basin is given by the existence of glacial moraines, as well as other climate records. Mono Basin moraine was used as a case study in order to propose the possibility that similar relationships exist and may be quantifiable for other landforms, other landscapes, and other regions. Further similar research in other regions may fill the gap and actually provide insights relevant to the other temporal and spatial scales and potentially provide a basis for comparing rates of topographic change through time resulting from forces acting at the different scales.

1.2 Background

Initial interest in landscape analysis centered on the observation of a slow reduction of landscape topography identifiable by reduction of landform gradient that was hypothesized to be driven by time, described by age cycles (Davis, 1902). Subsequent attempts quantified the unconsolidated mobile material mantling hillslope-shaped landforms with equations that expressed how rates of sediment transport changed with the natural reduction of gradients (Gilbert, 1909; Culling, 1960; Culling, 1965). However, as discussed in section 1.1, known forces external to the landscape that fluctuate on time scales independently of the regular courses of degradation, such as global climate fluctuations, were considered as a part of the natural inputs and were not independently quantified or assessed in relation to landscape changes.

The present study initiates an attempt to quantitatively incorporate known past climate fluctuations into a conventional diffusion equation long employed in geomorphology to model how landforms degrade. The equation is used to describe how sediment mantling landform surfaces is transported downslope and how the slope changes accordingly. Landforms, here, are understood to serve as elements of the larger landscape. Landscape evolution can be considered in various ways depending on the assumed temporal and spatial scales. The long term uplift, exhumation, and erosion at the mountain-range scale covering kilometers and occurring over spans of millions or hundreds of thousands of years reflect large spatial and long term scale change. However, at a smaller scale, regional landscapes also respond to global climate. This study investigates how such response may be quantified.

A lateral moraine, a hillslope-shaped landform deposited along the lateral edge of advancing alpine glacier, and left behind after the glacier has melted and receded, is an example of a response to cooling or warming temperatures that form or melt glaciers. The Sierra Nevada, California, USA, in particular, have exhibited sensitivity to shifts in the jet stream during glaciations in the Pleistocene (Benson et al., 1998; Gillespie and Zehfuss, 2004) as well as recorded lake level changes. The present study assumes that landform degradation and crest-lowering of sloping landforms can reflect much about regional modifications to the landscape on the time order of thousands to tens of thousands of years, a time scale that reflects the effects on the landscape of past glacial advances and retreats and the climates that drove that glacial activity.

While time scales on the order of hundreds of thousands to millions of years have been assumed be most relevant for landscape evolution models, the determination of whether critical processes occurring on smaller spatial scales and shorter time scales are resolvable and maintained in conventional modeling of landscapes is needed (Martin and Church, 1997). Difficulties in resolving data from geomorphic methods designed for incompatible resolutions must be addressed if processes occurring at different scales are going to be integrated in modeling (Martin and Church, 1997; Schrott et al., 2013). Due to the above mentioned difficulties of integrating different temporal and spatial scales, questions concerning the variability of degradation rates and hillslope processes on shorter time scales have been addressed much less frequently. As a result, the variable effects of climate on landform degradation have been studied in less depth than the effects of tectonics on the landscape, which is associated with mountain building at the scale of lithospheric plates. As an initial first order treatment of these issues, this study addresses questions relating topographic change to climate driven transport on natural landforms. Transport data from natural hillslopes occurring in locations with various averaged temperatures were correlated with past transport rates related with past temperatures from a glacial chronology of glacial advances and retreats in the region.

A hillslope diffusion equation that employs a general sediment transport law has been used to quantify and predict the elevation loss and smoothing that is undergone during landform degradation (Culling, 1960; Carson and Kirkby, 1972; Hallet and Putkonen, 1994; Putkonen and Swansen, 2003; Putkonen and O'Neal, 2006), and which expresses the cumulative effects of all the factors causing it. Such a transport law is encountered in many fundamental equations of physics and chemistry, and it relates two components of a system – amount of material in flux on one side and a concentration gradient on the other side – with a proportionality constant between them that is dependent on conditions in the particular environment being analyzed. The transport law applied to the physical process of hillslope degradation,

$$q_{vol,x} = \kappa(dz/dx) \qquad (1.1)$$

linearly relates a volume of material flux (regolith) $(q_{vol,x}\ [m^2/yr])$ with (dz/dx), its corresponding slope gradient, acting as the driver, and, $\kappa\ (m^2/yr)$, a constant coefficient expressing topographic diffusivity – how downslope sediment transport modifies topography. Topographic diffusivity is assumed to depend on the cumulative results of climate and substrate together at any point in time at a location. As such, changes in the cumulative results may be compared over time in order to assess the parameter at a particular point. The diffusion equation that employs the transport law will be explained in the Methods section.

The equation has been employed to numerically model the downslope mobility of sediment over the lifespan of a hillslope which results in its degradation (Hanks et al., 1984; Hallet and Putkonen, 1994; Putkonen and Swansen, 2003; Putkonen and O'Neal, 2006; Putkonen et al., 2008). The continual process of soil creep has been assumed to explain hillslope diffusion. The combined impacts of wind, rain splash, freeze-thaw cycles, and biotic activity, whose various influences depend on climate, are what the κ value represents (Hallet and Putkonen, 1994). Such influences are considered to act roughly continuously in contrast to other influences referred to as episodic, or "catastrophic," in geology, that include events such as debris flows, landslides, or floods. Such events sometimes result from large episodic weather events, such as storms, and sometimes they result simply from the passing of a stability threshold that could result from any number of causes.

This study assumes that sediment transport in similar climates on different slopes can be compared in order to make a first order assessment of how global climate changes on the scale of thousands to tens of thousands of years has affected sediment transport and thereby degradation rates. Local factors are assumed to have a cumulative effect over the time scale considered and on the single slope modeled through time. Examples of local factors include: slope aspect which, by affecting microclimate, can yield differences in diffusivity (Pierce and Colman, 1986) and above and below ground biological activity, of which the sum of mechanical processes results in a volumetric loss of regolith at the hillslope crest e.g. Gabet et al. (2003). Also assumed is the homogeneity of the substrate throughout the landform. The assumptions made in the present study in no way deny the many ways sediment on landform surfaces are mobilized. However the selected focus of the present study was on how evidence of past climates provided by a glacial chronology and temperature proxy records – can be used to reveal the variable effects of climate on the landscape for thousands to tens of thousands of years.

What has not been investigated in depth previously is the approach of a time varying topographic diffusivity that can be shown related to the past climates. Modeling hillslope processes is a common first step in modeling landscape evolution, from the earliest works (Davis, 1902; Gilbert, 1909; Culling, 1960; Culling, 1965) to the recent (Tucker and Hancock, 2010), although the techniques have changed. Given that κ is dependent on climate, expressed above as the cumulative effects on the substrate of the combined exogenic forces and the abundant evidence for past global climate changes, such an approach contributes a new perspective to consider for modeling hillslopes that represent natural landforms.

The linear diffusion equation has been shown to model hillslope profiles at selected times (t) with use of a mean κ value in a time interval of [0, t] regardless of the temporal variability of κ (Skianis et al., 2008). Results of that study are promising for the objectives of the present one. Because the point here is to show how exogenic inputs driven by times of global climate change are associated with relative changes in hillslope degradation rates, the results from the Skianis et al. (2008) study suggest that the application is sound even if the precise times when κ values change are uncertain.

The focus of the Skianis et al. (2008) work was in determining whether a difference in cross profile form and morphology would result from applying a time averaged κ value and a time-dependent κ value. While the work showed that a significant difference in form and morphology did not result, the physical relevance of the differences at specific times was not addressed. While a numerical difference amounting to a meter, for example, at the million year scale might have been assumed to be insignificant in terms of mass balance, relevant chemical processes occur within the uppermost 1 to 1.5 meters. If diffusivity over a thousand year scale is increased or decreased the result is increased or decreased surface exposure. Chemical processes, such as decay of cosmogenic isotopes is affected by exposure time at the surface. Exposure also affects isotopic fractionation, thermal penetration by solar radiation, and infiltration of precipitation. In other words, the physical processes occurring at different rates through climate shifts contribute to a long term average, but potentially in significantly different proportions at different times. Diffusivities in various climates may differ enough to significantly vary degradation rates at various times. Also regions, even within similar climates, may respond differently to climate shifts. Such variability can be significant for landform evolution and is lost when a time averaged value is used. Even if overall shape and morphology appear to differ little when a constant or time varying κ values are used, the physical results can be relevant and significant for upper-most surface processes responding to shifting climates.

Field observations have provided evidence that as sloping landforms age, their cross-section profiles become smoother as matrix is eroded from upslope, then transported and deposited on lower slope positions (Hallet and Putkonen, 1994; Putkonen and O'Neal, 2006; Putkonen et al., 2008). Modeling the process with a linear diffusion equation, the rate of sediment lost to crest lowering is linearly related with reduction in slope over time. Crest elevations can then be related to landform age (Hanks et al., 1984; Hallet and Putkonen, 1994; Putkonen and O'Neal, 2006; Putkonen et al., 2008; Skianis et al., 2008).

Similar observations have been used to relatively date glacial moraines in the eastern Sierra Nevada. Mono Basin moraine, located approximately 8 km south of the town of Lee Vining and Mono Lake and in a regional mean elevation of 2350 m asl, has been dated by cosmogenic isotopes and recognized as an older moraine, at least 60-80 ka, (Phillips et al., 1990; Phillips et al., 1996; Gillespie and Zehfuss, 2004; Phillips et al., 2001), in comparison to the neighboring younger Tahoe II moraine. Located in the Walker Creek valley, Tahoe II moraine exhibits a sharper crest and is dated within a range of 50-42 ka (Phillips et al., 1996; Phillips et al., 2001; Gillespie and Zehfuss, 2004). Mono Basin moraine was selected for modeling the evolution of its cross-section profile for this study because it exhibits the rounded crest characteristic of its older age (Gillespie and Zehfuss, 2004; Putkonen et al., 2008) and it thereby is assumed to have undergone the process that the hillslope model approximates.

Regional and global climate records show evidence that climate has fluctuated in the past as a result of temperature changes that coincided with glacial activity in both the

Northern and Southern Hemispheres (Shackleton et al., 1984). Examples of known changes in paleoclimate that coincide with global cycles are changes in incoming solar radiation resulting from orbital forcing, i.e. Milankovitch cycles occurring at 23-, 41- and 100 kyr intervals, advances and retreats of continental ice sheets, changes in sea surface temperature (SST) resulting from ice sheet instability (Hostetler and Clark, 1997; Licciardi et al., 2004; Clark et al., 2009), e.g. Heinrich events (Clark and Bartlein, 1995), and Dansgaard-Oeschger oscillations (Benson et al., 2003).

Each type of cause drives changes in temperature on a regional scale by means of atmospheric and oceanic circulation changes (Galaasen et al., 2014) that then affect regional climate and local weather patterns that affect erosion rates and landform degradation through time (Tausch et al., 1993; Woolfenden, 1996; Heusser, 1998; Minnich, 2007). Paleoclimatic proxies also indicate that large scale changes have themselves varied in duration and frequency, and that there is evidence for this globally and in the present study region (Rampino et al., 1987; Anklin et al., 1993; Dansgaard et al., 1993; Taylor et al., 1993; Smith and Bischoff, 1997; Lowenstein et al., 1998; Shackleton, 2000). Regional studies quantifying rates of topographic diffusivity related to different latitudes (Oehm and Hallet, 2005), as well as studies of ecological changes related to recent warming (Cannone et al., 2008; Field et al., 2011), provide evidence that small changes in regional temperatures over the scale of even decades can lead to significant ecological changes (Woolfenden, 2003). The present work relies on the overlapping evidence showing a relationship approximating an increase of topographic diffusivity with a decrease in temperature. By correlating past temperature changes in the eastern Sierra Nevada with topographic diffusivities recorded elsewhere in current climates, the effects of past climates on landform degradation were examined through an application of space-for-time substitution to be discussed in the Methods section.

Occurring during a time range for which proxy records provided evidence of alpine glacial advances and retreats, Mono Basin moraine was used as a record of how hillslope degradation responded to past climate changes triggering those advances and retreats. Published ages indicate deposition of the moraine occurred after the start of the last glacial period approximately 126 ka (Shackleton, 2000; Shackleton et al., 2003). A minimum age range is 80-60 ka according to revised published accounts (Phillips et al., 1990; Phillips et al., 1996; Gillespie and Zehfuss, 2004). The mid-latitude location at the boundary of the polar jet stream, considered to have shifted with the advances and retreats of the Laurentide ice sheet over the last glacial cycle (Clark and Bartlein, 1995; Benson et al., 1998), further supports the assumption that global climate changes drove the regional glaciations, thereby affecting landform surface processes. That there is considerable consistency in glacial advance and retreat in northwestern California with glaciations in east central California lends further support to the correlations of global and regional climate change patterns (James et al., 2002).

The location of the Mono Basin moraine in Mono Lake Basin, which is thought to have shared in the paleohydrological system of Owens River connecting Mono Lake to other lakes in the region, provides a physiographic basis for comparing proxy climate records from lake sediment cores (Benson et al., 1996; Litwin et al., 1997; Smith and Bischoff, 1997; Bischoff and Cummins, 2001) (Figure 1.1). Proxy climate data from

Mono Lake sediment cores can be used to correlate times of changes in the regional climate with conditions that would have affected erosion rates of the moraine in Mono Basin. For example, lake sediment records can indicate low stands which are associated with warmer temperatures that evaporated the lake water and, therefore, would have caused glaciers to melt and retreat. High stands are associated with cooler temperatures that would have maintained or advanced glaciers (Benson et al., 1998). Therefore Mono Basin moraine provides a temporal link with a glacial advance and it is spatially related to a drainage system for which proxy climate data indicates changes in climate during the evolution of the moraine.

1.3 Problem Statement

The diffusivity equation has been shown to closely model cross-section profiles of hillslopes (Putkonen and O'Neal, 2006; Putkonen et al., 2008). However, the coefficient of topographic diffusivity, κ, as it has been used as a time averaged constant, does not express the diversity of past climates that interacted with landform surfaces. Also, its use has thereby misrepresented variable degradation rates through the evolution of a landform. Given what is known about past climate fluctuations and the effect of temperature on current topographic diffusivities, this study addressed the problem by using numerical modeling to vary the coefficient of topographic diffusivity in accordance with documented variations in climate. With this approach, the cross-section profile of Mono Basin moraine was modeled and compared with models generated from the application of a constant topographic diffusivity.

Long term landform degradation has been modeled through application of the hillslope diffusion equation to an initial profile with an initial angle of repose, the steepest angle that a mound of unconsolidated material will remain at rest without sliding, as the initial state (Putkonen and O'Neal, 2006; Putkonen et al., 2008). The free variable in the equation, a constant κ, a parameter reflecting the integration of climate and substrate, has not been temporally constrained to actually reflect conditions it is used to represent. Rather, as a free variable, it is generated to produce a cross-section profile that agrees with an observed form given an initial angle of repose and application of the equation (Hallet and Putkonen, 1994). If assumptions about initial conditions of the slope are correct, then the method has been assumed useful in dating moraine age (Hallet and Putkonen, 1994). However, the result is that the use of a constant κ through the life of the landform misrepresents or does not include the variable effects of past climate fluctuations on the landscape, and so the conventional use of κ described by the transport law in the hillslope diffusion equation is limited in its ability to model landform evolution. Also, while current diffusivities are readily accessible in Mono Basin, they are only applicable to the most recent geological period of a global interglacial time, when climate has been warmer, drier, and more stable than it was prior to the last 10 kyrs (Holocene) since the start of the last interglacial time (Woolfenden, 1996; Benson et al., 1997; Benson et al., 1998; Mensing, 2001; Minnich, 2007). Therefore, use of present κ values are expected to misrepresent landform evolution as well.

1.4 Objectives

Hillslope diffusion equations typically are used to date sloping landforms rather than to sequence short time scale processes and perturbations, such as soil creep or landslides, during their evolution. Such smaller scale changes often are considered to lack relevance in quantifying long term geological processes because, for dating purposes, they are considered mainly for their contribution to the long term average erosion rate. This study focused on quantifying variable degradation rates in order to determine how past climates might have affected erosion and surface processes on time scales less than 100 kyrs. The objective was to quantify the variations in degradation that result from applying topographic diffusivities that change over time in accord with variations in climate. Comparisons of this model with those generated from a constant and optimal value showed: 1) the sensitivity of κ to climate fluctuations resulting from changes in air temperature and 2) the degradation variability lost when a constant value is used. The results produced: 1) generation of time dependent κ values that best model the current profile and 2) an analysis of the potential errors that result from using a constant κ instead of a climate dependent κ.

1.5 Geological and Climatic Setting of Mono Basin and Moraines

Although the Sierra Nevadas have been at the center of research endeavors to understand the petrogenesis and plate tectonic setting since at least the 1960's, interest in the geology of the mountain range and processes that modify its topography continues. A general summary has been published and is accepted as an introduction to the topic of Sierra Nevada geology in Hill (2006). A more complete compilation of the history of the research on which general scientific understanding is based has also been published in Moores et al. (1999). Since the 1980s and the advance of accelerator mass spectrometry (AMS), research specific to understanding glacial chronologies and the effect of

Pleistocene glaciations on the eastern Sierra Nevada landscape has been reexamined. Numerical age dating of moraine boulders using cosmogenic isotopes (Phillips et al., 1990; Phillips et al., 1996; Gillespie and Zehfuss, 2004) has significantly refined the earlier glacial chronologies of Blackwelder (1931). The following provides a summary synthesized from the above sources.

The eastern Sierra Nevada is an alpine environment shaped by the repeated advance and retreat of glaciers during a minimum of 9 recognized glacial/interglacial cycles occurring over the past 2.6 Ma (Gillespie et al., 1999; Gillespie and Zehfuss, 2004). The mountain range formed during the Late Jurassic, approximately 150 million years ago, as a result of subduction of the oceanic Farallon plate beneath the North American plate that produced a magmatic arc extending southward into Mexico and northward into the area of the Klamath Mountains (Moores et al., 1999; Hill, 2006). Renewed uplift began during the Miocene, ~20 million years ago, by Basin and Range extension of the crust, causing a westward tilting fault block of mainly granitic rock (Moores et al., 1999; Hill, 2006). The start of the Great Ice Age in the Pleistocene epoch, 2.6 Ma, marked the beginnings of glaciations occurring in the Sierra Nevada Mountains that carved mountain stream valleys into U-shaped valleys leaving behind long ridges of deposits as lateral moraines (Gillespie et al., 1999; Hill, 2006).

Moraines studied in Mono Basin and Bishop, California (Figure 1.1), as well as others occurring in the eastern Sierra Nevada, have been the subject of previous research efforts attempting to date the timing of glacial advances and retreats in this region as consequences of Pleistocene climate change in western North America (Gillespie et al., 1999; Gillespie and Zehfuss, 2004). Early work relied on mapping the extent of moraines (Blackwelder, 1931). Further progress was made through the use of relative dating techniques (Burke and Birkland, 1979; Bursik, 1991; Bursik and Gillespie, 1993; Sampson and Smith, 2006) and subsequently by exposure age dating of boulders and depth profile dating using cosmogenic isotopes (Phillips et al., 1990; Phillips et al., 2001; Phillips et al., 2009; Rood et al., 2011; Morgan and Putkonen, 2012). Moraines in the region are estimated to range in ages from approximately 2.6 Ma to 600 years old (Gillespie and Zehfuss, 2004), although the current interglacial time began ~11,500 years ago. Published relative and radiometric ages begin with the McGee glaciation between 2.7 -1.5 Ma, but records suggest that by circa 920 ka the landscape had become more continuous with the present landscape in terms of the preservation of moraines (Gillespie and Zehfuss, 2004).

Glacial chronologies have also been augmented by supplementary chronologies. Age constraints based on correlations of paleomagnetic field intensity of volcanic ash records with GLOPIS (Global Paleointensity Stack) (Zimmerman et al., 2006) have refined ages further. Age dating of other moraines in the broader region, extending from the Olympic Mountains in the northwestern United States to the Uinta Mountains along the Utah-Wyoming border (Thackray, 2008) to the far southwestern margin of California in the San Bernardino Mountains (Owen et al., 2003), indicate variable responses by regional glaciers to common forces that caused global climate fluctuations (Thackray, 2008).

Commonly, subsequent glacial advances remove previous deposits in their path or emplace younger deposits with older ones. For this reason, identifying some moraine deposits as distinct in age from others that might have been overridden or cross-cut during a glacial advance has been challenging and the subject of much debate. However, the latest published and cited ages distinguish the older Mono Basin moraine with dates ranging from 80-60 ka from a younger Tahoe II moraine, argued to be 50-42 ka (Phillips et al., 1996; Gillespie and Zehfuss, 2004), which was deposited by a glacier that traveled down the same valley but took a more northerly course cross-cutting the earlier deposit (Gillespie and Zehfuss, 2004). In addition to these moraines, published ages of other moraines in the region and augmented with published times of Mono Lake low stands (Benson et al., 1998) were used as motivation to vary the κ value (thought to reflect different climatic conditions) in the degradation modeling used in the present study and further described in Methods. Table 1.1 lists those times selected. The citations given as notes for Table 1.1 provide more complete accounts of the glacial and lake level chronologies and the sources of those chronologies, as their focuses centered on dating of the moraines. The focus of the present study was on modeling the evolution of the Mono Basin moraine using the latest updates employed for estimating the ages of moraines in the Mono Basin region.

Current κ values derived in the present study at Mono Basin will be discussed in Methods. Two additional moraines near Birch Creek, located approximately 11 km SW of the town of Bishop, CA. also were sampled as a basis for comparative analyses of current κ values in the region. However published dates of the moraines at Birch Creek

Table 1.1 Times used in degradation model and based on published moraine ages and proxy records

Event[1]	**Time (ka)**
Present	0
Recession	13
Transition	15
Tioga Start	25
ML LS 3	27
Tenaya	32
ML LS 4	34
Tahoe II	50
Mono Basin	80

[1] Events are based on glacial advances reported as the latest updates referenced in Gillespie and Zehfuss (2004) and occurring after the deposition of Mono Basin moraine. ML LS 4 and 3 are supplemented to the list to support inferred glacial retreats during reported Mono Lake Low Stands (Benson et al., 1998). The glaciation times are based on published dates compiled and reference in Gillespie and Zehfuss (2004). The times of "Transition" and "Recession" were also supported by qualitative proxy records discussed in the Results Chapter. The times shown were selected to be run in the degradation modeling program and based on published chronologies referenced in Gillespie and Zehfuss (2004).

are considerably older, between 150-130 ka (Phillips et al., 2009), than the moraines in the Mono Basin region and were not modeled in this study. The current diffusivity calculated for Mono Basin moraine was used together with other globally distributed values reflecting regional climates and related to an average air temperature reflective, though not necessarily definitive, of the location where the value was measured. The method of substituting geologically present diffusivities to a single location in the past under varying climates will be explained in the Methods section.

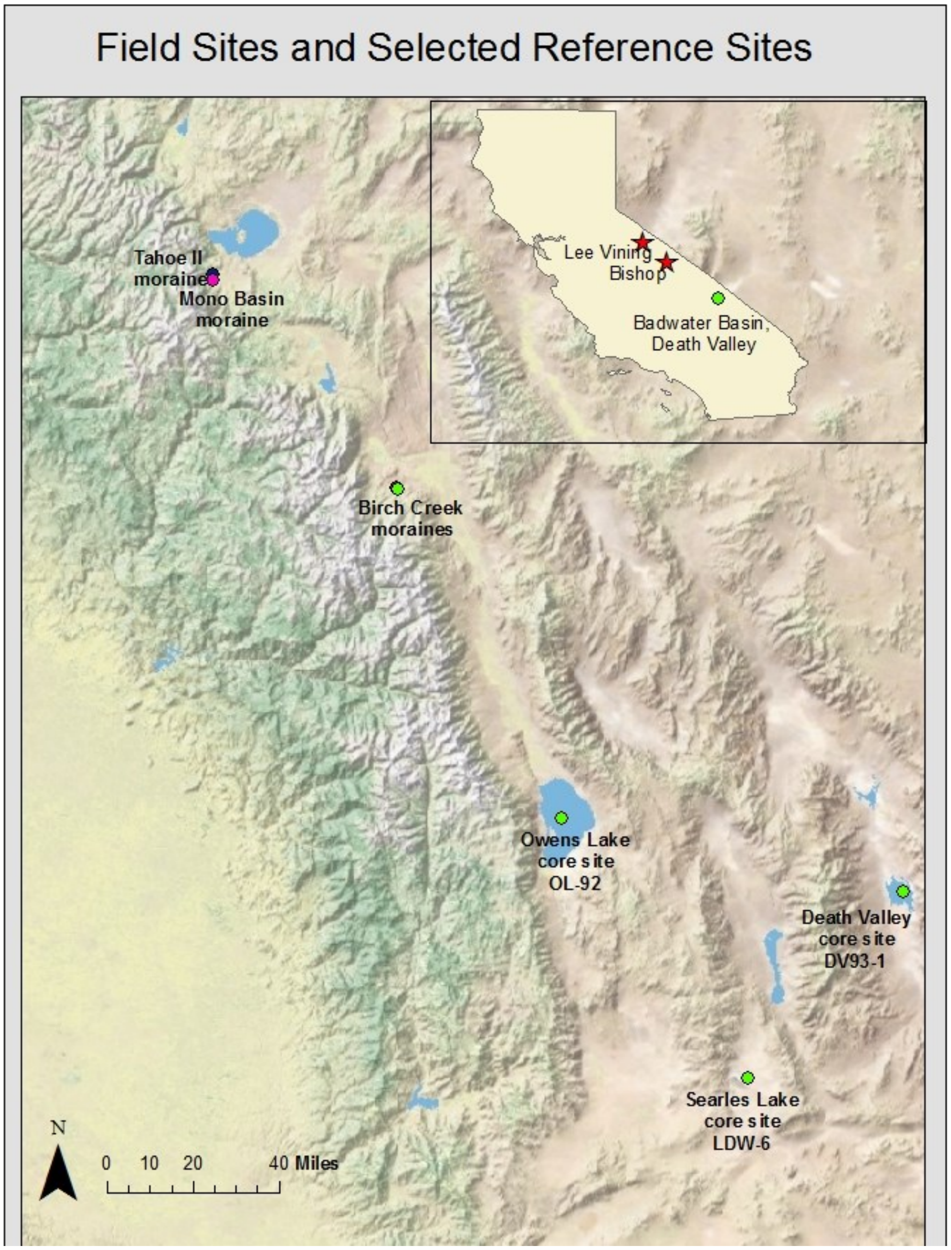

Figure 1.1. Relative locations of Mono Basin and Birch Creek moraines. Red stars in index map show nearest towns to field sites. Proxy data from Death Valley core site is referenced in the study. The topographic map has been compiled from multiple sources (ESRI, 2014).

CHAPTER II

METHODS

2.1 Overview

Current topographic diffusivities and related surface processes of the Mono Basin region were calculated through measurement from the following field methods: sediment traps, pebble lines, and repeat photography that are discussed in earlier professional literature of Tricart and Macar (1967) and a terrestrial LiDAR (Light Detection and Ranging) scanner. Multiple methods were used in this study for purposes of comparison and assessment of what may be learned from the resulting data given by various field methods. Present sediment transport was related to the current regional climate and assumed mode of sediment transport, which in a semi-arid alpine environment is considered to be surface wash (Leopold et al., 1966; Selby, 1993). Published data from studies on sediment transport on natural slopes in recent time and a similar arid climate supplemented measurements in the present study (Schumm, 1964; Kirkby and Kirkby, 1974; Abrahams et al., 1984).

Measurements in the present study were made for the year 2010-2011. The results, while given as an annual rate, therefore reflect only a single year. Measurements averaged over multiple years, of three, five, or ten for example would have better represented annual transport rates. However, financial and time limitations did not allow for annual data campaigns. The training in the installation of the apparatus, the data sampling, measuring, and collection and in the reconnaissance for assessing their suitability for future studies provided a foundation for more efficient campaigns in the future.

Installation of field apparatus was made on different moraines for comparison and in order to test the feasibility of their performance for future study. The practice of collecting data on bare earth areas, as explained in the individual methods, was to characterize the mobility of the substrate at the surface unhindered by obstructions such as vegetation, deadwood, and large boulders. Such obstructions hinder downslope transport, and the objective was to investigate how the regolith making up the mobile surface moved, in order to assess how the sediment that was in flux *contributed* to the degradation of the landform.

The method for studying past diffusivities in the region was a transference of present diffusivities in global locations that included Mono Basin with climates, identified by air temperature, to times in the past in the region of Mono Basin where proxy records indicate similar temperatures. The method will be described in section 2.7.

In Chapter 3, Data, an overview includes the novel applications that the data generated from the following methods were used for. The field methods themselves cited above in Tricart and Macar (1967) have a long standing history in land management studies around the world, because they have been viewed as the most effective way of measuring natural sediment transport as a measure of surface *change* on the landscape. However earlier published studies have not typically performed uncertainty analyses with these field methods. The studies compiled by Oehm and Hallet (2005), for example, provide no such analyses. Measurements are typically made to one or two significant figures depending on the sampling and measuring apparatus used. No assumed standard was used with which to compare field measurements and so analysis of uncertainty, rather than error, was performed. In the field of geomorphology field data of physical processes may be compared with model results with the assumption that the model results are limited to a restricted use of parameters that do not reflect the complexity and interactions occurring among the multitude of variables (Tucker and Hancock, 2010).

2.2 Sediment Flux Rates from Sediment traps

Sediment flux, defined as a bulk volume of regolith moving past a representative unit width on the hillslope per unit of time, was collected in sediment traps from various mid-slope to near-crest locations on the moraines in Mono Basin and Birch Creek. Sediment traps have been used as a standard method by the United States Forest Service (Wells and Wohlgemuth, 1987) and in recent sediment transport studies in Dry Valleys in Antarctica (Putkonen et al., 2007) to quantify the transport rate of volume of sediment that has moved past a point on a sloping land surface per unit of time. Dimensions and construction materials are often modified to adapt to environmental conditions to ensure sediment in transport has free entry into the trap and to minimize the loss of sediment by wind, water, or animals. For example, the traps in the present study were constructed with higher sides that those used in Antarctica. Due to an expected higher volume of material in transport in the Sierras than in Antarctica, where erosion rates have been measured to be the slowest on Earth (Putkonen et al., 2007), higher sides helped to ensure that the larger amount of sediment was not removed (Figure 2.1 A and B).

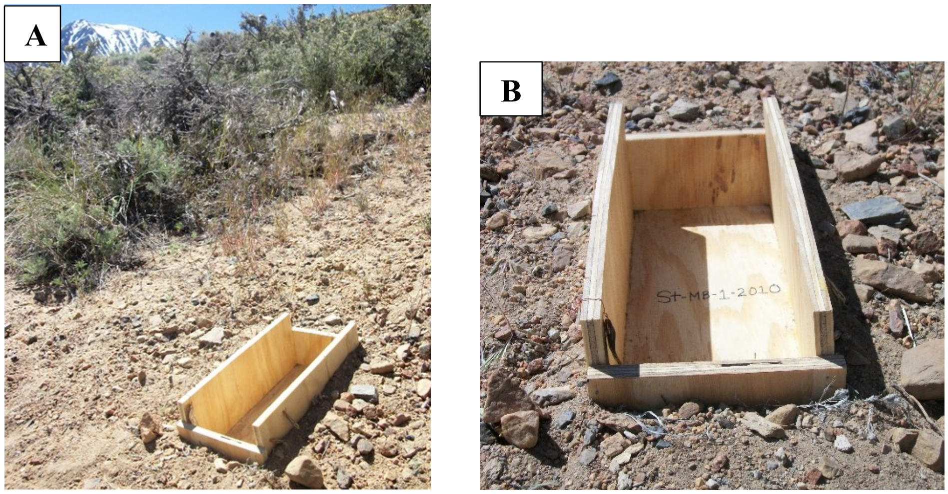

Figure. 2.1. Wooden sediment trap installed on hillslope surface. A. Oblique view shows pathway upslope (towards upper right) where sediment enters trap and back-end flush with surface. Front end does not need to be flush, as sediment only enters from up-slope. Sides are constructed higher in order to prevent sediment entering through the sides. B. View from above shows trap interior and relative dimensions with sample ID and metal ID tag attached at left for recovery if trap became covered with sediment.

As the volume of mobile regolith moving down the hillslope surface, sediment flux is represented in the equation of the general sediment transport law as q, indicated in equation (1.1). When q is not directly measured, but derived from measures of elevation loss and an assumed landform age, the volume can be time-averaged and expressed as an annual rate. However, the transport law itself is not restricted to certain time units. It is given simply as an expression of the general parameters involved in mobilizing sediment down a slope.

In this study, the volume of bulk regolith collected in the sediment trap was measured and used to assess the distribution of regolith sizes transported on the given slope. The volume of material collected in each trap was calculated from measurements of substrate densities. Densities were determined by packing the sediment into a vial of known volume and measuring the mass of regolith filling it. The average density of surface substrate in Mono Basin was 1.958 g/cm^3. In Bishop, the average density was 2.122 g/cm^3. The mass of the collected sample from the trap was then divided by the density to determine the volume of sample. Diffusivity was solved by substituting the tangent of the slope angle for the gradient in the equation (1.1) and presented in a similar form by Putkonen et al. (2007).

The sediment traps were constructed of plywood of 1-cm thickness and with dimensions 12 cm x 32 cm with the sides an additional 4 cm higher than the front and back (6 cm each). They were buried so that the upper lip of the back side would be flush with the surface of the hillslope so as to collect regolith moving downslope. The downslope end of the box did not need to be flush with surface, as the purpose of the trap was to collect sediment from upslope that was transported into the box. The sides extended above the land surface in order to avoid sediment being jostled or blown out of the box. Once installed in the above manner, the inclination of the trap was measured by a clinometer reading along the long edges of the sediment trap which was approximately parallel with the downslope angle on the hillslope at that location. However, the slope angle recorded for the location of the trap was measured by a clinometer reading of the slope between two persons standing approximately 5 meters apart upslope and downslope from the trap location. This two-person method provided the measure of the hillslope rather than the local slope where the trap was positioned.

The sediment transport equation (1.1) expresses sediment mobility as compared to similar slopes in other regions where the combined effects of climate on the substrate transport sediment more or less easily. The state of vegetation, therefore, is assumed to be a result of those combined effects in this kind of study. Other kinds of studies may focus, for example, on the contribution of the variety and density of vegetation to a landform surface by comparing the vegetation on different landform surfaces as a single parameter. However the present study treated the cumulative effects of a climate on a substrate in a general way similar to other studies of its kind, e.g. those that have focused on modeling hillslope degradation over a relatively long time as compared with shorter time scales that are used in considerations of vegetation species and density changes.

The current hillslope surface of Mono Basin moraine exhibited regular spatial patterns of sagebrush and bare earth and grass. A bare earth pathway was assumed to reflect areas where sediment on the slope was being transported. Areas containing brush, woody debris, and large rocks and boulders were assumed to be areas where sediment in transport might be obstructed and stored. If the climate had been such that there was less vegetation then, everything else being equal, it was assumed the sediment would have been transported more easily. The sediment that traveled through the pathway without obstruction represented the rate that sediment was transported in the particular environment, which was assumed to be a cumulative result of the climatic conditions on the substrate. The above, therefore, dictated where the traps were installed, which were locations of un-vegetated areas with an upslope pathway leading to the trap, the distance of which also approximated a downslope distance from the bottom edge of the trap, so that the slope where the trap was installed reflected the location on a hillslope, rather than a localized depression or mound. The trap was oriented perpendicular to the slope contour as closely as possible. The methods for recording slope were described above.

The top few centimeters of soil were sampled, not only to determine an average density of the substrate, but also to compare the relative proportions of regolith making up the surface layer of the landform with what had been collected in the traps as annual transport. The purpose of comparing the two was to assess the size of regolith that had not been transported into traps. This, together with data on transport distances, discussed in the next section, indicated how far various grain sizes were travelling downslope in a given year. This was done simply as a way of characterizing the mobile surface in more detail than simply sampling at a point source.

Collected samples were weighed first as bulk masses. Each, then, was sieved, according to the Udden-Wentworth scale, a commonly used geometric scale in sedimentology, where each value is twice as large as the one preceding. The scale extends from 1/256 mm to >256 mm, and is divided into three major categories (mud, sand and gravel). Each category is subdivided. The present study used the following millimeter divisions for sieving: 1.19 – 1.68 (very coarse sand), 2.83 (granule), 4-32 (pebble), >32 (cobble) (Boggs, 1995). For the purposes of the present study, fines were considered all sediment smaller than granule size. The different grain sizes were compared as percentages of the total bulk mass of each sample collected in a trap. These relative comparisons were also compared with bulk masses of the grain sizes collected from the top 3 cm of substrate.

2.3 Pebble Transport Distance from Pebble Lines

Pebble lines were used to measure annual transport of pebbles. Published accounts include similar uses of painted pebble tracking (Persico et al., 2005) as well as adaptations referring to erosion-monitoring lines (Kirkby and Kirkby, 1974; Abrahams et al., 1984).

Pebble lines were located at sites with continuous bare earth that extended an ample distance downslope in order to determine how far pebbles would be capable of travelling in one year on a representative surface of a landform. To measure the average distance travelled by pebbles on the slope, native pebbles 2 to 3 cm in diameter were labelled and placed in a row along a horizontal line along the slope contour. A typical row was 4 to 5 meters in length with 25 pebbles at 20 cm intervals (Figure 2.2 A and B). Rebar stakes were installed at the ends as bench markers. During the subsequent year

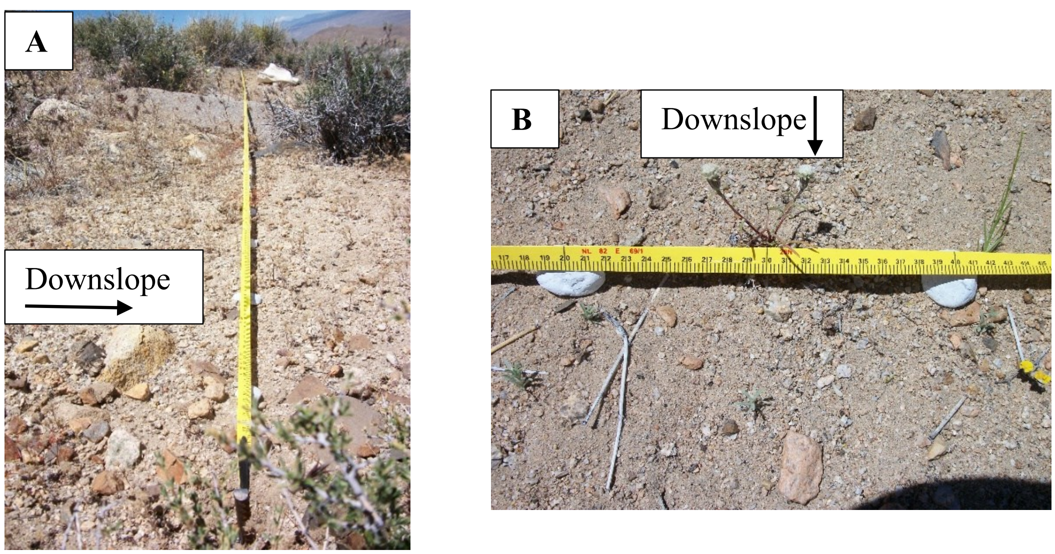

Figure 2.2. Pebble lines installed on hillslope surface. A. View shows pebble line, with downslope towards the right. B. View shows how pebbles were placed on the surface (down slope is down).

pebbles from the line were measured with a measuring tape from their point of origin to their destination position.

2.4 Transport Distance from Repeat Photography and Frequency Analysis

Tracking annual displacement of regolith in repeat photography is an additional way to measure transport rates of pebbles. The method was used together with the measure of pebble frequency over a square meter of bare earth surface. By using distances measured in pebble-line transport and pebble frequency determined in photo analysis, the average travel distance of a volume of pebble-size regolith was determined. Using the transport equation discussed earlier, this volume was used to calculate a topographic diffusivity that was compared with those calculated from sediment traps and terrestrial LiDAR repeat scans, discussed in the following section. The comparisons were made to assess how the rates at which annual surface transport measured to have occurred were related to regolith size variations. They were also used to compare how κ varied with grain size.

The use of photographs to track regolith broadened the range of pebble sizes that could be tracked. Whereas pebbles used in the pebble lines were restricted to 2-3 cm and were placed by hand at initial positions, displaced regolith in photos ranged in size from 0.85 to 8.5 cm and they travelled from natural positions, rather than having been placed, as the pebbles in the pebble line had been. Photographs were also used to assess a size of rock that appeared to have remained stationary. A stationary size of 12 cm was used to generate a curve relating grain size to transport rate. The curve generated from data in this study was then compared with curves generated from published travel distance data of similar sized regolith on shallower slopes. Similarity in appearance with sites used for neighboring sediment trap and pebble-line installations was used as a basis for photo site selection. Rocks observed to have moved a measurable amount were identified in photos taken the second year. Their distances were measured in Adobe Photoshop by determining the displacement of the long axis center.

The frequency of occurrence of pebbles 2-3 cm, determined through photo analysis, was used to calculate the volume of pebbles at field sites where pebble lines were used to determine travel distance. The method correlates two characteristics – size and frequency – by relating them to the third feature – transport rate – to calculate the volume of pebbles in annual transport per unit width. The volume was used to calculate and compare a topographic diffusivity for the pebble line and repeat photography methods with the other discussed methods, as illustrated in the Results.

A published method for determining the volume of a certain rock size transported over a designated reference area was adapted to this study (Putkonen et al., 2007). In the equation,

$$q_{vol,\,x,\,mean} = \sum_{1}^{n} \frac{\frac{V_n * d_n}{\Delta t}}{A} \qquad (2.1)$$

total volume of sediment flux (q) (in this case of pebbles) equals the sum of all pebbles of a certain size ($V = m^3$) multiplied by the distance per unit width they travelled over time and divided by A (the reference area) in units of m^2/yr. With this equation, the q for 2-3 cm pebbles, was used in the transport equation (1.1) given in section 1.2 to calculate a κ value for the pebbles only. Equation 2.1 differs from 1.1 in that the flux rate is defined by a measured distance in 2.1. However, equation 1.1 was used to calculate the κ value from the volume of sediment collected in a sediment trap where the combined mix is assumed to represent the mobile surface. Equation 2.1 was used to determine the volume of a certain regolith size traveling a measured distance in order to calculate a transport rate for a grain size. The grain sizes and their relative proportions together constitute the substrate of the moraine and, for the purposes of modeling, were assumed to be constant over the surface.

In order to incorporate grain sizes smaller than pebbles that could not be physically tracked like the larger regolith into the descriptive curve of size versus transport distance, a theoretical determination was made, intended to reflect an intermediate value discussed below. The theoretical value was derived from calculating a length of assumed volumetric dimensions measured from the average topographic difference between LiDAR repeat scans (see explanation in section 2.5), the width of a sediment trap, and the volume of fines collected in the trap. The average topographic difference of the scan area is here assumed to represent an amount of flux in transport that occurred when sediment entered the sediment trap. For this to be true, the slopes would need to have been comparable and the average topographic change collectively would need to have been generated predominantly by fines. Given the caveats and uncertainties, this theoretical value was employed to reflect an intermediate value. A minimum value would result from fines that were transported into the trap from the edge of the trap opening, while a maximum distance value would originate from some unknown point near the crest of the slope. Given that the start of the pathway was not at the crest top but, rather, downslope from sagebrush, the maximum distance possible for a fine likely did not occur on the landform under study. The calculated distance for fines was at a reasonably greater distance than those reported for pebbles. This theoretical calculation was interpreted to reflect the historical experiments that produced a classic curve showing the velocity needed to transport various grain sizes. It illustrated that for sand-sized and larger grains, the larger the average diameter, the higher the velocity required to initiate transport (referred to as critical current velocity) (Sundborg, 1957). Here, the principle is used to illustrate that given a transport event, the smaller the grain size, the further the movement, all else equal, i.e. no obstructions.

2.5 Topographic Change Detection with Terrestrial LiDAR

In the present study terrestrial LiDAR (Light Detection and Ranging), also referred herein as terrestrial laser scanning (TLS), annual repeat scans were used to observe and document, each year, the topography over approximately 1 square meter of bare earth on the moraines in Mono Basin and Bishop. A set of annual repeat scans taken of approximately 1 square meter of bare earth surface patches on the moraines in Mono Basin and Bishop were taken using a Leica ScanStation (Figure 2.3). The scanner was programmed to emit laser pulses at 2 millimeter spacing with an electromagnetic wavelength documented to be emitted by laser scanners of 10^{-3}-10^{3} (eV) (Heritage and Large, 2009). The instrument is capable of 2 millimeter modeled surface precision during scanning with a 6 millimeter accuracy of position and 4 mm accuracy of distance according to the instrument specifications.

Mid-slopes and near-crest areas were scanned by transporting the LiDAR and setting it up on a tripod positioned to face upslope. The distance between the scanner and

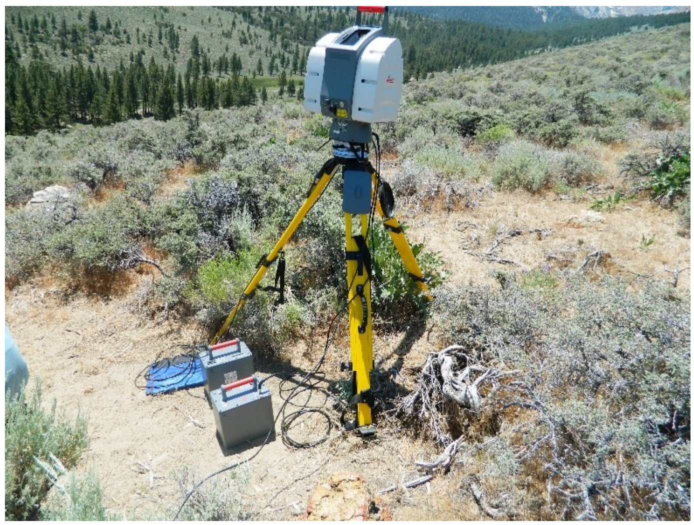

Figure 2.3. View of LiDAR set-up on hillslope. All set-ups have instrument facing upslope to minimize distance between scanner and area scanned.

the area scanned typically ranged from 1 to 3 meters, appropriate for the scale of square meters under study. A typical range for studies in geology and geomorphology are on the scale of 10s to 100s of meters with errors that scale with those distances, centimeters to 10s of centimeters. However, those studies typically are not designed to measure sediment transport rates at a fine scale, which is a unique feature to measure with repeat scanning in the field of geomorphology. The laser was programmed to emit pulses that interfaced with the surface at 2 millimeter spacing with use of the Cyclone software which accompanies the instrument.

Decreasing the distance between the scanner and scan area increased precision by minimizing interference and increasing the likelihood of returns, hence increasing the signal to noise ratio (Heritage and Large, 2009). Vegetation between the scanner and the bare surface could cause interference with the emitted pulses. Also, the higher the density of return points, the more accurate will be the triangulations between points used in creating a digital surface once the points are downloaded (Heritage and Large, 2009). Further, the better the precision for each scan, the better the precision between repeat scans of the same area. The scanner recorded the digital returns as point clouds with each point carrying coordinate information relative to an arbitrary reference point – x-, y-, z-distances – and intensity information – a measure of the reflectance of the surface (Reshetytuk, 2009).

The scans were aligned with the help of targets with which subsequent scans were rectified in the instrument's software. Three to four targets were drilled with bolts into large boulders around the periphery of the scan areas. Initial processing of the LiDAR scan data entailed rectifying the scans with alignment to target scans. The software used the target coordinates as tie points recorded within the instrument's internal frame of reference. Upon return the following year, the LiDAR was set up over a nail used as a benchmark placed in the ground the previous year. With the targets in the same place, the second year scans had the same tie points in the first year's frame of reference. Several swath areas were scanned each year. Because overlap of all of them was not possible, only those areas that did overlap were selected for analysis.

Because the purpose of the scanning was to quantify topographic change related to the natural removal and deposition of sediment, the area within the periphery of the targets was bordered off to restrict any human disturbance of the sediment during the campaign itself. For this reason, vegetation or other obstructions could not be approached and removed. Therefore, Cyclone software was used to remove those point clouds whose intensities were produced from sources other than bare earth, such as from vegetation returns. The coordinate data were then imported into MatLab. MatLab code was written to create continuous surfaces from non-uniformly distributed data points, which produced DEMs of the surfaces scanned. Surfaces were created from the TLS data from each field season. The differences between elevations generated from the surfaces of the two field seasons – 2010 and 2011 – were calculated and superimposed as an independent matrix over one of the previous year's surfaces showing where there was net deposition, erosion, or no change. The difference surface gave a measure of overall loss (erosion) or gain (deposition) in elevations over the selected swath study area.

By mapping the topographic differences, not only was cumulative difference of the topography quantified, but distribution of the differences was quantified. The purpose in so doing the latter was to assess potential areas for sediment storage, flow routes, and spatial patterns relating the two surfaces. Topographic highs, defined by elevations higher than the average, of each year were mapped. The mapping scheme used a sliding window of approximately 5 cm by 5 cm to determine an average elevation as the datum for each window. Spatial patterns of the highs were used to locate storage areas in relation to the high areas of the first year.

The above discussed methods were performed as means to quantify observations of surface changes that otherwise are extremely difficult to make and to quantify as they occur naturally in the landscape. Limiting the controls contributing to natural transport means that many factors involved in the regolith mobility and degradation of the landforms are unknown. Therefore, as mentioned earlier, documentation of surface change was limited to what could be measured and observed after one year. Use of multiple methods provided a way to compare results and to assess the suitability of the locations of the apparatus for considerations of future study.

2.6 Modeling Hillslope Diffusion

While present-day diffusivities and erosion rates were quantified from regional measurements, degradation modelling was used to analyze the effects of past climate on the topography. Degradation of Mono Basin moraine was quantified by modeling hillslope diffusion and evolution of its profile cross-section. A diffusion equation expressed by a basic law of sediment transport (1.1) was used to model the effects of fluctuating climate over the age of the moraine. As indicated in section 1.2 (Hallet and Putkonen, 1994), soil creep and, in addition, surface wash, round out the crest and smooth the edges so that the resulting profile follows a gradual reduction in hillslope gradient over time (Selby, 1993). However, because rates of soil creep were shown to be influenced by climate (Oehm and Hallet, 2005), this study employed degradation modeling to test whether known variability, tracked as regional air temperatures in a climate record and assumed to be affected by glacial activity that altered past global climates during the last glacial period, could be shown to significantly affect regolith erosion rates through time.

One of two other possibilities are that global climate change did affect regional climates and, therefore, land surfaces, but that such correlations cannot be determined through the climate records. In other words, no physical evidence of past effects on the landscape by those climates can be used for numerical modeling. The other possibility is the global climate changes triggered by glacial activities of past glaciations, of ice sheets for example, did not significantly alter all regional climates enough to affect rates of surface processes. In other words, in such a case, climate is not a significant factor in the long term degradation of the landscape. Results from the modeling employed in the present study were used to address such possibilities.

For the purpose of modeling hillslope degradation using the transport law (1.1), an initial hillslope angle was assumed and assigned the angle of repose for the initial cross-section profile. A required initial angle is intended to represent starting conditions when the landform was deposited. The maximum slope angle at which the hill-shaped landform, in this case a moraine consisting of glacial till, remains stable, i.e. where the grains would not slide, called the angle of repose, is a subject little examined in natural environments, particularly for such a complex medium. Published works modeling natural landforms have cited and employed values ranging from 31° - 35° to generate model profiles that conform to observed profiles (Hanks et al., 1984; Hallet and Putkonen, 1994; Putkonen and O'Neal, 2006; Putkonen et al., 2008). The values also fall within ranges found through laboratory experiments where the deposition angle was measured for mixed shape and angular gravel (Deganutti et al., 2011). The behavior of the sediment transported appeared to follow observations of grains sliding over a thin boundary layer at the surface studied experimentally and reported in Jaeger and Nagel (1992) and Deganutti et al. (2011). Given that Mono Basin moraine had a high sand content and former modeling of the landform profile employed an initial angle of 31° (Hallet and Putkonen, 1994), a 31° angle of repose was employed in the present study as well.

The sediment flux per unit width down slope is linearly related to slope (dz/dx). The κ, measured in m^2/yr, parameterizes the integrated effects of climate and substrate (discussed in the Introduction) by expressing a rate of degradation that is independent of slope. The transport equation generates a flux proportional to the decrease in slope angles as regolith is eroded (removed) from the crest, sent into transport (mobile state) and deposited (settled state) down slope. As regolith is transported from upslope and deposited down slope, the slope profile changes as a function of curvature or the second derivative of the slope. The cumulative sum of the change is represented as a volume of material at a particular point on the slope at a corresponding time. The slope is multiplied by the diffusivity coefficient κ which the model assumes to expresses the cumulative exogenic effects of climate on degradation irrespective of slope. While local features may affect κ, in the application of the degradation model in the present study and in the time scales of thousands to tens of thousands of years used in the model, such effects were not factored into modeling independently. Rather, any such local factors were integrated through time, so that long term effects were compared relatively at times associated with climate records indicating glacial activity, as will be discussed in the following section.

The physical descriptions above are formalized in equations: The transport equation (1.1), given in section 1.2, expresses that a volume of material passing a line parallel to a slope contour is quantifiable as a linear relation to slope gradient. The basic parameters are: q (volume of flux/year), z (local elevation difference in meters), x (horizontal unit distance in meters), and κ (topographic diffusivity in m^2/year). By the principle of conservation of material, where the loss of elevation (z) over time (t) is proportional to the volume of material (q) transported over a horizontal distance (x),

$$-(dz/dt) = (dq/dx) \tag{2.2}$$

the continual transfer of material from up slope toward down slope positions approximates a linear differential equation, which follows:

$$dz/dt = \kappa(d^2z/dx^2) \tag{2.3}$$

Diffusive processes thereby are said to shape the moraine profile to conform to the diffusion equation, a second order derivative of the combined transport and conservation equations. Progression from the initial conditions to the current profile as it results from degradation as defined by the diffusion equation described above is illustrated in Figure 2.4. The MatLab code written and used to generate elevation profiles applying the transport law and different scenarios for κ is in the Appendix.

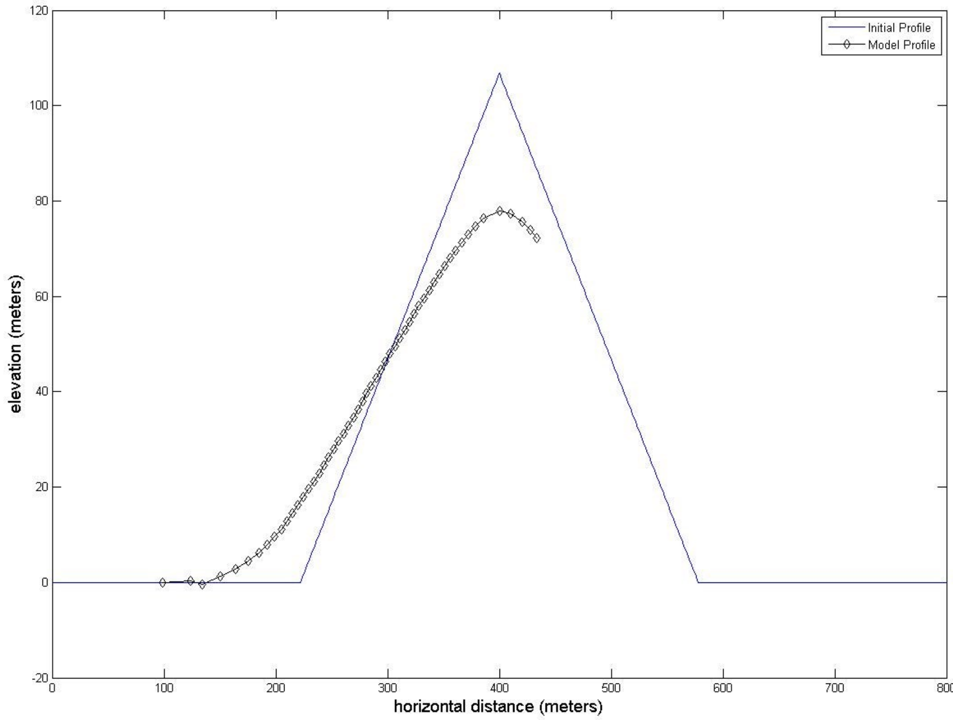

Figure 2.4. Assumed initial profile of a hillslope at angle of repose, 31° (blue), and current hillslope profile of Mono Basin moraine (diamonds) based on elevations measured in the field. Differences in profiles, i.e. the differences in elevation and in curvature, exemplifies the underlying processes of diffusion expressed by the degradation equation. Initial crest elevation would be 106.8 m above an arbitrary base level.

In order to examine the effect of past climate fluctuations on hillslope degradation over the age of Mono Basin moraine, three versions of the model using different κ values were compared. All models use the maximum age of the moraine as 85 ka, which was selected on the basis of the most recent published ages and recent publications of the same author on considerations of updated calibrations and error limits related to exposure age dating of boulders using cosmogenic isotopes (Phillips et al., 1996; Phillips et al., 2001; Phillips et al., 2009; Marrero et al., submitted 2014). While studies have employed degradation modeling to date fault scarps for example (Hanks et al., 1984), radiometric age dates typically are used when they have been published because they are considered absolute chronological markers. Therefore, modeling was not used here to explore ages that would generate an improved fit given constant κ values. Rather, the purpose was to test and compare the constant κ value, assuming a given age, with a time-varying sequence of values. Each model starts with the same initial conditions of the angle of repose discussed earlier in this section. In the first case, a constant κ optimized to generate a cross-section profile closely approximating the current moraine profile was used to model the evolution of the landform from initial conditions to the present morphology. In the second, κ was held constant and defined by present-day degradation values. In the third, κ varied with time based on current climate-related diffusivities and the documented variation in the paleoclimate. Determining the κ values that correspond with paleoclimate required a series of steps described in the following section.

2.7 Past Degradation and Climate from Space-for-Time Substitution

A physical quantifiable basis for varying κ through time was needed, but past climate features, such as temperature, cannot be measured directly. Published diffusivities compiled in Oehm and Hallet (2005) provided a physical starting point for relating temperatures broadly related to regional climates that could be identified with an average air temperature. The authors had organized diffusivities by latitude with a goal of assessing how much surface mobility was affected by climates as they approached higher latitudes. Their work was more focused on determining how rates of soil creep, the slow downslope movement of hillslope surfaces, differed across broad stretches of climates found in different latitudes, from the tropics to the polar regions. The authors found only two other earlier publications that examined the relationship between global climate and the mobility of the surface layer, and those focused on the periglacial processes of solifluction and gelifluction, soil flow associated with the melting of frozen ground (Kirkby, 1995; Matsuoka, 2001). The compilation in Oehm and Hallet (2005) was intended to increase attention to the effects of climatic factors (in the broad exogenic sense explained earlier) on the mobility of hillslope surfaces.

The two earlier works focused on surface mobility in periglacial environments, those regions either located near glaciers or that undergo freeze-thaw conditions due to seasonal variations in temperatures. The Oehm and Hallet (2005) work, in particular, assessed typical rates of soil creep in order to compare if and how soil creep operated across different climates and environments. In the compilation the authors examined how such regions across the globe might undergo changes during times of future climate change that might accelerate the release of CO_2 when the mobility of the active layer increased as a result of increased temperatures. The present work focuses on the mobility of a particular landform surface and how that mobility might have changed through times in the past as a result of the cumulative changes in climate and expressed through a temperature proxy. The purpose of using a temperature proxy was to produce numerical results that could be compared through time, as an improvement on comparing results from qualitative proxies.

Many workers have investigated relative changes in past temperatures for the Sierra Nevada through the use of proxy records that include pollen in packrat middens and lake cores, cosmogenic exposure age dating of moraines, mineralogy of rock flour, and chemical analysis of lake cores (Koehler and Anderson, 1995; Woolfenden, 1996; Litwin et al., 1997; Benson et al., 1998; Heusser, 1998; Litwin et al., 1999; Minnich, 2007; Street et al., 2012). However these provided largely qualitative assessments of past climates, e.g. in terms of being warmer or colder, wetter or drier than the present. Although relevant and important, qualitative information was not applicable for executing the modeling technique of the present study. However, some of the above works were referenced for comparative purposes.

Space-for-time substitution, as applied in the present study, related present topographic diffusivities and the current air temperatures in which they were measured, with Mono Basin's past air temperatures, and derived past diffusivities for Mono Basin from a transfer function. The application is a case of the geological principle of Uniformitarianism, the foundational principle in Geology that processes and rates operating in the present are the same as those operating in the past. The method also has been widely used, although highly debated, in the field Ecology (Pickett, 1989). While space-for-time analyses have been shown to pose problems for ecological data, where species and community changes can occur on much shorter time-scales than those applied in the present study (Blois et al., 2013), long-term applications on the scale employed in the present study, have been accepted in ecology, particular with respect to studies examining long term climate changes (Blois et al., 2013).

The resolution of the ecological sensitivities associated with small spatial scales combined with short time scales were not considered as part of the scope of the present study. In relative terms, small scale effects on the landscape resulting from climate and expressed through ecological variations, were considered cumulatively when time scales of thousands to tens of thousands of years were compared. Although, future studies could focus on the effects of short time scale vegetation changes brought about by episodic events (related to climate, fire, mass movements) on the spatial extent of erosion, for example. The relevance of the method for the present study was simply of using a set of known κ values related spatially by temperature, and applying those values to past temperatures. While the goal was to address larger temporal scales than those often investigated in ecological studies, the scale of thousands to tens of thousands of years is relatively smaller than what has been addressed by landscape evolution studies that often quantify at the scale of hundreds of thousands to millions of years. The purpose here was to show that if the given knowns could be accepted, or be shown to have firmer ground than qualitative measures, then the method would be better able to quantify variability in long term degradation than the application that assumes a constant κ value, where no variability can be derived.

As far as the acceptability of space-for-time in geological studies, the general form of reasoning has been used most recently by Hilley and Arrowsmith (2008) to associate periods of erosion in assumed tectonically-related drainage basins to slip rates along a pressure ridge along the San Andreas Fault Zone. Their study substituted measures within the same geologically related area, whereas the present study used globally diverse areas in transferring measured rates. While the application of the substitution method used in the present study could be questioned because of underlying variability in the different landscapes, the physical bases for measured κ values given by temperatures was viewed as an advance on the common application of a constant value with no physical basis.

Published diffusivity values from field areas compiled in Oehm and Hallet (2005) included data from several sites at each latitude represented and, therefore, the minimum and maximum values from each region were used to derive transfer functions relating κ values with air temperatures at the location of the sites (see explanation below). The transfer function generated from maximum values was selected for modeling, because the maximum values were more reflective of a climatic zone than the minimum values, which spanned multiple latitudes and could reflect multiple climatic zones. Reports from the compiled sites were selected based on criteria explained below. The sites compiled in Oehm and Hallet (2005) whose current average April/May temperatures (see explanation below) fell within an approximate range of the paleotemperatures of Mono Basin originally were published in: Rudberg (1964), Finlayson (1981), Mackay (1981), Gamper (1983), Smith (1988), Jahn (1991), Price (1991), Smith (1992), Matsuoka et al. (1997), Matsuoka (1998). The references are listed in Table 2.1 with corresponding climate zones and diffusivities. The compiled diffusivities were published as illustrating a relationship between latitude and diffusivity. The present study used the compiled findings to generate a transfer function relating κ values with temperature as a basis for relating past diffusivities with temperatures ascertained to have occurred in the past in the region of Mono Basin moraine. The transfer function also included the current diffusivity measured for Mono Basin moraine as a data point. The purpose of using a transfer function was to broadly quantify the temperature and diffusivity relationship in the presence of a scattered set of points with each based on non-uniform methods and landforms. Use of the function provided uniformity to the application of the relationship.

Table 2.1. Selected References Compiled in Oehm and Hallet (2005) for Diffusivities

Location	Lat	Lon	Climate Zone	k-min	k-max	Reference
Mackenzie Delta, Garry Is, NWT	69.50	-135.71	subpolar-polar	1.19E-01	1.19E-01	Mackay (1981)
Tarfala Valley, Sweden	67.92	18.60	subarctic-alpine	2.00E-04	8.23E-02	Jahn (1991), Rudberg (1964)
Ruby Range, Yukon Territory	61.74	-137.59	subarctic-alpine	4.80E-03	3.63E-02	Price (1991)
S. Rockies, Mt. Rae	50.66	-115.20	temperate	1.00E-04	1.10E-02	Smith (1988, 1992)
Engadine Valley, Switzerland	46.50	10.00	subarctic-alpine	3.00E-04	4.70E-03	Matsuoka et al. (1997), Gamper (1983)
Karkonosze Mts, Poland	50.79	15.60	temperate	6.00E-04	9.30E-03	Jahn (1975)
Mt. Ainodake, Japan Alps	35.65	138.23	subtropics	3.60E-03	1.35E-02	Matsuoka (1998)
Mendips, UK	51.30	-2.73	temperate	7.00E-04	3.89E-02	Finlayson (1981)

By quantitatively relating diffusivity with temperature, the transfer functions were generated from the current global distribution of diffusivity measurements. A log scale for the y-axis (κ) of the graph was generated in Excel and the choice of function was selected by visual inspection of a line produced by a function that spatially divided maximum values equally. The function was exponential, but it does not reflect a numerical average or a minimal least square difference. The Oehm and Hallet (2005) work did not provide a formal assessment of a numerical correlation between latitude and diffusivity, but rather an observation about the spatial distribution of diffusivities. The authors suggested a subtle correlation, though not tight, between higher diffusivity values and higher latitudes. The function selected conformed best to that observation.

Paleotemperatures, starting with the age of the moraine to the current temperature reported in regional climate records, were then substituted in the transfer function to derive diffusivities occurring in the past. Because the present time was included in the overall chronology used in modeling, the diffusivities derived from transfer function also included diffusivities for the present time, which differed from those measured (further discussed in Discussion). The paleotemperatures were derived from halite fluid inclusions in the ephemeral lake sediment core of Death Valley, DV93-1, Figure 1.1, a 200 kyr proxy record that provided absolute temperatures at the times in the past (Lowenstein et al., 1999) that also correlated with evidence for glacial advances and retreats in the present study. Studies on the halite inclusions found that the maximum homogenization temperatures of salt crystallized in fluid inclusions in saline lakes conform to late April through early May air temperatures (Li et al., 1996; Lowenstein et al., 1998; Lowenstein et al., 1999). For this reason, only April/May average temperatures were assigned to the current locations compiled in Oehm and Hallet (2005). The relevant temporal portion of the plot relating maximum homogenization temperature from the Lowenstein et al. (1999) study is shown in Figure 2.5.

Glacial advance requires temperatures that accumulate enough snow to permit an alpine glacier to move down a mountain valley and thereby erode and deposit the sediment that will be deposited as lateral moraines. The ages of such preserved moraines The ages of such preserved moraines in the region of Mono Basin were taken as evidence for the times significant for temperature fluctuations relative to times for which there was other evidence of warmer conditions, such as the Mono Lake low stands (Benson et al., 1998).

Times at which salt homogenized were interpolated from uranium series ages of tufas dated on the eastern side of Death Valley, which provided the 200 ka paleoclimate

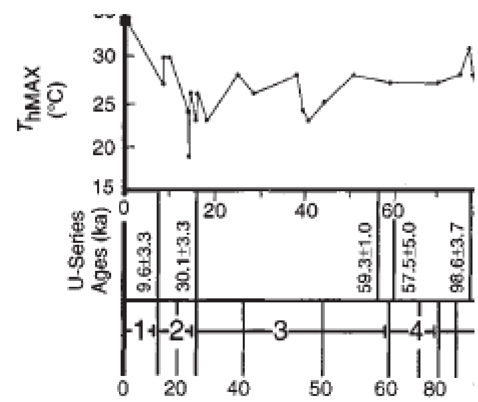

Figure 2.5. Maximum homogenization temperatures T_{hMAX} of halite fluid inclusions in DV93-1 and corresponding times (ka) (lower-most numbers) in the past from Lowenstein et al. (1999). Displacement with current value of 34°C was applied to current April/May average in Lee Vining, CA.

record. While Death Valley is over 400 km from Mono Lake, it is considered climatologically related. Mono Lake adjoins the northern edge of the Owens River catchment system, which was hydrologically connected to a chain of lakes that, during high stand, fed into Death Valley (Smith and Bischoff, 1997). Based on this shared drainage routing with Mono Lake and Owens Lake, the times of temperature changes, as indicated by the advance and retreat of glaciers in the eastern Sierra Nevada, are considered to have affected all the lakes in the drainage system. Therefore, the displacement between absolute April/May average differences of present air temperatures with paleo-temperatures at Death Valley were applied to current temperatures at Lee Vining, California given by the Western Regional Climate Center (WRCC, 2010). Paleotemperatures for Lee Vining, then, were derived and applied in the transfer function.

The air temperatures assigned to current locations cited in Oehm and Hallet (2005), from which the transfer functions were generated, were based on the average long term, from 1900 to 2008, mean air temperatures of April and May. These months correspond to the season from which the proxy temperatures were taken. However because the compiled sites did not include weather data, the long term mean temperatures were taken from reanalysis data through NOAA's Earth Systems Research lab, Physical Sciences Division, from the University of Delaware's global climate data sets (Matsuura and Willmott, 2010) (Figures 2.6 and 2.7). Reanalysis data is produced by integration of real time weather data by using climate models. Available station observations every 6-12 hours over the time period analyzed are used in the assimilation models. While specific data values are products of the model and are not real for a particular location, they are based on a systematic and consistent application of weather patterns derived from real data (Dee and Fasullo, 2014). Gaps in in coverage of local variability of air temperature measurements were spatially interpolated and corrected for elevation as explained in Matsuura and Willmott (2012). Recent, from 1981-2010, mean April and May temperatures and precipitation for Lee Vining and Bishop were taken from the Western Regional Climate Center (WRCC, 2010).

While long term monthly means for air temperature and precipitation are available for the most geologic recent times of approximately 100 years, comparable direct measures of absolute precipitation do not exist in the same way for the past 100 thousand years in the study area. States of precipitation are complex and sensitive to numerous factors. They vary between the land surface and subsurface, they vary seasonally, and with changes in temperature. For the purposes of the present study, which relied on a specific chronology based on the time scale that glaciers in the region would have advanced and retreated and for which moraine records were preserved, the paleo-temperature record was more effective for modeling hillslope degradation. The degradation effects from the kinds of precipitation states that might have coincided with the past temperatures were generated through the transfer function by application of the substitution method explained earlier. This means that whatever precipitation and its state accompanied the soil creep measured in the accounts compiled by Oehm and Hallet (2005) also coincided with an average April/May air temperature that was part of a climate state which, when integrated with the substrate cumulatively, resulted in a measured diffusivity.

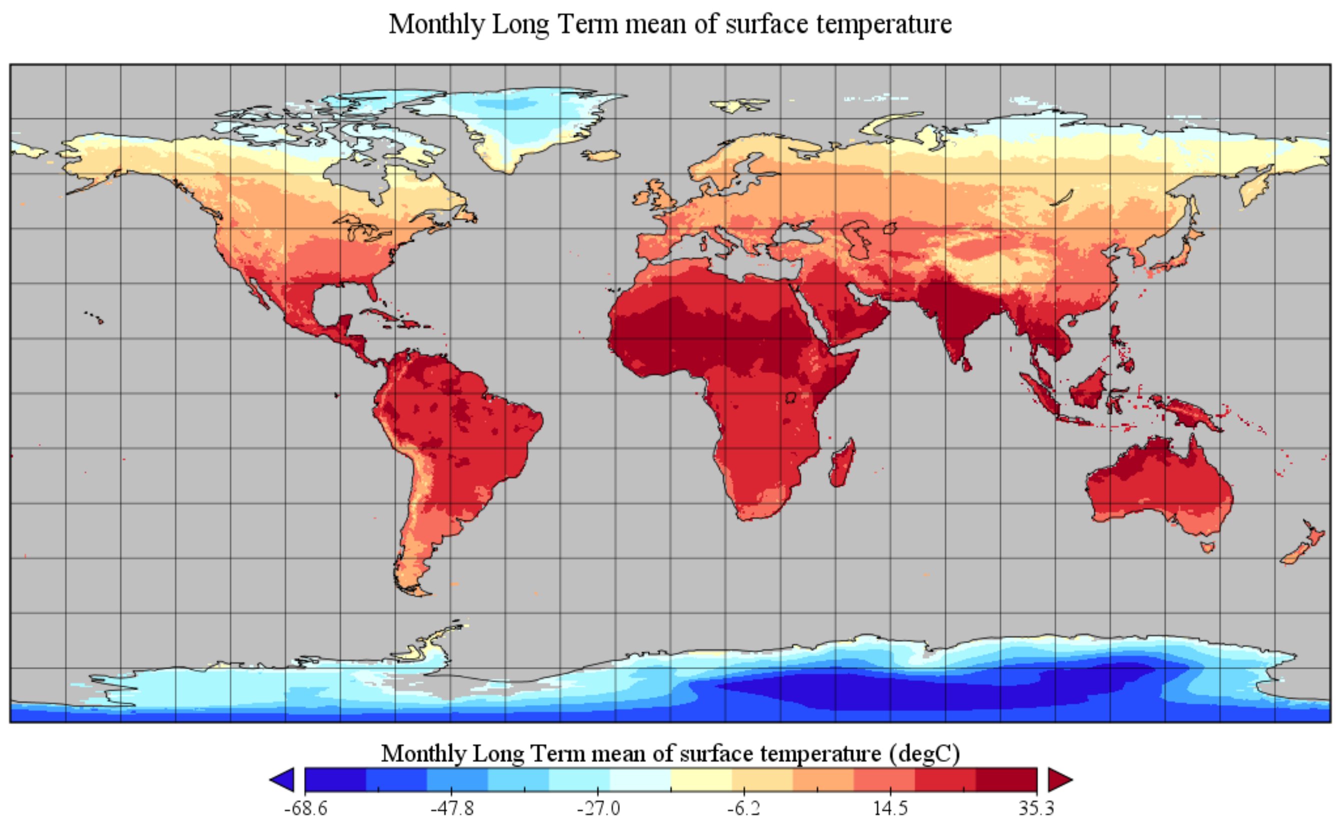

Figure 2.6. Long term April mean monthly temperature given as an example of a reanalysis map of long term global mean monthly temperatures for April for 1900-2008. Produced from University of Delaware's data set (Matsuura and Willmott, 2010).

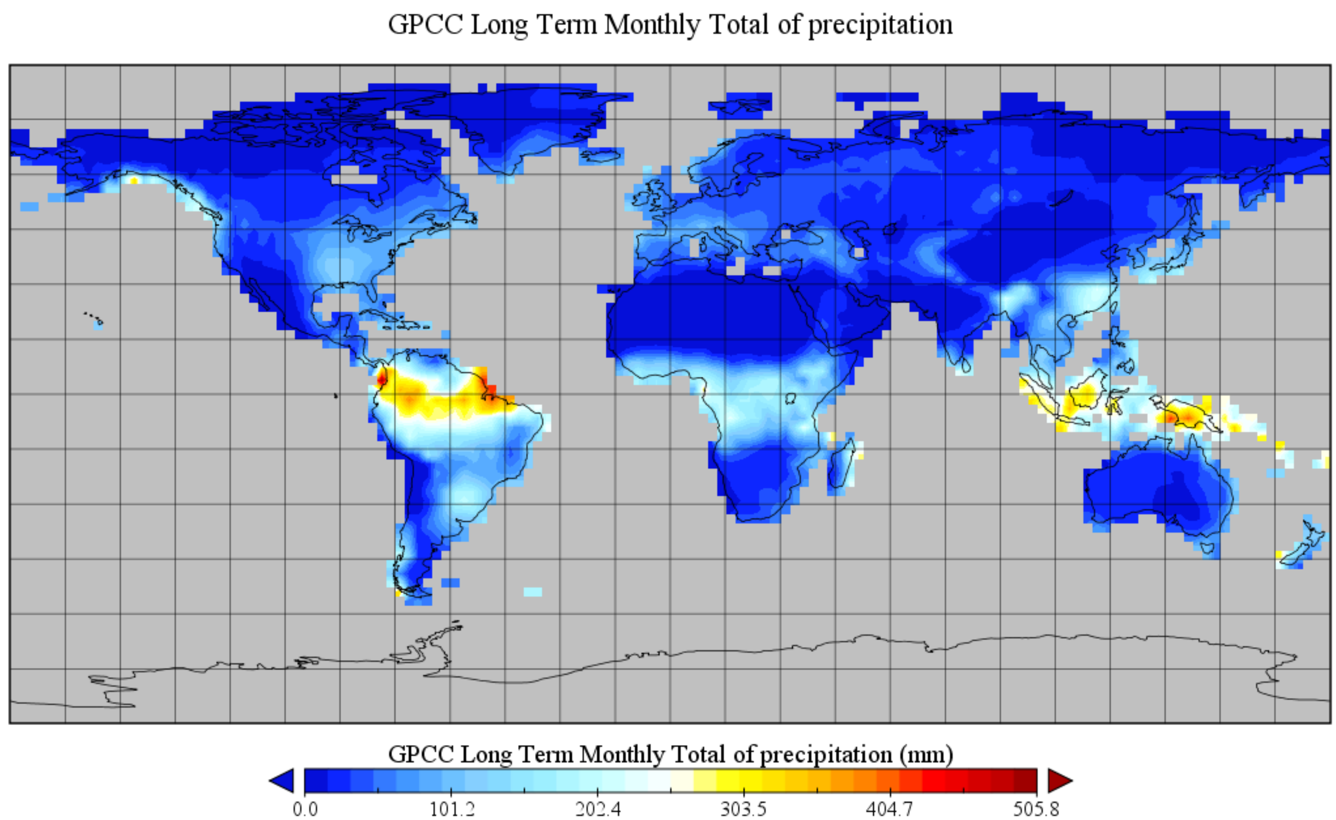

Figure 2.7 Long term April mean monthly precipitation given as an example of a reanalysis map of long term global mean monthly precipitation (mm) for April from 1981-2010. Produced from University of Delaware's data set. (Matsuura and Willmott, 2010).

Even though surface runoff is often considered responsible for sediment transport, it would not have accounted for all of the surface lowering that might have occurred in the past, particularly under climate regimes more comparable to periglacial or glaciated environments that the proxy records indicate. Also, the field of geomorphology considers the drivers of landscape change – climate, gravity, and heat generated inside Earth – interacting with resistance forces - lithology and structure of the geology - as the broader framework for understanding an Earth surface process such as degradation and quantifying erosion (Selby, 1993; Ritter et al., 2011). In this framework, the distribution of heat energy originating from the sun varies greatly with latitude (Ritter et al., 2011). This was the reason that Oehm and Hallet (2005) used latitude to organize topographic diffusivity measurements. Their study investigated global rates of soil creep, and they found certain latitudinal trends that were associated with temperature differences between the equator and the poles. The present study adopted the assumption and used the reanalysis data associated with geographic coordinates of the field sites where the diffusivities were recorded. Also, because precipitation here is assumed to be controlled by the same processes that distribute temperature, and patterns of precipitation generally follow zones of atmospheric temperatures (Ritter et al., 2011), it is assumed that the transfer function relating κ and temperature is acting to represent in a general way those combined conditions that would produce a certain range of diffusivities, assuming a constant substrate.

The temporal scale is stressed here because the specific chronology is employed for the purpose of illustrating the effects that past climates as they were tracked through times for which there is evidence of glacially driven temperature changes. The presence or absence of numerous factors may contribute to climate, from what are considered part of large spatial scale cyclic patterns, such as El Nino, and changes in atmospheric-ocean circulation patterns and sea surface temperature (SST), which have been modeled for climates in the past, such as the Miocene (23-5.3 Ma) and Pliocene (5.3 – 2.6 Ma) (Goldner et al., 2011). While important to consider, such models do not focus on how regional responses to ice sheet activity, for example, can affect a region's climate. As with all models, comparisons with physical bases are needed for them to be informative about physical features they are being purported to affect. Late Pleistocene megafaunal extinctions have been used in climate modeling to test the potential impact of biogeographic changes on the land-atmospheric CO_2 exchanges and the resulting effect on global climate, modeled in (Brault et al., 2013). However, the focus of the present study was not to examine the causes and effects of past climates. The focus, as part of geologic study, essentially was on a sedimentary record, not on a climate record. The climates were inferred from the use of the discussed proxy records and how they correlated with a glacial chronology obtained through published moraine ages that employed absolute age dates using geochemistry. In fact, the purpose of landscape evolution modeling, as practiced in the present study, is to understand something about how past climates, however they were generated and however they were expressed regionally, in terms of regional temperatures and precipitation, affected the land surface. So, a physical basis was employed through substitution and related to past temperatures by means of a chronology to propose physically based degradation model as an improvement over a degradation model based on a constant parameter optimized to fit a shape and morphology, not to track the variability in form over time.

Although a landscape, or a landform, evolution model is not a climate model, it depends on climate-based parameters and, as the present study argues, how those parameters might have varied in the past will affect our understanding of how Earth's surface has changed and can change in the future if those parameters change. As a geologic study, use was made of sedimentary records and glacial chronologies, but it did not rely on results from climate modeling, except for the reanalysis data, for the purpose of assigning locally relevant temperatures to locally measured diffusivities. Climate models that have been generated and cited in the field of geomorphology and that incorporate physical based parameters include Hostetler and Benson (1990), Hostetler and Clark (1997) who used coupled modeling. Examples of such parameters include glacial mass balance or lake level stands and the temperature and precipitation required to achieve those measures that correlated with evidence of past glaciations or with lake sediment cores. However, the objective of the present study was to show a legitimate physical basis for variable diffusivities through the course of time for which landform degradation was modeled. The focus was on how sediment transport rates could have varied through time on a scale relevant for exploring the effects of past climates as the results of past glacial times. Although many might have speculated that they had varied, and even varied as result of past climates, a physical basis had not been shown. Future work may involve improvements on parameterizing κ. Other, more focused work, might employ coupled modeling of temperature and precipitation with specific processes or with specific kinds of landforms.

Qualitative assessments of climate also often are made with proxy records, such as vegetation speciation, which is both an important climatic indicator and a significant factor in surface processes. Past climates are often interpreted with the use of regional pollen records. Two well documented lake cores in the region from Owens Lake (OL-92) and Searles Lake (LDW-6) are referenced in literature on the topic for their age controls and length of record and their correlation has been used for interpreting late Quaternary climate signals in the region, and their locations are shown in Figure 1.1 (Smith and Bischoff, 1993; Litwin et al., 1997; Litwin et al., 1999).

In the eastern Sierra Nevada, lake sediment cores have been correlated intra-regionally with other sediment cores and paleobotanical records on the basis of organic and inorganic material (Heusser, 1995; Koehler and Anderson, 1995; Litwin et al., 1997; Heusser, 1998; Litwin et al., 1999; Mensing, 2001; Street et al., 2012), as well as globally, such as with ice cores and ocean sediment cores, in order to assess the timings of climate changes and events that might have triggered them (Adam et al., 1981; Benson et al., 1998; Bischoff and Cummins, 2001; Woolfenden, 2003; Potito et al., 2006; Jimenez-Moreno et al., 2010). For this reason, also, relative vegetation zoning patterns found in the pollen records are used to further qualitatively support temperature changes over certain past time intervals.

Previous climate reconstructions based on pollen assemblages compared modern analogues to lake core sediments (Adam et al., 1981; Mensing, 2001; Woolfenden, 2003) or to packrat middens (Koehler and Anderson, 1995) and used radiocarbon to date the changes in assemblages. Published literature on vegetation change related to past climate cycles contain overlap on distinctive patterns and types: cold glacial phases are characterized by maximum TCT (*Taxodiaceae, Cupressaceae, and Taxaceae)* – pollen grains, typically of juniper, combined together due to difficulty in distinguishing the different taxa; cool transitional times are associated with Greasewood (*Sarcobatus),* big sagebrush (*Artemisia*), and oak (*Quercus*); and warm (interstadials) by increase in pine pollen frequency (Litwin et al., 1999). Important to note is that vegetation continued to adapt individually and as communities as climate changed, so quantifying frequencies of pollen occurrences and using modern analogues is limited as a method for relating temperatures and precipitation to past time intervals. Present day assemblages are only a consequence of adaptive and dynamic interactions to past environments; they are not especially indicative of a particular temperature (Tausch et al., 1993; Woolfenden, 1996). For this reason, proxy records that could only provide relative comparisons with other records were used to support the temperatures derived from the maximum homogenization temperatures of the halite fluid inclusions from the Death Valley core that were applied in the transfer functions.

In order to model degradation with temporally-varying diffusivities, specific times were used through which a given κ would run. As given in Table 1.1 and explained earlier, the time periods were based on the latest revised ^{36}Cl dates of moraines in the region (Phillips et al., 1990; Zreda et al., 1990; Phillips et al., 1996; Gillespie and Zehfuss, 2004) as well as on recent calibration and error analysis limits cited earlier. They were assumed to represent times of glacial advances starting with Mono Basin moraine and followed by revised age dates for other moraines in the region. Published dates for Mono Lake low stands (Benson et al., 1996; Benson et al., 1998), based on $\delta^{18}O$ of low-magnesium calcite of Mono Lake sediments from the Wilson Creek Formation, Mono Basin, CA and ^{14}C dating of Owens Lake Core OL-92, are assumed to reflect short periods of warming and glacial retreats. Boulder erosion can complicate ^{36}Cl and may decrease its concentrations thereby causing younger apparent ages. Regional boulder erosion rates were published after the revised published dates for Mono Basin moraine, and so the age of 85 ka was used in the degradation modeling based on recalculation with 3.3 mm of boulder erosion using the CRONUS ^{36}Cl Exposure Age Calculator (Phillips et al., 2009; Marrero et al., submitted 2014).

CHAPTER III

DATA

3.1 Overview

The present study examined sediment transport on a naturally occurring landform in order to quantify sediment mobility as the cumulative effect of climate on the substrate. Direct measurements of regolith transport using sediment traps, pebble lines, repeat photos, and terrestrial LiDAR were collected and recorded in 2011, with the field apparatus installation, described in Methods, made in 2010. Laboratory experiments, while better able to establish controls, are less able to characterize natural environments. Optimal physically based landscape models can only be substantiated by field data and understanding of field processes (Tucker and Hancock, 2010).

The methods applied in the present study, although not new by themselves, were synthesized to integrate the resulting data in a novel way for the field of landscape evolution modeling. Volumes of regolith were used for calculating diffusivities. Transport distances were used to characterize the contribution of various regolith sizes to erosion and degradation of the hillslope. While the data reflects smaller areas than the catchment-size scale landscape models have used, the data also reflects measures of actual processes. Published records of paleo-temperatures, both absolute and qualitative, were organized according to time periods noted in the literature. The collected data were quantified in ways described in Chapter II, Methods. However, present and paleo-ecologies were identified and associated with published data on the basis of relative climatic trends with related vegetation records. Although the current diffusivities were calculated for the field sites in the present study, the diffusivities used in modeling were derived from a transfer function that also included as points the current measured diffusivity and corresponding average April/May temperature for Mono Basin.

The substitution method described in Methods and the use of proxy records were used as a first attempt in landscape evolution modeling to relate field based data and sediment transport processes to a degradation model. Use of the method was not intended to establish one-to-one correspondences between past and present processes or parameters. The application used parameters based on the occurrence and rates of surface processes measured to have occurred naturally and to relate them to modeling similar processes and rates in the past on the basis of a reasonable point of comparison, with that being temperature. How temperature was considered to relate to surface processes has been discussed in earlier chapters. However, such parameterization could be further refined and improved, and that is the task of field based modeling.

3.2 Paleoecologies

The present vegetation in Mono Basin was compared with paleo-pollen records to provide a qualitative framework to check against the changes in climate that were based on quantitative records. The current vegetation on the eastern slopes include uppermontane sub-alpine forest (*Abies-Pinus)* with Red Fir at lower elevations, dense graminoid communities (grasses) that decrease in height to 10 cm with decrease in elevation, and sagebrush steppe (Barbour and Major, 1977). The primary vegetation on the moraines is sagebrush. Bare earth patches with varying densities of grasses occurred regularly between the sagebrush. The above described vegetation conditions are assumed typical for what is considered the warm dry pattern beginning with the last interglacial at the start of the Holocene 10 ka, as noted in Chapter 1.3. This vegetation pattern is often inclined to higher pine frequencies and contrasted with colder wetter times of glaciations when juniper prevailed, or with cooler transitional times associated with sagebrush (Litwin et al., 1999).

3.3 Sediment Flux

Regolith transport rate, or sediment flux, is an essential element in calculating the topographic diffusivities for the moraines. The bulk mass of the regolith as well as of the various grain sizes sieved from the samples – fines, granules, and pebbles - were measured. Table 3.1 lists the data associated with sediment trap samples (ST): GPS locations, slopes, and masses. Slopes represent the general hillslope over several meters upslope and downslope from the trap. Sediment traps were installed at all sites. The flux transported into the traps was assumed to represent the regolith transport of the hillslope, and so ST samples were used to measure the present day κ values of the region. In addition to measuring the volume of flux, comparative assessment was made between the relative proportions of grain sizes that the surface is composed of and of the relative proportions in a transport year, inferred from sediment trap collection and the sieved quantities of the grain sizes. This comparison provided some indication of the sizes that moved too slowly to have been transported into the trap at the end of one year and how this compared with sizes measured in the repeat photos. Such data provides compositional characteristics of the mobile layer and how it moves. Figures 3.1-3.4 plot the relationships between grain sizes and their bulk masses collected in the traps and sampled at the surface. Comparisons of the graphs between the sediment trap samples and the surface samples indicate that 50 mm -140 is a significant size range, because it

Table 3.1. Sediment Traps ID, Location, Slope, Mass

	GPS coordinates decimal degrees			
ID	N	W	Slope (°)	Mass (g)
ST-MB-1-2010	37.909	119.124	26.2	360.4
ST-MB-2-2010	37.9091	119.124	20.9	45.1
ST-MB-3-2010	37.9014	119.131	22.0	308.4
ST-MB-4-2010	37.9015	119.131	17.0	86.5
ST-MB-5-2010	37.8974	119.131	26.2	52.8
ST-BC-1-2010	Missing	Data	15.0	261.5
ST-BC-2-2010	37.3207	118.513	19.0	91.7
ST-BC-3-2010	37.3204	118.514	19.0	2278.1
ST-BC-4-2010	37.3257	118.517	8.0	79.3
ST-BC-5-2010	37.3257	118.516	0.5	57.9

ST = Sediment Trap; MB = Mono Basin; BC = Birch Creek

appears in the surface samples, but the appearances of sizes within that range vary in their proportions in the sediment trap cases when compared with the surface samples. In the younger Tahoe moraine the significant size that is represented at the surface, but not in transport, is 140 mm. The plots also show that the bulk mass of fines is higher than the bulk mass of other grains smaller than 50 mm in the surface samples. Also in the sediment traps, while the bulk mass of fines never reached the amounts of that in the surface samples, the bulk mass of fines in the traps were higher than the bulk mass of the

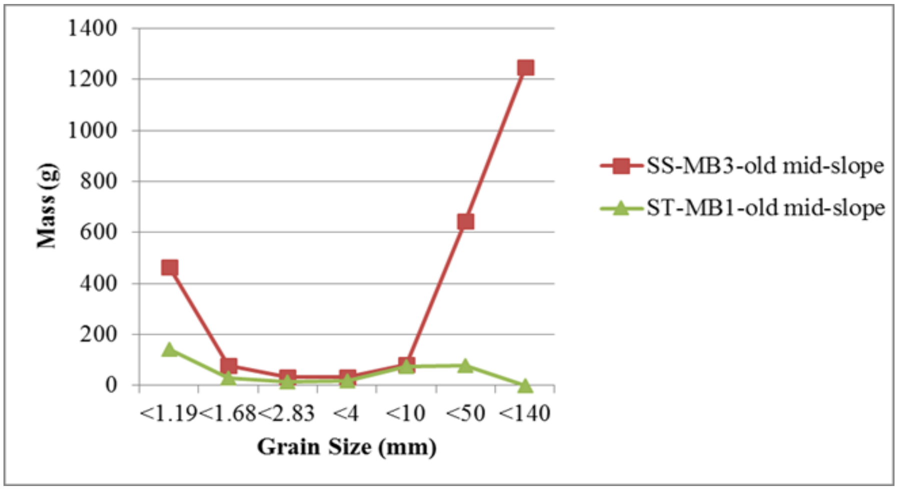

Figure 3.1. Mid-slope ST (sediment trap) sample and SS (surface substrate) sample bulk masses of grain sizes collected on Mono Basin moraine. Comparisons between bulk masses of fines and 50 mm and higher in the SS and ST show that 50 mm is a significant size that distinguishes what is mobilized downslope in one year and what is moving at a slower rate or remaining stationary.

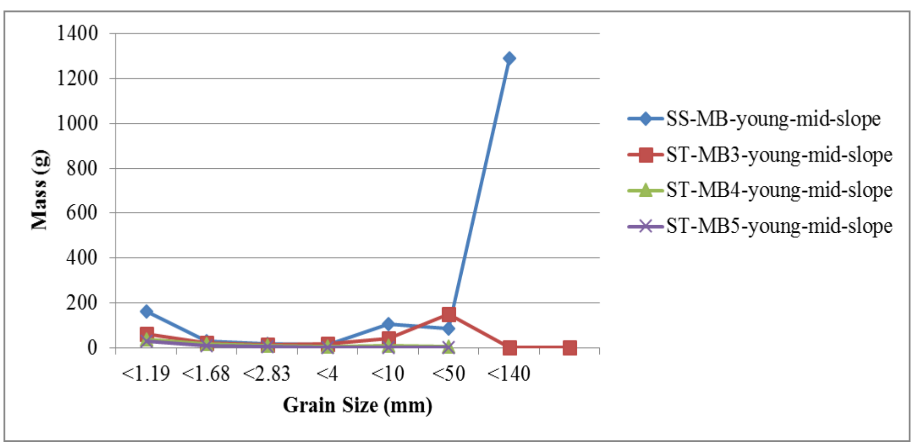

Figure 3.2. Mid-slope ST (sediment trap) sample and SS (surface substrate) sample bulk masses of grain size fractions collected on Tahoe moraine. Bulk mass for fines and pebbles in both SS and ST are higher than sizes between them and 140 mm is the significant size represented at the surface, but not in transport.

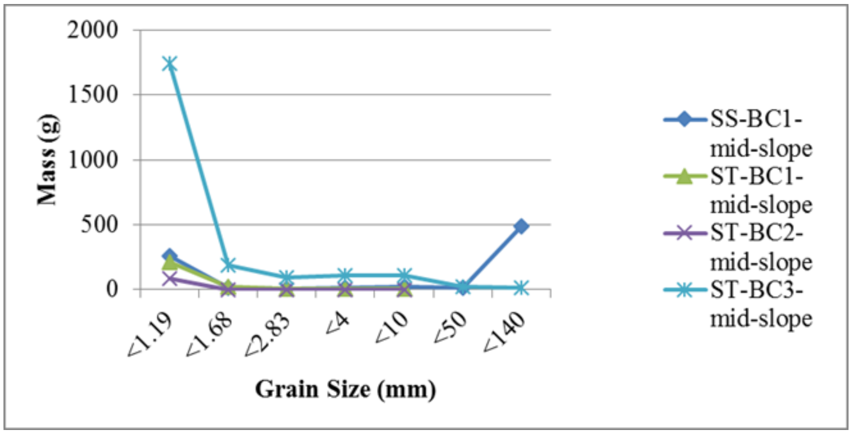

Figure 3.3. ST (sediment trap) and SS (surface substrate) from Birch Creek moraine 1. Fines represent the majority of bulk mass in annual flux. ST sample exhibited similar relationship of a higher representation of fines 1.19 mm and less as the other ST sample at BC 1. 10 mm – 140 mm were represented at the surface.

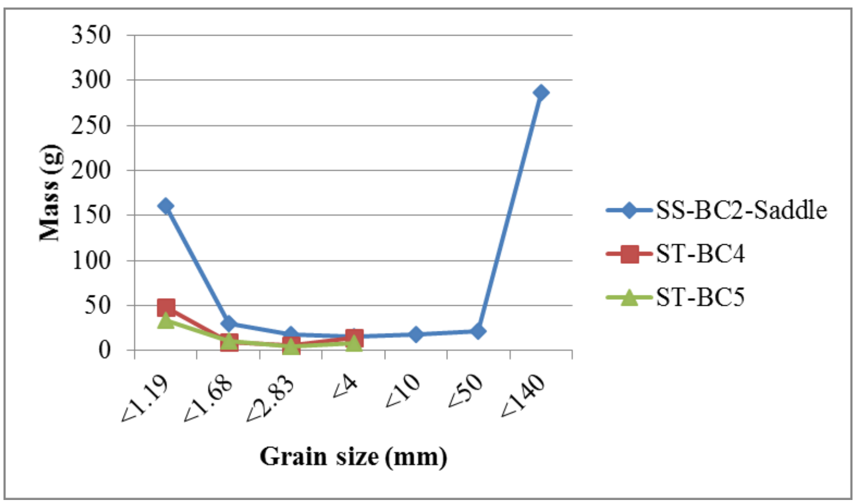

Figure 3.4. Mid-slope ST (sediment trap) sample and SS (surface substrate) bulk masses of grain size fractions collected on Birch Creek moraine 2 (~0.6 km northwest of BC moraine 1). Fines (<2.83 mm) represent the majority of bulk mass in annual flux. Proportions of regolith transported is similar to proportions in surface substrate, except that the surface substrate had a higher proportion of 140 mm or higher.

other sizes smaller than 50 mm. If the fines are indeed moving at a faster rate during transport events, this would explain their representative proportions in the surface samples and in the traps. Other factors might explain their occurrence as well. For example, the substrate could have higher percentage of fines, giving a higher probability that more would enter the trap and that more occur on any point on the surface at any point in time than other sizes smaller than pebbles.

Further in depth analyses of sediment size and their relative proportions and masses were not performed for this study. The data was interpreted as suggesting that, in general, regolith in annual flux in the region sampled in sediment trap collections resembled surficial composition of the hillslope for sizes from fines to 10mm to 50 mm (depending on the moraine). However, the components of the mobile layer of regolith are not moving at the same rates between the moraines. The regolith sizes in the mobile layer are moving at different rates between the older Mono Basin moraine and the younger Tahoe moraine. Therefore, the relative proportions of material in annual flux for a mixed granular till in a comparable arid to semi-arid climate depends largely on transport rates of grain sizes ranging from fines to large pebbles, which are the sizes with the highest percentages represented in flux in this study. Specific percentages depend on additional factors. Moraine age may be one factor in addition to other local differences that were not investigated in the present study. The relevant point is that the mobility of the surface is determined by the transport rates of grain sizes fines through 50 mm when they have a free path to move. Whatever climatic conditions produce events capable of moving these sizes, besides the hillslope gradient, are the predominant factors controlling sediment transport and hence degradation. Such factors are likely surface wash and snowmelt runoff in the present climatic regime. However, variability of past diffusivities would support the occurrence of variability of predominantly controlling factors on sediment transport. Future studies could advance the topic by quantifying the various contributions of such processes to annual sediment transport, perhaps by investigating in greater depth particular processes, their associated climates, and their mechanics.

The rates of movement will depend on the cumulative effects that the results of the climatic conditions have on the substrate. Such effects include infiltration and compaction, which effect the mobility of the grains. Certainly vegetation density is a factor that could hinder transport, and it also results from climate, but it is not a primary control on regolith mobility; it is a secondary factor in overall transport. Mobility was the feature of the hillslope surface that the present study was investigating. A more in depth study of the sediment transport would include measures of all the above mentioned features, how they change over the year, and the surface activity, which may be monitored with weather stations and specified control points.

As part of the overall objective of examining relationships between climate and sediment mobility, the transport data measured in the present study was related to average April/May temperatures given by the Western Regional Climate Center for Lee Vining. Because transport rates also depend on climate as well as slope, the data reflects the current climatic regime. The current climate overall, occurring in an interglacial time (Holocene), is interpreted as warm and dry as compared with glacial times, as referenced in section 1.3. The current climate of the region is considered semi-arid alpine (Barbour and Major, 1977; Litwin et al., 1999), with an average of ~40 cm/yr of precipitation with the majority, ~35 cm, as rain (NOAA, 2014). The assumption that rain is the primary transport agent in this climate, by generating surface wash, is consistent with the professional literature (Selby, 1993) and with the field observations that indicated a range of grain sizes in annual transport that included fine sand through pebbles (Figures 3.1-3.4). Their annual transport on slopes that averaged 20°, as exhibited in the sediment trap samples and the average distances traveled by pebbles in the pebble line, was assumed to be explained primarily by surface wash.

3.4 Transport Distances

Regolith transport rates were used to characterize degradation of the hillslopes. A travel distance curve relates grain size, as defined by the intermediate axis of regolith, and the annual distance measured to have been travelled by that size. The densities of the various regolith size fractions are assumed to be the same, so their intermediate axis size is the variable tested with respect to their transport rate. Pebble travel distances that were measured from pebble lines (PB), as well as those measured through photo analysis, were compiled in a graph of travel distance curves (Figure 3.5). Included also are travel distances theoretically extrapolated for the fines in the study as noted in Methods, Chapter 2.

The shift between curves correlates with different slope angles on which pebbles were measured. Published data from earlier work in a semi-arid environment (Kirkby and Kirkby, 1974) are shown by curves interpolating red-colored data points, which show overall lower transport rates than the curve interpolating the other colored data points. However, as the legend shows, the shallower slopes are associated with lower transport rates. On steeper slopes occurring in the present study, pebbles travelled at higher rates.

The trend lines generated in Excel were power equations for all the curves. The green points identified as “observed pebble travel,” were all recorded with lower rates than the pebbles measured from pebble lines. One reason could be the observed pebbles had been left in their natural place and reflect original motion, whereas pebble line pebbles, although representative of the size of pebbles at their location, had been hand-placed along a pebble line. A proposed explanation is that the pebble line pebbles experienced less initial resistance to removal and travelled further in the same time.

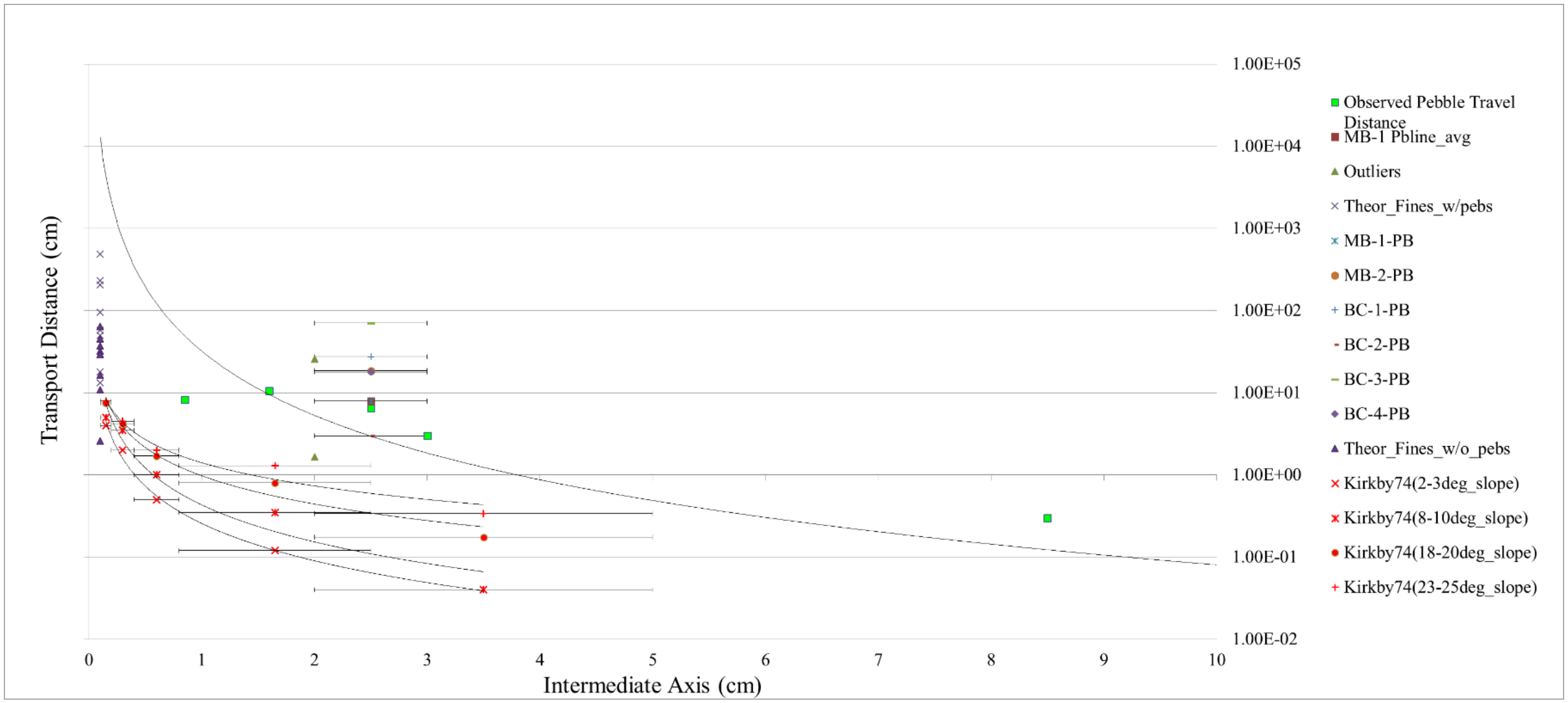

Figure 3.5. Rock size (intermediate axis) versus travel distance curves. Power laws best express the relationship between grain size and transport rate, further supported by published data for transport in a similar climate. Observed pebble travel (green square) were measured from photo analysis and pebble line averages. Data from Kirkby and Kirkby (1974) reported lower slopes show corresponding lower transport distances.

3.5 Topographic Change

A second element in surface characterization is the rate of surface lowering. As such, transport rates and sediment flux may be compared with landform degradation. For the purposes of physical based modeling, data from sediment flux was compared with average topographic change – gain or loss – measured at a surface. The average of difference between the terrestrial LiDAR repeat scans was calculated and modeled (Figure 3.6). In the figure, the color bar indicates where sediment was added in deposition or lost in erosion in the first year.

Visual inspection of Figure 3.6 also offers some insight into how sediment was transported. The difference overlaid on the first year's topography shows that material is being deposited or "filling in" micro-lows in a pattern that crosses the downslope direction, suggesting transport is down slope as well as across slope. This cross-grading has been attributed to the formation of rills, micro-channels with cross-sections of a few centimeters to a few tens of centimeters, typically obliterated between storms and with parallel rills becoming integrated and draining into a deeper rill (Selby, 1993). Cross-grading has been considered as a process that accompanies surface wash. Such a process suggests that the mobility of regolith on this landform was primarily controlled by the cumulative effects of climate on uppermost surface of the mobile layer. This contrasts with mobility that could occur as a result of freeze-thaw conditions occurring within 30-50 cm beneath the surface and which is more common in colder or periglacial climates. A more complete study in the future could investigate the variety and predominance of patterns of surface transport and what they suggest about surface processes and degradation rates.

Because sediment transport data from this study are comparable with published sediment transport data in Kirkby and Kirkby (1974), and the evidence from field data shows that transport processes appear to follow trends that are typical for a semi-arid climate indicated in Selby (1993), diffusivities calculated for the site were assumed to be reliable for an annual time scale at the present time for the current climate. Although certainly the inclusion of more years would have provided a more comprehensive characterization of the mobile surface in the present climate.

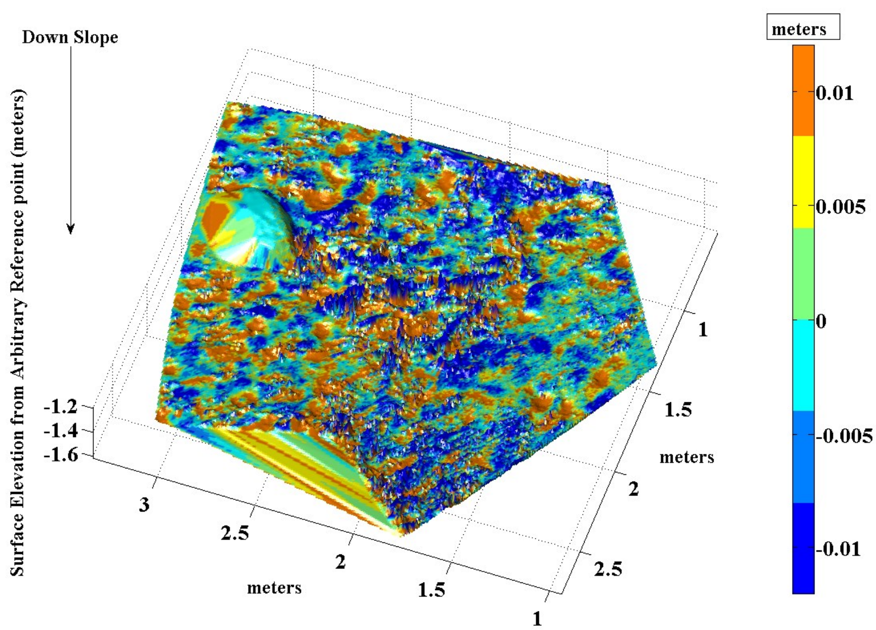

Figure 3.6. LiDAR surface (2010) of Mono Basin moraine with annual scan difference superimposed. Difference is superimposed on first year's surface. Positive values on the color bar are areas of addition or deposition; negative values areas of removal or erosion. The average difference was calculated of the combined loss and gain as 2.65 mm/ m^2.

3.6 Space-for-time Substitution

Data were compiled from published accounts of proxy temperature records for use in the space-for-time substitution method used to model hillslope degradation with different scenarios for diffusivity. The scenarios relied on 1) published diffusivities measured globally and used to generate transfer functions from which diffusivities related to past climates in the region were derived, 2) documented surface exposure ages, and 3) absolute proxy records of paleo-temperatures occurring during the recorded times.

Time periods used for establishing when a different range of diffusivities would be selected from in the program were based on glacial advances and retreats reported in the literature (Gillespie and Zehfuss, 2004). The time periods were assumed to represent the effects of a change in regional temperatures, as evidenced by dated glacial deposits. Published data from Mono Lake core sediments that showed two significant low stands, suggesting a climate warm enough or dry enough to cause enhanced lake evaporation, were also used for selecting times of glacial retreats (Benson et al., 1998). These time periods, then, were used to select temperatures for which halite inclusions from DV93-1 (a sediment core from a perennial saline lake in Death Valley) have been identified. The method for transferring the displaced temperatures has been explained in Methods.

The laboratory studies of halite inclusions exhibiting maximum homogenization temperatures of the brine from which halite crystals formed, which equilibrated with air temperature, supported correlation of the paleotemperature record from the last 100 ky in Death Valley with other proxy records in the Great Basin, as well as another continuous proxy climate record for the past 160,000 years in the Vostok ice core (Lowenstein et al., 1998; Lowenstein et al., 1999). So by correlating the difference between the current air temperature and the homogenization temperatures at Death Valley with the present air temperature at Mono Basin, the paleo-temperatures of the Mono Basin area were derived and used in the transfer function. When the transfer function was applied and minimum and maximum κ values generated for the paleo-temperatures, paleo-κ values were generated for the time intervals when there were known glaciations in the region.

Table 3.2 summarizes the times compiled from published sources giving the latest revisions and the temperatures adjusted to the Mono Lake region from the Death Valley drill core (DV93-1), as explained in Methods 2.7 and summarized above. The additional qualitative climate records provide supporting evidence for the timing of past changes in glacial activity and associated climate changes. The qualitative records were taken from regularly referenced sources often cited in paleoclimate research in the region for the time under study. The times and the corresponding paleo-temperatures were the values employed in generating final degradation models that could be compared with degradation models using three different κ values based on 1) past climate change, 2) evolution based on an optimized value that closely approximates the current moraine profile, and 3) measured diffusivities of the current landform from the present study.

Table 3.2. Compiled paleo-temperatures and associated glacial chronology with supplementary proxy records

Event[1]	Time[2] (ka)	End[3]	T(°C)[4] T_{hMax} salt inclusion	Rock Flour %[5]	T (°C)[6] from Pollen (modern analogues)	Qualitative from Pollen[7]	Vegetation Record[8]
Present	0	0	9.5	30			
Recession	13		5.2		7.5		
Transition	15		4	65	4.5	transition	reversal to pine expansion
Tioga Start	25	20	-5.5	70		full glacial (26 -23.5 ka)	juniper increase (20-25 ka)
ML LS 3	27		2	65			
Tenaya	32		0.5	40		warm interstadial	
ML LS 4	34		1.5	30.5			
Tahoe II	50	42	1	75			
Mono Basin	80	60	3	20-50.5			decrease in pine

[1] Glacial events cited from Gillespie and Zehfuss (2004), ML LS (Mono Lake Low Stand) cited in Benson et al. (1998) indicate warming and glacial recessions in the region. [2] Times (ka) are given as cited maximum start times and [3] some of the end times of ranges based on ^{36}Cl exposure age dating (Phillips et al., 1996; Gillespie and Zehfuss, 2004). [4] Homogenization temperatures of salt inclusions from Death Valley 93 -1 sediment core (Lowenstein et al., 1999) at maximum age shown in [2]. [5]Rock flour % indicative of glacial advances at maximum times given in [2] (Bischoff and Cummins, 2001). [6] Modern pollen analogues used to infer paleo-temperatures (Mensing, 2001). [7] and [8] inferred from multiple sources cited above and used to describe relatively timed glacial landscape ([7]) and vegetation ([8]) features. Pine/juniper frequency ratios are used to infer warming or cooling, where higher pine occurrence is associated with relative warming and higher juniper with relative cooling (Litwin et al., 1997; Woolfenden, 2003).

CHAPTER IV

RESULTS

4.1 Overview

The main objective of the present study was to show with numerical modeling relative effects of past climates on landform degradation using Mono Basin moraine as a case study. Numerical modeling provided a means for quantifying regolith erosion rates and, by chronological association, the possible effects of global climate change on hillslope degradation. To stress, however, the purpose was not to propose particular erosion rates or κ values for certain times in the past. The purpose was to provide a physical basis that could be quantified for variability of past degradation rates that a constant diffusivity parameter could not be relied upon to express.

The model that describes the hillslope degradation is based on a diffusion equation. The parameter, κ, in the hillslope diffusion equation that expresses the effect of climate interacting with substrate on hillslope degradation was derived for the present time in the eastern Sierra Nevada. The cumulative effects occurring in the geologically present interactions between the climate and substrate were assumed to produce the surface processes from which sediment transport measurements were recorded and calculated. However, the complex physical and chemical processes that cause various surfaces to degrade under certain climatic regimes or erode in certain ways were not the focus of this study. Current records of global climates and published values of topographic diffusivity were used to compare and analyze what could be discerned about past climates from proxy records in the study region.

4.2 Current Sediment Transport and Diffusivity

As noted in the Methods section, observations and data collected from the field sites were made in order to characterize the sediment transport of the mobile surface. The point in doing this was to assess whether use of the methods could produce data that reflected sediment transport. While no single method could be used to ensure an expected standard rate, using multiple methods that could measure the travel distance of similar sized regolith, for example, provided a means for assessing whether the data could be used as reflective of the surface mobility. Additional comparison with published rates using a similar method, in a similar climate further supported the relevance of the data.

Sediment traps, pebble lines, repeat photos, and repeat scans from the terrestrial LiDAR were used to measure how regolith transport contributed to topographic change in terms of flux, transport distances, and surface lowering, or erosion. Current diffusivities, derived by calculating volumes of sediment flux, pebble frequency, and erosion were used to quantify sediment transport and to calculate a current diffusivity value for use in generating the transfer function. Table 4.1 lists the calculated volumes and diffusivities for each site where the data was gathered for each method.

Table 4.1. Compiled calculated volume, erosion, and diffusivity

ST_{BLK}	V_{ST} (m^3)	V_{PBL} (m^3)	V_{RPT} (m^3)	ER_{LDR} (m^2)	$\kappa_{(ST)}$ (m^2/yr)	$\kappa_{(PBL)}$ (m^2/yr)	$\kappa_{(RPT)}$ (m^2/yr)	$\kappa_{(LDR)}$ (m^2/yr)
MB-1	1.84E-04	3.71E-04	3.27E-05	2.65E-04	4.36E-03	1.08E-03	3.27E-05	4.57E-03
MB-2	2.30E-05		1.43E-04		3.53E-04		1.43E-04	
MB-3	1.58E-04	1.75E-04	4.91E-05	2.25E-03	3.18E-03	4.29E-04	4.91E-05	6.11E-04
MB-4	4.42E-05		4.91E-05		1.18E-03		4.91E-05	
MB-5	2.70E-05	7.36E-05	8.91E-06	2.61E-01	4.47E-04	1.73E-04	8.91E-06	2.40E-02
BC-1	1.23E-04	1.50E-04	2.67E-05	2.09E-03	4.07E-03	4.34E-04	2.67E-05	7.28E-03
BC-2	4.32E-05	8.92E-04			1.11E-03	3.22E-03	1.08E-04	
BC-3	1.07E-03		1.08E-04		2.76E-02			
BC-4	3.74E-05	1.76E-04	4.57E-05	4.69E-03	2.35E-03	4.47E-04	4.57E-05	1.32E-02
BC-5	2.73E-05				2.76E-02			

MB= Mono Basin; BC=Birch Creek; V=volume; ST= sediment trap; PBL=pebbles; RPT=repeat photos; LDR=LiDAR; ER= erosion; κ=kappa;

The κ values from Table 4.1 were derived through use of the sediment transport law where the volumes of regolith were calculated from each method.

Uncertainty analyses for measurement related to Mono Basin moraine are shown in Table 4.2. Upper-lower limits of κ, based on the uncertainty of each measurement, are shown in the table. Also shown are percent of relative uncertainties for each measurement and their propagation calculated from the square of the sum of squares of each uncertainty (Deardorff, 2000). Only the largest relative uncertainty is shown for repeat photos because when a relative uncertainty is significantly higher the propagation of uncertainty is approximately equal to it. The relative uncertainty for slope was shown to be much smaller in the other methods. The primary uncertainty for the LiDAR data was the distance between the scanner and the point measured which gives the elevation at a point, so it is shown as the only relative uncertainty for that method.

For the purpose of illustrating the typical uncertainty for each method and the effect on κ, the propagated uncertainties of the methods measuring sediment transport rates for Mono Basin moraine were applied to the calculated κ values at all sites where measurements were taken (Figure 4.1). The small uncertainties reflect that the margins of error for the measurements with the apparatus used were not large sources of error. The use of photos to determine a volume of pebble size regolith had the highest uncertainty because the pebbles selected in the photos were 2-3 cm, so each measurement included in equation (1.2) had up to 1 cm of uncertainty. Equation (1.2) that used pebble frequency to calculate a volume q used an intermediate axis of 2 cm. Error could be reduced in future studies if more accurate measures were recorded and used in each application of the equation.

Table 4.2. Bounded and % of relative uncertainties of κ and methods

	Bounded Uncertainty κ	% Relative Unceratainty
ST		
Box Opening	3.71E-05	8.33E-01
Scale Measure	1.24E-06	2.77E-02
Slope	2.53E-05	2.77E-02
		9.86E-01
ST_{PB}		
Box Opening	3.71E-05	8.33E-01
Slope	1.88E-07	5.26E-01
Scale Measure	1.21E-07	3.65E-01
		1.05E+00
RPT		
Slope	1.88E-07	
Size	1.54E-04	
		5.00E+01
LiDAR		
Distance	4.99E-01	
		2.54E-01

ST=sediment trap; ST_{PB}= sediment trap pebbles; RPT=repeat photos; LiDAR= terrestrial LiDAR

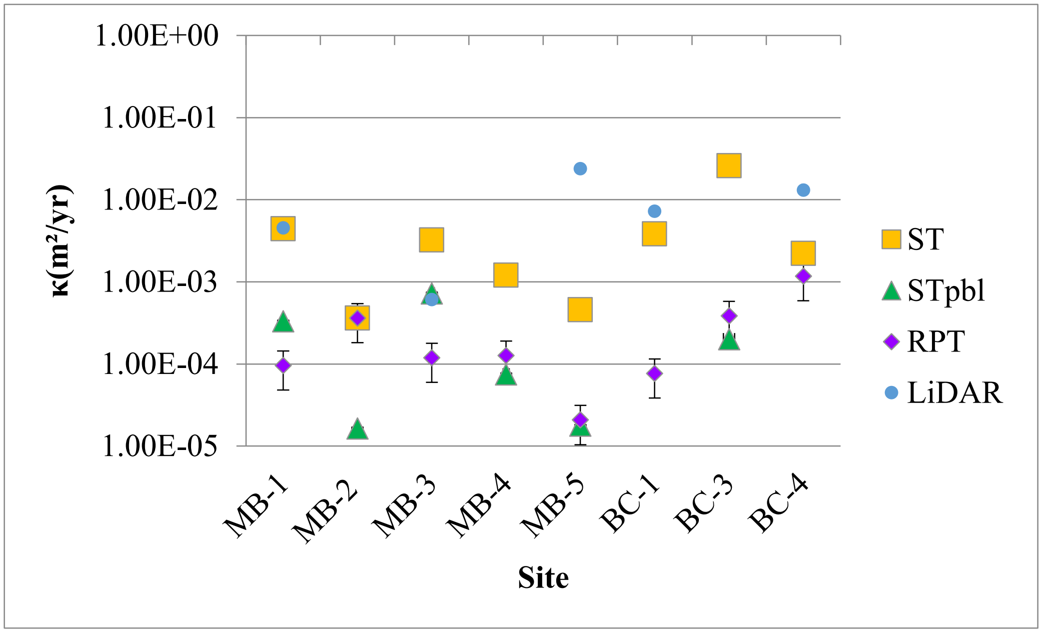

Figure 4.1. Derived kappa values from all sites for all methods shown by legend markers and applied % uncertainties from Mono Basin. Overall, relative comparison of values shows that grain size affects diffusivity. Sediment trap κ values represent best the range of diffusivities of the granular mixed regolith in annual transport, because sediment in flux most closely resembles the landform surface. Bounded uncertainty intervals representing percent uncertainty is the square of the sum of squares of the uncertainty for each method. Uncertainties were calculated for Mono Basin moraine and applied to all sites as they were within the bounds of the other sites and Mono Basin moraine was the one modeled. Relatively small uncertainties for the methods indicate that the measuring methods were not a large source for error.

The values from each method, although varying between sites, show some spatial trend in alignment. For example, the sediment trap, and the LiDAR values that employed the mass from the sediment traps, are mostly higher than the diffusivity derived from the pebbles transported into the trap and that calculated from the frequency analysis. So when direct comparison are made, the fines with a higher mobility rate are contributing to the mobility of the surface. While not surprising, the characterization provides insight with a quantitative basis into the transport of the mobile layer, showing that the fines have higher mobility, while the mobility of pebbles is 1-2 orders of magnitude less. This also indicates that the larger cobbles and boulders beneath the uppermost surface are being unearthed by the transport of fines and pebbles as they move over and around them. This observation, too, is not new and has been cited in (Hallet and Putkonen, 1994). However, the observed mobility and its measurements confirm that the methods used follow expected processes that have been documented in the professional literature.

By a broadly accepted definition discussed in earlier chapters, κ expresses the effect of climate interacting with a given substrate as independent of slope on the mobility of sediment, which results in degradation. In this study, the substrate is composed of a mixture of various grain sizes that were shown earlier to have different transport rates (Figure 3.5). So the transport rate measured from the sediment trap determines the flux and approximate travel distance for a given climate, whatever the combined effects of temperature and precipitation might have been to produce the transport results. Also, because large sizes will move slower than the fines, a certain percentage of larger pebbles and larger regolith will act as barriers behind which fines will be stored. In other words, given a diffusivity, a climate, and transport rates of grains in a regolith substrate, surface processes will result that coincide with corresponding erosion rates. However, an erosion rate, the rate at which a volume of sediment is removed from a point, is not the defining cause of sediment transport, it is a result of how the surface regolith is mobilized. Therefore, increases or decreases in erosion rates are not the telling factors for the effect of climate on landform degradation. The factors that inform about degradation are diffusivities of the substrate and surface processes that result and, because these do depend on climate, their quantified changes are what are used to correlate past climates with landform degradation rates.

Variable diffusivities of regolith combine during transport events, based on the above discussed evidence relating diffusivities to grain size, to generate topographic change. While the total effect of this change is crest lowering, the surface processes, which are the result of variable diffusivities, are storage and transport. The ratio between storage and transport is what ultimately determines the rate of degradation. Therefore, the combined effects of climate, which include both the mechanisms contributing to storage, such as vegetation species and density and surface stability, and also the forces driving transport, result in processes that cause rates of degradation.

The ratio of storage to transport in the current relatively warm dry time at the sites in the present study resulted in diffusivities lower than those found to occur in colder wetter climates. The latter exhibited broader ranges that contained higher diffusivities in the Oehm and Hallet (2005) compilation. The ratio of storage to transport was quantified in the present study and is illustrated in Figure 4.2. The figure is a map of the change in topographic highs of the second year with the respect to the first year. The change covers an approximate square meter located several meters downslope from the crest. The small topographic changes indicated in the figure quantitatively show that up to three-quarters of regolith transported by the end of the year was either re-deposited adjacent to or overlying the topography of the previous year. Hence this scan area may be characterized

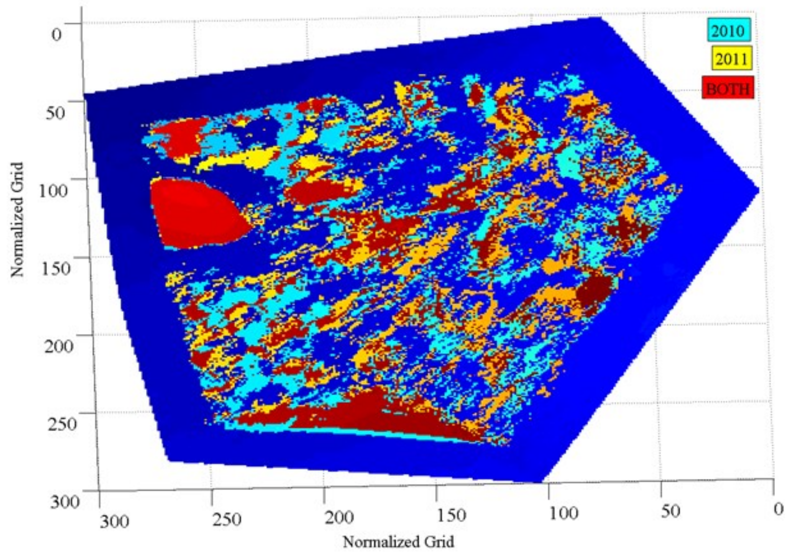

Figure 4.2. Relative spatial distribution of topographic highs (sediment accumulation) between second- and first- year. The first year (blue), second year (yellow/orange), and second year on top of first (red) shows how annual transport results in 74 % adjacency. This adjacency is interpreted as storage that is contributing to slower degradation.

by a diffusivity represented by the flux sampled in a nearby sediment trap, as well as by mobility of pebble sized grains given by κ values and transport rates, and by a degrading or mobile surface where up to three quarters of the regolith in a transport year is stored by the topography generated by the stationary or slower moving regolith of the previous year. Results of the characterization suggest a relatively stable surface that may be interpreted as resulting from a climate relatively drier and limited in the precipitation rate needed to move a higher percentage of the regolith that is winding up in storage. Certainly, a higher number of scan areas on the same moraine, on different locations, and over more years would lend more support for such an interpretation.

When compared with published diffusivities for landforms degrading by landslides, for example Martin (2000), the current surface characterized in Mono Basin shows relatively slow degradation with shallow topographic changes. The small isolated topographic changes at the sub-centimeter scale are both depositional and erosional and dot the surface. However, the average change for the measured surface is at the millimeter scale and is a net gain of 2.65 mm over the particular area shown in Figure 4.2. These results are consistent with findings that in arid climates it is the "upper soil zone" that drives downslope movement and which contrasts with soil transport in high latitudes and humid regions where soil creep plays a larger role (Schumm, 1964). This again suggests that degradation is not a measure of surface loss, or simply erosion, but the depth to which the cumulative effects of climate are interacting with the substrate to result in its mobility at and/or near the surface.

Soil creep, described as the progressive and intermittent downslope soil motion arising from the combined actions, of wind, rain splash, freeze thaw cycles, and biotic activity (Hallet and Putkonen, 1994), was measured globally in a study that found that higher latitudes exhibited a broader range of diffusivities (Oehm and Hallet, 2005). While that range may include the lowest diffusivities, as reported by others, e.g. Martin (2000), the implication interpreted here is that it is the depth to which climate *can* affect transport that dictates the effect of climate on degradation. In warm arid climates the depth is shallow, on the order of millimeters to centimeters. In cold wet climates, the depth has a broader range, on the order of centimeters to a meter, due to the variability of insolation over the year (Anderson and Anderson, 2010). This partly explains why higher latitudes exhibited a larger range of diffusivities in the Oehm and Hallet (2005) work. The results and implications lend support for the occurrence of variable diffusivities in the past, as a result of temperature fluctuations, i.e. that they reached higher values in colder and wetter climates related to the activity of past glaciations, and that an active layer or upper soil zone was deeper and exposed at a higher rate than during relatively warmer and drier or interglacial times.

4.3 Past Temperatures and Diffusivities

As noted in Chapter III, Methods, the compiled global topographic diffusivities in (Oehm and Hallet, 2005) were organized by latitude in order to relate a climatic region, such as tropical, polar, or temperate, to rates of soil creep. Because soil creep occurs in polar as well tropical latitudes, globally distributed records were used to serve the purpose of broadly comparing global diffusivities in terms of regional climate, but not to causally assign a latitude limit to a diffusivity. Using the substitution method, (described in Methods), current average air temperatures of April and May at globally distributed locations given by reports cited in Oehm and Hallet (2005) were used to generate a numerical relationship, or transfer function, between current climate, based on the air temperatures at those locations, and diffusivities measured at those locations (Figure 4.3). Included also as a point used to generate the function was the current relationship for Mono Basin moraine.

The functions then were used to calculate the diffusivities that correspond with the past climates, derived from applying the halite inclusion temperature proxy record, explained in section 2.7. The paleotemperatures for the region were only selected for the discrete times given in the published literature for which dated moraines provide evidence of significant and preserved glacial advances in the region, indicating times when climate conditions allowed for the formation and advance of glaciers. The temperatures are not assumed to reflect continuous conditions, but those diffusivities derived from them at those times selected were used to model degradation of the model profile between times of assigned temperatures.

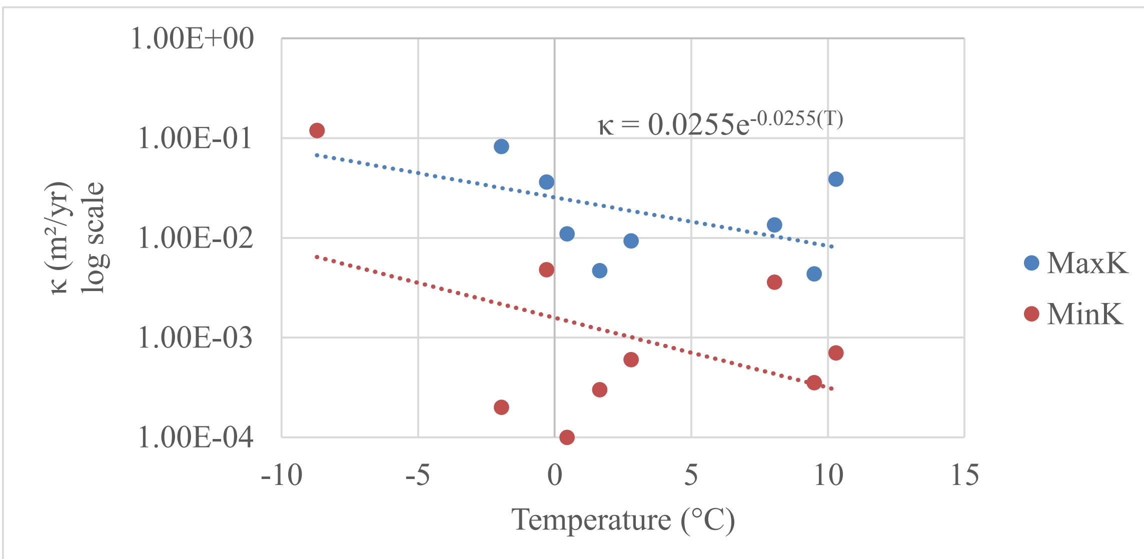

Figure 4.3. Transfer function based on reanalysis April/May average temperatures for current site locations where κ values were recorded (Oehm and Hallet, 2005). Points shown are the set selected to represent the range of paleo-temperatures and does not include the full global set. This transfer function produced the closest fitting cross-section profile to the current observed profile, with an underestimation of 0.9 m.

The results from applying the transfer function to the times of past temperatures is illustrated in Figure 4.4 which relates past temperatures with derived maximum κ values. The plot shows past variability in diffusivity, previously not shown with application of a constant optimized κ, and it shows the times when the temperature has produced a relatively large increase or decrease in κ, which is relevant for understanding the effects of past global climate change and glaciations on landform degradation.

A set of three transfer functions were assessed for performance in modeling the climate driven degradation through time: 1) The first one was based on every location cited in Oehm and Hallet (2005) (Global κ), 2) in the second function the selection is

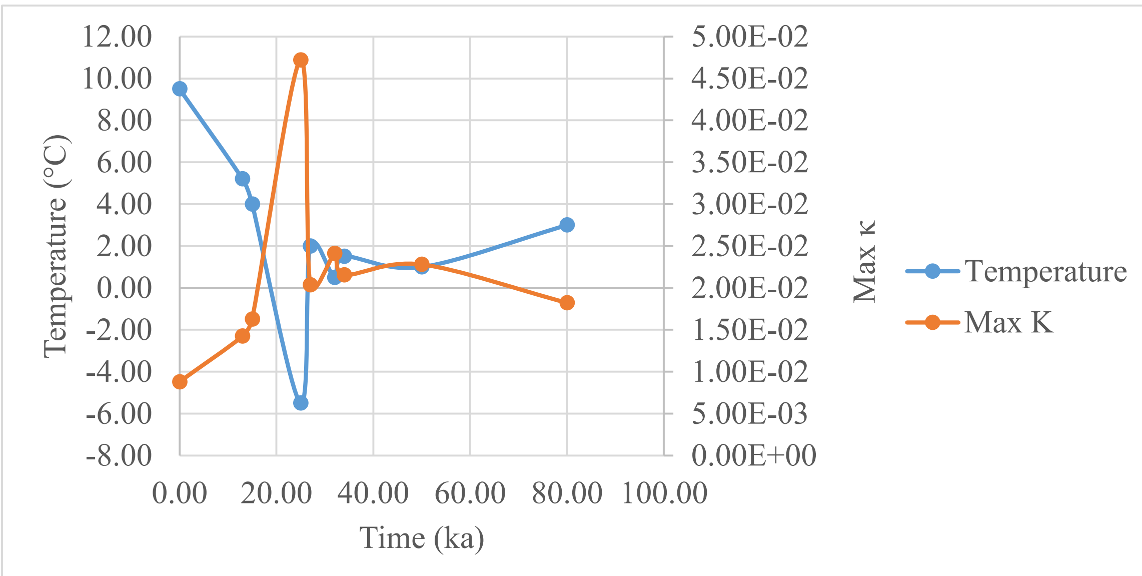

Figure 4.4. Maximum derived paleo-diffusivities (orange) and their associated average April/May temperatures from halite inclusion proxy record (blue) plotted against the times from the glacial chronology. If the transfer function reflects an accurate relationship between temperature and diffusivity and the chronology of past temperatures at Mono Basin is accurate then the relationships can be used to assess degradation rates in climates with related temperatures in the past and the present.

limited to sites that fall within the limits of the actual documented paleo-temperatures (Paleo-T-Range κ), and 3) the third function, is a compromise between the two previous versions (Partial-Global κ). The transfer function based on the locations with temperatures that fell within the range closest to the paleotemperatures generated a cross-section profile with the minimal least square difference. An additional reason for choosing this transfer function was that the other two were based on locations whose temperatures fell well outside the paleo-range, suggesting that the processes at those locations were not reflective of the processes occurring in the past. Table 4.3 lists the diffusivity results of applying the three different transfer functions. It also lists, separately, the set of chronologies based on calibration updates and considerations in selecting ages for the degradation model. Explanation was given as to how the selection decisions were made.

However, application of the substitution method in this study was not constrained by use of transfer functions or ages given with a least uncertainty or error. Other selections are possible. The amount of difference between the model profile and the observed profile, while shown as a difference in the application of parameters, may also be the result of missing chronologies, missing points and temperatures in the transfer function, and episodic events whose effect on degradation were not represented. The difference between, for example, the current measured diffusivity on Mono Basin moraine and the result of the current time diffusivity generated from the transfer function may result from any one or multiple issues – a common discrepancy between localized measurements and those generated from averaging between points being fit by a curve, points contributing different weights and generating a curve that does not equitably represent various points, gaps in representation between climate/diffusivity data points also causing a curve to misrepresent the relationship.

When the maximum Paleo-T transfer function was applied together with the selected ages, the cross-section profile with minimal least square difference was generated, underestimating the current profile by only 0.9 meters (discussed in the following section). The selections made are offered both as alternative sets of criteria to a constant optimized κ in the application of the degradation model and as a suggestion for how to integrate disparate data according to understandings of naturally occurring physical processes. The profiles were based on modeling, but the time-varying parameters used in modeling were based on physical measurements that were integrated to generate the physical process of degradation.

Based on the methods and evidence used, the purpose of the above selection was to have a basis for replicating whatever conditions might have prevailed in past climates that together would have generated the current observed profile. Achieving the objective also required applying shifts to climate conditions at times for which there was some physical evidence for doing so. Certainly other climate conditions might have prevailed that are not being considered which might have accelerated or decelerated the mobility of the surface at times not included. A different study could focus on considering the many modeling scenarios that employ different combinations of climatic indicators and how they could possibly affect erosion. However such a focus is outside the topic and scope of the present study.

Table 4.3. Three scenarios of ages and transfer function - derived paleo-κ values

Glacial Activity	Error	Transfer Function	Transfer Function
	Age	**Min K**	**Max K**
	0	Globak K	Globak K
Present	0	8.74E-04	1.11E-02
Recession	13	1.21E-03	1.57E-02
Transition	15	1.33E-03	1.73E-02
Tioga Start	25	2.73E-03	3.73E-02
ML LS 3	27	1.55E-03	2.03E-02
Tenaya	32	1.73E-03	2.30E-02
ML LS 4	34	1.61E-03	2.12E-02
Tahoe II	50	1.67E-03	2.20E-02
Mono Basin	80	1.43E-03	1.87E-02
	12 ka	Paleo-T-Range	Paleo-T-Range
Present	0	3.47E-04	8.80E-03
Recession	13	6.93E-04	1.42E-02
Transition	15	8.40E-04	1.63E-02
Tioga Start	25	3.88E-03	4.72E-02
ML LS 3	27	1.16E-03	2.04E-02
Tenaya	32	1.48E-03	2.41E-02
ML LS 4	34	1.26E-03	2.16E-02
Tahoe II	54	1.36E-03	2.28E-02
Mono Basin	92	9.87E-04	1.82E-02
	4 ka	Partial-Global	Partial-Global
Present	0	8.08E-04	1.02E-02
Recession	13	1.19E-03	1.47E-02
Transition	15	1.33E-03	1.63E-02
Tioga Start	25	3.12E-03	3.65E-02
ML LS 3	27	1.59E-03	1.93E-02
Tenaya	30.4	1.82E-03	2.19E-02
ML LS 4	34	1.66E-03	2.02E-02
Tahoe II	47.5	1.74E-03	2.10E-02
Mono Basin	76	1.45E-03	1.77E-02

4.4 Varying Diffusivities through Time

Also shown in Table 4.3 are the ages for the times in the varying κ degradation model. Several criteria were considered when modeling and selecting times to ensure accurate representation of the most updated records and to understand their effects on optimization of model results. Selection of times was based primarily on the latest published data for evidence of glaciations and glacial retreats in the region compiled in (Gillespie and Zehfuss, 2004) for glaciations and in Benson et al. (1998) for retreats identified by Mono Lake low stands. The oldest glaciations provided the oldest times and were considered significant contributions to long term degradation. The latest revised published age for Mono Basin moraine was given as a range 80-60 ka. Based on earlier published dates, the range implies an average of 70 ka with 10 ka margin of error. For Tahoe II, the age range given was 50-42 ka, which likewise implies a 4 ka year margin of error. However, the oldest in the ranges were selected for use in modeling, because reports have documented that degradation can make cosmogenic isotope dates appear to be younger than the true ages (Hallet and Putkonen, 1994; Putkonen and Swansen, 2003; Putkonen et al., 2008). This is why choosing the oldest possible age within a distribution of ages is a common practice and was followed in the published revised dates of Phillips et al. (1996).

However, in the selection process, unpublished ages falling within uncertainties cited by recalibration studies (Phillips et al., 2001) and the original reported geochemistry of the two oldest ages associated with Tahoe II and Mono Basin age moraines (Zreda et al., 1990; Phillips et al., 2001; Marrero et al., submitted 2014) were used by the

CRONUS calculator, introduced at the end of section 2.7. Uncertainty findings on recalibration studies reported in Phillips et al. (2001) were incorporated so that the maximum age used for modeling degradation was 85 ka. This age has not been published and the recalibration studies had not been applied to Mono Basin moraine in updated glacial chronologies in Phillips et al. (1996), so 85 ka remains speculative. However, because it was within the maximum uncertainty generated with the CRONUS calculator derived as the 92 ka age shown in Table 4.2, which considered the latest calibration studies (Marrero et al., submitted 2014) and boulder erosion (Phillips et al., 2009), 85 ka was used for modeling, because it improved the results by reducing the least square difference in profile elevation compared to the modeling results that had applied the published age of 80 ka, and because it reflects a relatively conservative estimate considering the updated parameterizations. Because age determination was not the focus in the present study, published and experimental results of recent sources (Phillips et al., 2001; Marrero et al., submitted 2014) were selected and applied for age parameters in order to test model scenarios. The focus was not on testing the degradation model with different ages falling within the margins of error. The objective in the selection of ages was to represent the documented age of the moraine within limits warranted by 1) latest published ages, which were based on ^{36}Cl concentrations in cosmogenic isotope dating of exposed boulder surfaces and 2) representation of possible boulder erosion included in the recalibrated ages, given in the latest documentation (Phillips et al., 2009).

The CRONUS-Earth calculator was used to determine oldest possible ages given by uncertainties, which increased with older ages. The oldest age with uncertainty of 12 ka on the 80 ka for the recalibrated age of Mono Basin moraine was 92 ka. When boulder erosion of 3.3 mm was incorporated, the exposure age decreased to 74 ka. So if erosion occurred then the exposure ages are younger than the actual age of the moraine. Therefore the age of 92 ka is a minimum, but it is uncertain how much so. A recalibration gave an absolute error of 5% for granodiorite in the region (Phillips et al., 2001). A 5% error on the 80 ka, gave a lower age of 76 ka. This age was used as the lower age limit, assuming no erosion, because it was within the negative uncertainty of the published age calculated by CRONUS.

The same approach was applied to the Tahoe II age moraine. However, as the moraine ages decreased, so did the uncertainty. Ages younger than Tahoe age moraine of 50-54 ka, gave uncertainties 2.8 ka or less. These low uncertainties were not applied because applying them pushed a documented glacial event into the previous or next interstadial, which were deemed important to include. Also, the adjusted ages with low uncertainties did not contribute significantly to changing degradation rates when modeled. The resulting three age representations shown in Table 4, include 1) the oldest revised ages published assuming no new error recently calculated by CRONUS and no erosion, 2) the oldest ages given the highest positive uncertainties calculated by CRONUS, and 3) lower ages given a low 5% error on the published dates of the high end range. The age extents were combined with the three sets of κ values generated by the three transfer function described above.

Results from degradation modeling and application of a least square difference between the modeled cross-section profile and the observed profile gave a 0.9 m underestimation of the crest elevation even with the optimal set of conditions (Figure 4.5). The figure shows profile results when the time varying κ value was applied in the diffusion equation for an optimal age of 85 ka. The set of time-varying κ values was based on selection of the transfer function restricted by paleo-temperature ranges, where the restriction did not exceed more than one temperature higher than the warmest (current temperature) or lower than the coldest paleotemperature. The age of 85 ka was used and justified by falling between the maximum published age with no recalibration error (80 ka) and the maximum published age with the maximum recalibration error (92 ka). Application of boulder weathering rate of 3.3 mm as a potential occurrence cited in Phillips et al. (2009) generated the final CRONUS calculator age of 85 ka. Therefore, 85 ka, which was the age that yield the lowest least square difference with optimized κ was the age employed for the age of the moraine and, therefore, the time in years used in profile modeling of the degradation of Mono Basin moraine.

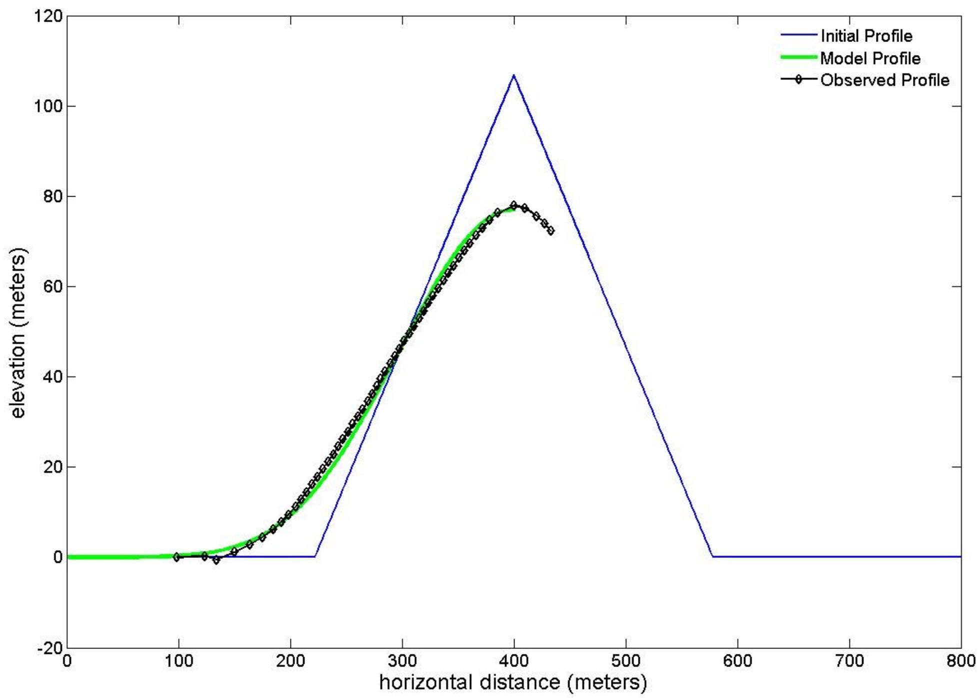

Figure 4.5. Degradation model with application of a time varying κ value. The profile in green differs in crest elevation from the observed profile by 0.9 m.

4.5 Diffusivities and Degradation Modeling

Three scenarios, each modeling degradation through the age of Mono Basin moraine, applied different κ values: 1) the first, a diffusivity based on sediment flux at the current time in the region, 2) the second, a value generated to optimally model the current elevation profile, and 3) the third, multiple κ values derived from the substitution method and transfer functions, as discussed earlier. The κ values resulting from application of the transfer function are shown in Figure 4.6 to illustrate their variability against time. Except for the current time and the last 10 ka, which exhibit the lowest diffusivities,

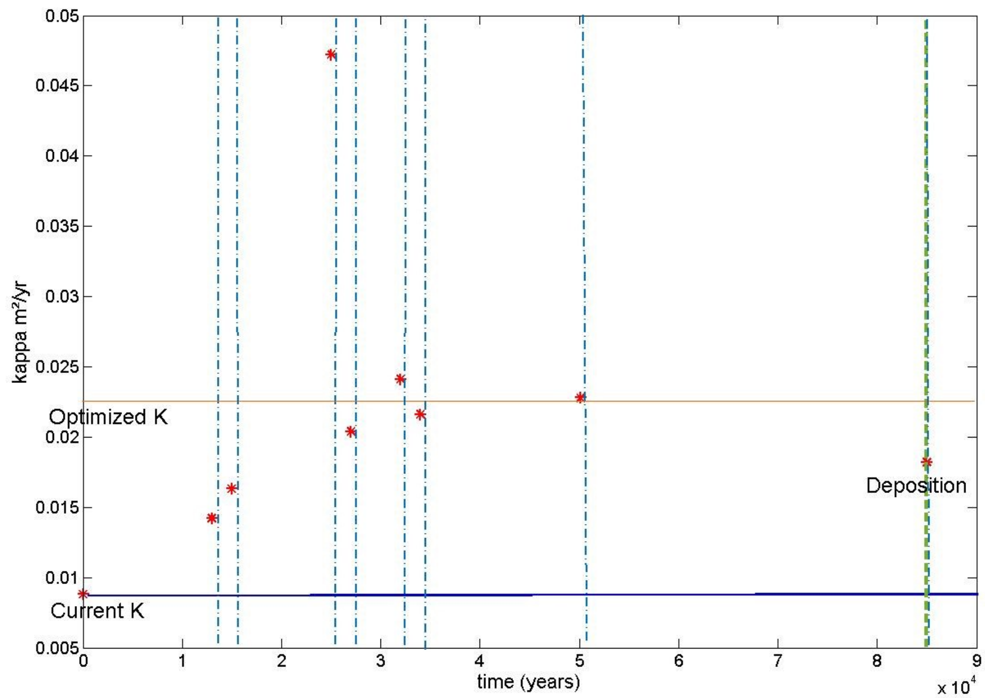

Figure 4.6. κ values varying through time and illustration of temperature based chronology bins. The current value is shown as the lowest overall and the last 13 ka also the lowest in comparison to the past. The highest value at ~25 ka corresponds to the LGM. Blue dotted lines divide the bins in which individual κ values were applied in the degradation model, starting with the earliest after deposition and changed to a temperature based diffusivity at the start of the subsequent time based on glacial chronology.

degradation is shown to have been higher during past times with the highest occurring approximately 25 ka during the Last Glacial Maximum, when the Laurentide ice sheet was at its furthest extent. Compared to the present, considered an interglacial time, previous glacial periods need to have been wetter and colder for the existence and advance of the glaciers that deposited the moraines that provided the dates for the glacial chronology and for which proxy climate records provide supporting evidence. Measured global diffusivities showed that higher latitudes, which generally support climatic conditions that produce glaciers or periglacial regions, those areas of intense frost action and a ground surface free of snow cover for part of the year (Ritter et al., 2011), exhibited relatively higher maximum diffusivities. Therefore, the results of the diffusivities through time follow a pattern for which there is evidence, both in the past and the present. The significant point is not *when* precisely certain degradation rates occurred, but rather 1) that there is a strong basis that they did vary and 2) that their variability was driven by changes occurring globally as a result of glacial activity.

When the varying diffusivities are used to track crest lowering or degradation through time, comparisons can be made showing the consequences from modeling with the different κ values (Figure 4.7). While the occurrence of variability in the values of the diffusivities through time may not be surprising, what is revealing is both the ability of the model to reveal any noticeable elevation changes resulting from varying the parameterization of κ and the order of magnitude of its variability at corresponding times. While κ was defined from the beginning as reflecting climate, the quantified effects of changing climate, with respect to temperature, on topographic diffusivity had not been apparent, and therefore the effects of past climates on landform degradation had not been quantified.

Transfer function derived diffusivities for the current time using the paleo-restricted temperature set and reflecting the lowest throughout the age of the moraine, generated a profile that underestimated the current moraine profile by up to 32%. When compared with degradation modeling that used an optimized value (constant κ), which generated a close approximation to the current elevation profile, using the constant value

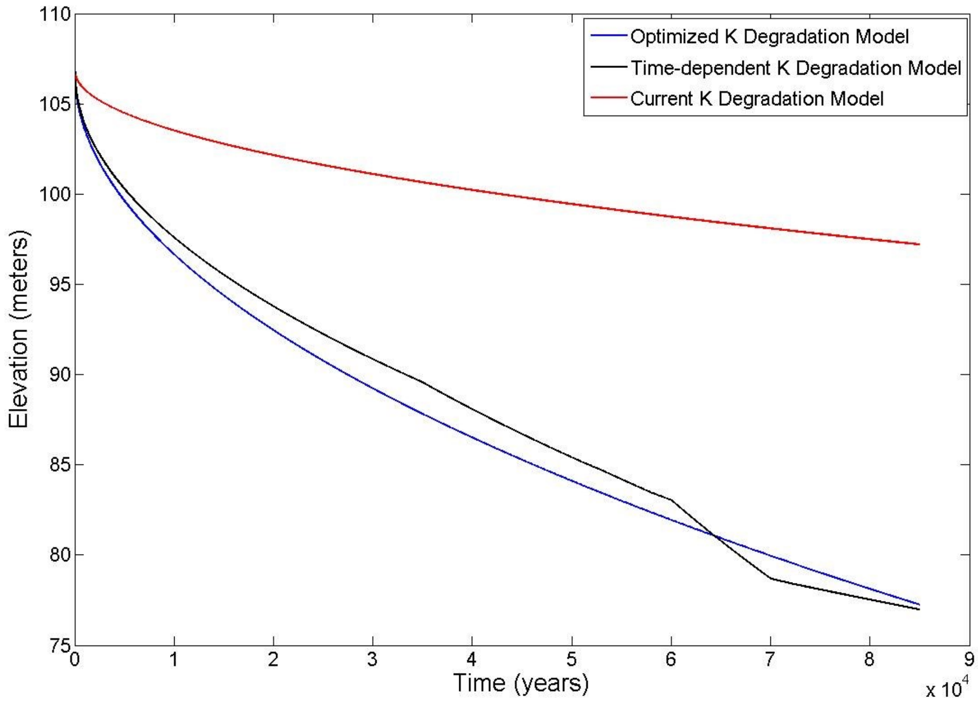

Figure 4.7. Degradation through time of three cases, where each uses a different value for topographic diffusivity. The current value, $\kappa=8.8 \times 10^{-3}$, generates a model that underestimates degradation by up to 32% of the current moraine profile. Use of a constant optimized $\kappa=2.2 \times 10^{-2}$ generates a model that overestimates degradation by up to 10 % during the first 60 kyrs and during a 5 thousand year time span 20 to 15 kyrs ago.

generated a profile that overestimated degradation by up to 10% during the first 60 thousand years and underestimated it the same amount during a 5 thousand year time span 15 to 20 thousand years ago. When viewed on a long time scale, the differences may not seem significant enough to warrant using varying κ values. However, the quantified differences support 1) a physical basis for diffusivity variability through time on a scale of thousands to tens of thousands of years, 2) quantified rate differences over time and 3) a link of the rate differences to past climates, whose mechanisms and causes can be assessed by climate records or climate modeling. Also, the differences can be significant with respect to the exposure of the upper-most millimeters to centimeters for drier climates and for the uppermost 50 cm in periglacial environments. Variability of the rates at which these depths are exposed, which depends on κ values varying through time, is critical for extrapolating cosmogenic isotope exposure ages, the dating of moraines and, hence, for determining the timing of past climate fluctuations.

Because the error between the optimized degradation model and the degradation model applying varying diffusivities is determined by a least square difference with the observed moraine profile, the overestimation and underestimation includes the cumulative error along the entire length of the slope, not merely the crest. The three different scenarios employ κ values throughout the degradation of the landform profile during modeling. Given that the present landform, like other landform surfaces in the region, appears unchanged for at least 80 years when compared with historical photos, no other surface processes, such as debris flows and landslides, were considered to have occurred during the last 10 thousand years. The occurrence of such events prior to that could not be assessed.

Further illustrating the relative elevation differences in moraine profiles produced from employing the optimized κ value and the time varying κ values, Figure 4.8 plots the relative differences between the two curves and shows when those differences occurred. The first 35 thousand years reflects the time span when greatest difference between a κ that reflects a long term average and the κ reflecting the earliest degradation of the moraine. While both steeper slopes and the cumulative effects of a colder wetter climate than the both contributed to early degradation, the degradation model from time varying κ values still produce higher elevations (less degradation) than the degradation model from the time averaged κ. Also, for the past 15 thousand years, the difference has been decreasing, and so it is a time range when application of an optimal constant κ would most closely reflect the conditions associated with a degrading the hillslope.

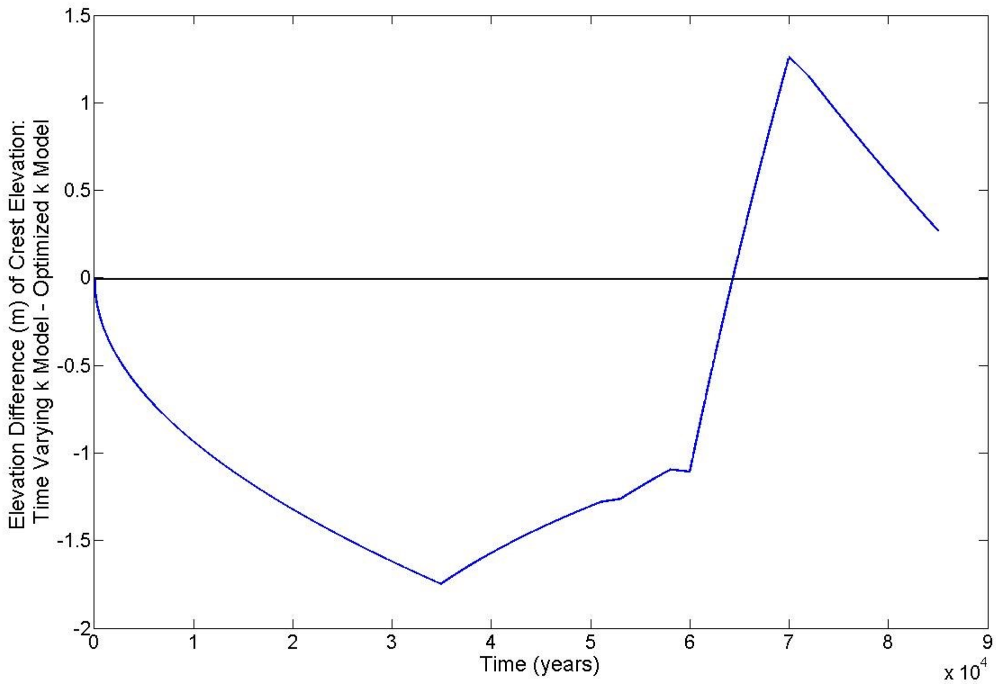

Figure 4.8. Difference between moraine crest elevation profiles generated with time varying κ values and with a constant optimized κ through age of the moraine. Assuming the same initial elevations, differences express how the different applications of diffusivity affect degradation modeling of the current profile through time in units of meters.

CHAPTER V

DISCUSSION

5.1 Overview

Results from degradation modeling quantified the effects of applying a time varying diffusivity parameter in the hillslope degradation model. The results of applying an optimized constant and a present day constant were quantitatively compared. As sediment transport rates were quantified according to grain size and the diffusivities of respective sizes were found to vary accordingly, the resultant effect on topographic change was mapped. The results, based on current field data, demonstrated the relative cumulative effects of the present climate on sediment transport and, hence, on the degradation rate of Mono Basin moraine. When compared with results based on proxy records of past climates, the variability of degradation rates over time was revealed and contrasted with the present rate and with the rate given by an optimized constant. The present degradation rate was based on diffusivity found to be an order of magnitude lower than climates occurring prior to recent geologic time of the Holocene. Also, the optimized constant diffusivity that produced a cross-section profile fitting the current moraine profile was found to only incidentally correlate with a time dependent diffusivity. Otherwise the generated profile using a constant optimized κ misrepresented degradation occurring during past climates.

5.2 The Effect of Climate on the Magnitude of Diffusivity

In conventional usage, the topographic diffusivity parameter is the free variable in the hillslope diffusion equation. As such, it is adjusted to produce the best fit model to the current hillslope profile. The aspect of climate that κ represents in such usage amounts to whatever the resulting optimal value happens to be. However, given that the climate dependent diffusivities were based on documented accounts of actual climatic conditions and numerical temperatures, not qualitative accounts and, further, that they produced a model profile that underestimated the current one by less than 2% shows that climate is a stronger force on erosion than is expressed in its typical application in the hillslope diffusion equation. The results suggest that climate fluctuations that have generated glacial and interglacial events in the past have affected erosion rates accordingly.

Through the modeling approach taken in the present study, where the variability of κ was related to relative changes in temperature that were assumed to follow past glacial advances and retreats, landform degradation rates were shown to vary in accord. With diffusivities derived from functions associating climates, defined in the present case by air temperatures at known locations, variations of degradation through time were tied to a physical basis that otherwise is unobservable. While the modeled profile employing time varying κ exhibited slightly more error than the optimized κ value, the varying κ is more reflective of conditions that occurred in the past that are not represented otherwise. This variability is not reflected or even accounted when an optimized, constant, value is applied.

The results are interpreted to indicate that slope is not the driving factor for degradation rates through time at all scales and in all cases, unless an average climate over thousands of years is approximately constant throughout that time. The temperature changes that result in climates that generate glacial advances or retreats affect the conditions controlling how sediment is transported and, therefore, the rates at which hillslopes degrade. Conditions referred to include the cumulative results of that would follow from temperature changes, such as precipitation, whether in terms of rain, snow melt, or thaw, as well as all the responses of the substrate and its ability to sustain biota in those conditions. While such conditions occur seasonally and annually, at the time scales employed in the present study, such conditions were considered as cumulative and compared relatively over thousands of years in terms of sediment transport. This was done through the use of the substitution method described in earlier sections.

The observation resulting from the application in the present study forces the reconsideration of 1) low degradation rates that may appear to result from age and lower slopes, may be the result of a climate 2) likewise, high degradation rates may not necessarily occur during the earliest times or even during brief episodic transport events, but rather result from global climate changes that are linked in complex ways to modifying the climate that effects rates of sediment transport. The point has been established in previous sections that the focus of this study was not to attempt to unravel those complex links. Rather, the focus was on establishing a physical basis for which evidence could be tied to show how diffusivity varied through thousands to tens of thousands of years when climate is known to have been modified by the climate forcing of ice sheet activity, for example.

The transfer function generated from a compilation from data collected in the Oehm and Hallet (2005) work indicated some trend relating temperatures at higher latitudes with higher diffusivities. Assuming the validity of the trend used and given the accompanying scatter likely resulting from the contribution of other local factors, such as elevation, varied substrates, varied landforms, varied precipitation, varied soil properties and vegetation, the small percentage of error between the model profile and the observed profile may be interpreted in two ways. One, the small error may be coincidental and the diffusivities used in the program do not actually reflect the relative changes in climate from one time to the next. In other words, the climate dependent κ values that were selected may be too scattered to have produced a reliable and relevant transfer function. Two, the physical evidence and its associated chronology *is* reflected in the relative sequence of time varying diffusivities. Certainly a function with less scatter would provide stronger support for a resulting profile with low error. Higher resolution could show more continuity between diffusivities, possibly revealing small degradation differences caused by the above factors contributing to the scatter in the transfer function.

Another limitation with the methods in the present study may lie with the chronological resolution. As indicated in Results section 4.3, the chronology used in the model employs discrete time periods, but the modeling requires that κ values be applied in the degradation model as constants until the following time when the value changes to reflect a change in climate evidenced by the halite homogenization temperatures from

DV93-1. The hillslope diffusion model is modeling in the same way as when an optimized constant κ was used. The only difference is that different κ value constants are used over different times to reflect corresponding changes in climate assumed to have occurred from glacial advances and retreats. However, chronological resolution is limited by the preservation of the glacial record. Because this study has focused on variability in degradation through time as resulting from past glacial activity, an indicator of global temperature changes, analyses of hillslope degradation of other moraines in this region as well as in comparison with other neighboring regions where timing of past glaciations was similar might lend further support to the methods employed in this study.

The current κ value is based on an interglacial climate that is warmer and drier than climates occurring during prior glacial times. When the current κ value is applied in the diffusion equation degradation rates underestimate degradation throughout the age of the landform. Evidence that the present landscape has changed little, as seen in 80 year old historical photos, lends further support to the present landscape reflecting relative stability associated with conditions of an interglacial. In other words, low diffusivities measured from the present landform are not simply reflective of the landscape today, and the results of recent effects of fire suppression for example, possibly allowing vegetation density to increase and decrease erosion. They are interpreted here as reflective of an interglacial time that can be shown to contrast with known past glacial times, in terms of the effects of diffusivity and therefore landform degradation.

The methods carried out in the study where sediment transport was measured over bare earth patches or pathways allowed measurement to reflect how sediment has been transported regardless of the vegetation. While vegetation density will affect overall degradation, the derived κ value from a volume sediment transported over bare earth will reflect a relative mobility that can be compared with other such rates in the past or in the present. As mentioned previously, the substitution method provided a physical basis to which chronologically-based evidence could be tied. So that even though precise diffusivities should not be assumed to correlate exactly with the time selected and used in the degradation model, the physical basis for their temporal variability provides a basis for when in the past degradation rates should be assessed against the optimized κ value or compared with current κ values. Even with the given limitations in the paleoclimate data and the scatter from a relatively low distribution of global diffusivities, the substitution method generated a degradation model that closely approximated the present landform when κ values based on actual climate conditions were used.

5.3 Correlation with Past Times

Modeling results from the application of hillslope diffusion showed that the selected time periods, together with the selected κ values applied to each time, produced a profile that underestimated the current one less than 2%. So, given the uncertainties calculated by CRONUS for ^{36}Cl cosmogenic exposure age dating and the error associated with the methods used for the revised ages, the degradation model based on time varying κ value produced a profile that approximated the current while reflecting past climate variability in doing so. The evidence, therefore, strongly indicates that climate variability through the time scales defined by the chronology has been at least a significant, if not driving force, at some times in the past, controlling variable erosion rates in this region.

While other regions may have additional forces affecting erosion rates, such as earthquakes, mass movements, and anthropogenic activity, the effect of climate is ongoing everywhere, even though regionally responses differ. Because the variability accompanying climate during glacial and interglacial periods was shown in this study to contribute to degradation, whether it was by accelerating, decelerating, or maintaining it through time, the basic role is assumed to apply to all regions, although in various interactions with other forces relevant for a particular region.

As indicated in earlier sections 2.7 and 4.3 this study, while the attempt was made to determine times of the climate variability that occurred over the life span of the landform, each κ value was not assumed to correspond continuously between times, except insofar as needed to be able to model the degradation that generated a model of the profile. During the intervals of selected times climate very likely varied on smaller time scales, from seasons to years. Precipitation likely varied, just as it varies in the current time. This study did not focus on variability at that scale, for the main reason being that proxy records, particularly those that can provide numerical data, do not exist at the annual and seasonal scales. Proxy records that could provide definitive values for precipitation do not exist at all. However, the state of climate that produced the numerical temperatures for which proxy records did exist was assumed to have also generated all the climatic conditions that resulted in the diffusivities that were measured. Also assumed was that those conditions accompanying the temperatures in the current time, generating the measured diffusivities, also accompanied those temperatures that were applied to the past in the Mono Basin region.

5.4 Significance of the Results for Degradation Modeling

Varying topographic diffusivity through time and using time varying values showed variability in degradation rates that application of a constant κ did not show. Designating κ values to times associated with different temperatures, reflecting climates modified by glacial activity, provided a physically based scenario for time varying degradation. Because glacial advances require relatively colder temperatures and enough precipitation to accumulate ice and to push an alpine glacier down slope, the time associated with a moraine deposit is also associate with a glacial advance and the needed climatic conditions. For this reason, relative to the present, times in the past with higher diffusivities were associated with colder and wetter climates. However, within the duration of past glacial times, climates were wetter or drier, colder or warmer compared to each other. The halite fluid inclusions provided the only means for assessing the relative temperature differences in the past on any numerical scale. Together with the transfer function, relative differences in diffusivities were discerned.

The results show, for example, that the climate subsequent to the one that resulted in the glacier that deposited Mono Basin moraine, such as the one that resulted in the glacier that deposited the Tahoe moraine, kept κ values even higher than when Mono Basin moraine was deposited. Evidence for this is shown in Figure 4.5. If conditions had been warmer than during Mono Basin time, Tahoe moraine would not have been deposited further out ahead of Mono Basin moraine. The results also show significant increase in κ at the time associated with the Last Glacial Maximum where the evidence shows a significant decrease in temperature and, as discussed in earlier sections, a likelihood of increased precipitation in some regions. Again, the point here is not to explain causal connections, but to link the physically based evidence with a chronology and values, in this case of temperature, that can be assigned, in the least relatively, to times in the past, thereby providing grounds for temporally varying diffusivity and showing how degradation rates can vary through time.

Considering the two scenarios for κ, one where it is a constant and optimized to closely approximate the observed profile and the other, based on time-dependent climate records, the parameter may be viewed in two ways. Used as an optimized constant to model the current profile, it functions to express all factors in a generic way that are not related to slope, with climate being primary. So it is expressing the contribution to the overall degradation by climate in a general sense. Used to express diffusivity related to past climates, it functions both to produce a model profile approximating the current as well to quantify degradation rates through the age of the moraine. In the latter case, the parameter contributes to the transport and erosional processes and how their rates might have varied through time and contributed to the current elevations. For understanding the rates at which surfaces became exposed through time, when using cosmogenic isotopes for exposure age dating for example, such parameterization is more relevant than one given by a constant κ. In such cases, knowing that erosion rates might have been significantly different for a duration of time might be useful in calculations. For simply generating a diffusion equation that provides a curve that fits a current landform cross-section profile, use of an optimal κ value may be sufficient if, for example, one wanted to assign an approximate age to a landform or calculate an average long term erosion rate.

CHAPTER VI

CONCLUSIONS

As an exogenic force, climate acts on Earth's surface directly and continuously. The rate of regolith transport within the uppermost 30-50 cm of hillslope surfaces responds to climate. So as climate changes through time the regolith transport rates change accordingly. Therefore the rates at which underlying regolith is exposed and the rates at which uppermost regolith is delivered downslope and into streams and rivers depend on climate as well.

Regolith transport and hillslope degradation today and through the age of Mono Basin moraine (~80 kyrs) in the eastern Sierra Nevada were investigated for the purpose of understanding the effect of climate on landform degradation and erosion rates. Hillslope degradation was quantified with the sediment transport equation, $q=-\kappa(dz/dx)$, where (q), the volume of regolith per meter width of the slope that is transported, is a function of slope (dz/dx). Topographic diffusivity (κ) is a coefficient that expresses the effects other than slope on degradation. Besides slope, climate and substrate are typically considered the primary factors that determine the rate of sediment transport. Annual transport rates of glacial regolith, making up the substrate of Mono Basin moraine in the eastern Sierra Nevada, were measured in 2011. The data was used to determine current hillslope processes and to quantify current regolith erosion rates. The field measurements were correlated with the climate records that span the past 30 years.

The main objective of the research was to relate the variations in climate known to have occurred in the past to corresponding variations in degradation rates. This was accomplished both by comparing the present climate, which has been relatively stable since the end of the Last Glacial Maximum, with climatic conditions resulting from the cooling and warming related to past glaciations for 100 ka. Climate driven topographic diffusivity was calculated by making use of the published paleoclimatological data for the region and correlating it with current global topographic diffusivities. This climate driven and, therefore, time dependent topographic diffusivity was then used in a degradation model to resolve the past fluctuations in the hillslope degradation.

Typically, in degradation analyses that are based on regolith transport laws and expressions of conservation of mass the topographic diffusivity is the free variable. In other words it is determined by fitting the results of the sediment transport equation to a present landform cross-sectional profile. However, given that κ is assumed to express the effects of climate on erosion rates, the question arises of whether its value is expressing what is intended if it has been derived on assumptions or records other than climate, such as erosion, elevations, and slope. To test how well the parameter is actually performing the role that is intended in the hillslope diffusion analyses, three scenarios were used to model the cross-section profile of Mono Basin Moraine, and the results of degradation modeling were compared with the current observed profile.

The first was a κ value based on current sediment transport records and, hence, reflective of the current climate, which is the warmest and driest over the last 100 ka. The second κ was generated as an optimal value to produce a profile fitting the current one based on observed elevations. The third was selected through the space-for-time substitution method and is a time-dependent κ based on past climate changes in the region. While the second case above is based on a best fit with the current profile, it is not the diffusivity responsible for degrading the moraine to its current shape and elevation. It will be the values truly reflective of their respective climates that provide the truest final profile when the diffusion-based degradation model is run. A constant κ value can never truly model the degradation of a landform because on the scale of tens to hundreds of thousands of years, a constant climate has not persisted.

Results from modeling showed that the current diffusivity underestimated the degradation and resulted in a current profile that is taller than observed today by 32%. When considered together with current erosion rates of 2.65 mm/yr for Mono Basin and an average diffusivity for the region of 2.20 x $10^{-2}m^2/yr$, the results are consistent with a moderate regolith transport processes quantified in the study, although relatively slow erosion, and correlated with the current warm dry climate. These results suggest that transport is likely related to surface wash related to seasonal rain events so that sediment on the slopes is replaced by sediment traveling downslope. This produces a slow rate of cumulative erosion.

Modeling results based on diffusivities that applied varying diffusivities to past climates showed an underestimation (the modeled profile is taller than observed) of the current and final profile by less than 2% with the use of varying κ. Comparisons between the degradation rates generated from an optimized constant κ and from variable κ show that there is overestimation of the optimized model of up to 10% during the first approximately ¾ of landform age and underestimation of approximately the same amount, but for a brief time during approximately the last third of the landform age. While such differences are not presented as results with high certainty occurring at certain times, the significance is that a relatively small difference can amount to cumulative differences over thousands of years, which may be significant, even if some error pertains in the results. How well κ expresses the true value(s) that have led to the current profile depends on the frequency and magnitudes of changes in climate over the age of a landform. Given what is known from paleoclimate records and the correlation with current diffusivities, a time-varying κ best expresses the topographic diffusivity related to the erosional history of the landform.

The main finding in this study is: because topographic diffusivity is based on climate and climate is known to have fluctuated in the past on thousand, ten-thousand, and one-hundred-thousand year time scales, therefore also the topographic diffusivity varied with time in accord with the cumulative climate states. These variable climates impacted changes in interaction with landscape substrates and, hence, with the mobility of landform surfaces and, thereby, landform degradation rates. The climate conditions producing colder and wetter conditions that promoted glacier growth and advance are viewed akin to those conditions that produce similar temperatures in colder wetter climates at current times. The affinity of climatic conditions supports a transference of diffusivities to past sediment transport.

While the natural course of landform evolution therefore is variable degradation, assessments on the significance of the variability are not in agreement. Those who have been interested in a long term average of diffusivity have found that use of an optimized constant κ value sufficiently satisfies modeling results of the degradation profile. However physical processes occurring within the upper-most 1-1.5 meters of a landform surface that affect sediment transport within even a small percent of deviation from the optimized κ can affect regolith exposure time and depth. The findings in the present study identifies unaccounted variability resulting from application of the constant κ value. The finding is problematic for techniques that rely on surface exposure and surface stability for purposes of dating the landform or for determining the length of time the surface has been stable. Often, when a landform is assumed to have been stable for thousands to hundreds of thousands of years as a result of tectonic quiescence or an absence of catastrophic events its surface transport is also assumed to have been stable. However, as shown in this study, the rates of surface regolith transport can vary temporally in significant amounts on a time scale when global climate changes are known to occur.

While the results in this study show the variability of landform degradation as an effect of climate variations through time for a particular landform, they are relevant for the landscape scale. The longer the time scale and the larger the spatial scale the worse the problem becomes. The further back in time is the record of the landform, the weaker are the environmental proxies for indicating when changes to the surface occurred. The larger the spatial scale, such as kilometers for mountain ranges, the greater the difficulties in locating and quantifying variations in transport and storage. This problem makes environmental interpretations of the past difficult to make and to use as explanations for landscape evolution, even though factors in the environment, such as climate, are fundamental and continuous causes in the change.

The rate of degradation is well known to be related to the climate. As the climate is known to have varied in the past so must the rates of degradation have varied. Here it is shown that either assigning a constant rate of degradation based on modern rates or an average rate based on total lifetime degradation leads to erroneous estimates of past degradation. Moreover, those rates almost never coincide with actual rates of degradation, and do so occasionally only incidentally. Furthermore it is shown that in the eastern Sierra Nevada study area the difference between time varying degradation and degradation modeled with an optimized constant can be up to ~10%. Even though these findings force us to reconsider commonly made assumptions in exposure age dating, i.e. where the exposure of a chemical system that is part of a landform surface is used to date the landform, or the general stability of landform surfaces, they also warrant a means for using sedimentary records together with Quaternary dating methods to improve assessments of how landscapes have evolved over time in response to past climates.

APPENDIX

MatLab Code for Degradation Models and Observation Profile

```
clear all

%----------------------DATA FILES-----------------------------------------------
load pub_dates_3er.txt%text file of publication dates, times when k changes
load MB_profile.txt %Mono Basin moraine profile data
load maxK.txt% max k values from Oehm and Hallet (2005)
load maxKM.txt

%--------USER CHANGABLE PARAMETERS---------------------------------
 runs=1;% Number of runs
% slope_rise=slope angle expressed as this much rise over a 1 meter
% horizontal distance
   % slope_rise=0.6745;% tan 34 (optional)
   % slope_rise=0.532;% tan 28 (optional)
   slope_rise=0.60;% tan 31
% initial conditions of hillslope profile, start slope needs to be adjusted
% with angle of repose
start_slope=223;
mid_slope=400;% don't touch this
end_flank=800;% total width
end_slope=end_flank-start_slope;% don't touch this

dt=1; % timestep
k=2; % Change to 1(if modeling time varying k; paleo-restricted), to 2
(kappa_field),select constant or optimized selections dependent on angle of repose;
to 3 (if modeling time varying k; global data set)

   % kappa_field=2.36E-3; % Mono Basin moraine current degradation
   % kappa_field=2.6E-2;% k 34° (angle of repose)
   % kappa_field=1.65E-2;% k 28° (angle of repose)
   % kappa_field=2.10E-2;% k, 31° (angle of repose)
   kappa_field=2.2E-2;% k, 31, to start with vary-k

%----------------------------Model Parameters--------------------------------------

maxtime=pub_dates_3er(end,1)*1000; % the max time steps that the program runs
time1=maxtime;
time2=pub_dates_3er(end-1,1)*1000;
time3=pub_dates_3er(end-2,1)*1000;
time4=pub_dates_3er(end-3,1)*1000;
```

```
time5=pub_dates_3er(end-4,1)*1000;
time6=pub_dates_3er(end-5,1)*1000;
time7=pub_dates_3er(end-6,1)*1000;
time8=pub_dates_3er(end-7,1)*1000;
time9=pub_dates_3er(end-8,1)*1000;

time_file=[time9;time8;time7;time6;time5;time4;time3;time2;time1];

figure(1)
clf %clear current figure window
%
tic
for run_counter=1:runs;
elevations=zeros(1,end_flank);
elevationsr=zeros(1,end_flank);

for counter2=start_slope:mid_slope;
   elevations(counter2)=elevations(counter2-1)+slope_rise;
   elevationsr(counter2)=elevationsr(counter2-1)+slope_rise;

end
for counter2=mid_slope+1:end_slope
   elevations(counter2)=elevations(counter2-1)-slope_rise;
   elevationsr(counter2)=elevationsr(counter2-1)-slope_rise;

end
figure(1)
   plot(elevations)
   hold on
kappa_file(:,run_counter)=elevationsr(:); %collects final elevations in a file

if k==1;%time varying k (paleo-restricted)
ranu1=maxK(9,1);
ranu2=maxK(8,1);
ranu3=maxK(7,1);
ranu4=maxK(6,1);
ranu5=maxK(5,1);
ranu6=maxK(4,1);
ranu7=maxK(3,1);
ranu8=maxK(2,1);
ranu9=maxK(1,1);
else k==2;% constant k
ranu1=kappa_field;
ranu2=kappa_field;
```

```
ranu3=kappa_field;
ranu4=kappa_field;
ranu5=kappa_field;
ranu6=kappa_field;
ranu7=kappa_field;
ranu8=kappa_field;
ranu9=kappa_field;

else k=3;% time-varying k, global
ranu1=maxKM(9,1);
ranu2=maxKM(8,1);
ranu3=maxKM(7,1);
ranu4=maxKM(6,1);
ranu5=maxKM(5,1);
ranu6=maxKM(4,1);
ranu7=maxKM(3,1);
ranu8=maxKM(2,1);
ranu9=maxKM(1,1);

end

ran_k(:,run_counter)=[ranu9;ranu8;ranu7;ranu6;ranu5;ranu4;ranu3;ranu2;ranu1]';%k list
starts with youngest

data_lengthr=length (elevationsr);

%start plotting the figure with initial profile
time_counter=maxtime;
crest_file_counter=1;

while time_counter>0 %loop through the time steps

   if and(time_counter<time1+1,time_counter>time2);
      ran_inpt_kappa1=ranu1;

   elseif and(time_counter<time2,time_counter>time3);
      ran_inpt_kappa1=ranu2;

   elseif and(time_counter<time3,time_counter>time4);
      ran_inpt_kappa1=ranu3;

   elseif and(time_counter<time4,time_counter>time5);
      ran_inpt_kappa1=ranu4;
```

```
    elseif and(time_counter<time5,time_counter>time6);
       ran_inpt_kappa1=ranu5;
    elseif and(time_counter<time6,time_counter>time7);
       ran_inpt_kappa1=ranu6;

    elseif and(time_counter<time7,time_counter>time8);
       ran_inpt_kappa1=ranu7;

    elseif and(time_counter<time8,time_counter>time9);
       ran_inpt_kappa1=ranu8;

    elseif (time_counter<time9);
       ran_inpt_kappa1=ranu9;

    end %end of elseif statements

        step_counter=2;

while step_counter<mid_slope+1; %loop through the elevation data array

elevationsr(step_counter)=elevationsr(step_counter)+(((elevationsr(step_counter+1)-...
         elevationsr(step_counter))-(elevationsr(step_counter)-elevationsr(step_counter-
         1)))*ran_inpt_kappa1)*dt;

       step_counter=step_counter+1;

    end %end of elevation array loop

    elevationsr(1)=elevationsr(2);

    elevationsr(mid_slope+1)=elevationsr(mid_slope-1);

    crest_file(crest_file_counter)=elevationsr(mid_slope);

    time_counter=time_counter-dt;
    crest_file_counter=crest_file_counter+1;

lowering=crest_file(:,1:end)';

end %end of time loop

kappa_file(1:end,run_counter)=elevationsr(:,:);%File collects elevations of kappa inputs
from each run
run_counter=run_counter+1;
```

```
end
%---------------------------------------Degradation Profiles--------------------------------------
 figure(1)

   axes('Fontsize',18,'FontName','Arial','XTickLabel',[0,200,800])
   xlim([0 800])
   ylim([0 120])

   plot(elevations,'-k')
   hold on

   plot(elevationsr,'-ok','MarkerSize',7);
   plot(MB_profile(:,1)+99,MB_profile(:,2),'dk');

   xlabel('horizontal distance (meters)','FontName','Arial','Fontsize',18);
   ylabel('elevation (meters)','FontName','Ariel','Fontsize',18)
   legend('Initial Profile','Model Profile','Observed Profile')
   legend('Boxoff')

DIF=MB(1:1:mid_slope-99,1:end)-kappa_file(100:1:mid_slope,1:end);
LSD=sqrt(DIF.^2);
LSDM=mean(LSD(1:end,:))';

%-------------------------------------------Observed Profile-----------------------------------
x=MB_profile(1:end,1);

Y=MB_profile(1:end,2);

xi=1:1:mid_slope;

yi=interp1(x,Y,xi)';

i=find(isnan(yi));
yi(i)=zeros(size(i));
[m,n]=size(kappa_file);
MB=repmat(yi,1,n);
MB=repmat(yi,[m,n]);
%--------------------------------------------------------------------------------------------------
elapsed_time_in_minutes=toc/60;
```

References

Abrahams, A.D., Parsons, A.J., Cooke, R.U., and Reeves, R.W., 1984, Stone movement on hillslopes in the Mojave Desert, California: a 16-year record: Earth Surface Process and Landforms, v. 9, no. 4, p. 365-370.

Adam, D.P., Sims, J.D., and Throkmorton, C.K., 1981, 130,000-yr continuous pollen record from Clear Lake County, California: Geology, v. 9, no. 8, p. 373-377.

Anderson, R.S., and Anderson, S., 2010, Periglacial processes and forms. *in* Geomorphology: The Mechanics and Chemistry of Landscapes: Cambridge, UK, Cambridge University Press, p.270-303.

Anklin, M., Barnola, J.M., Beer, J., and Blunier, T., 1993, Climate instability during the last interglacial period recorded in the GRIP ice core: Nature, v. 364, p. 203-207.

Barbour, M.G., and Major, J., 1977, Terrestrial Vegetation of California: New York, Wiley, 1002 p.

Benson, L.V., Burdet, J.W., Kashgarien, M., Lund, S.P., Phillips, F.M., and Rye, R.O., 1996, Climatic and hydrologic oscillations in the Owens Lake Basin and adjacent Sierra Nevada, California: Science, v. 274, no. 5288, p. 746-749.

Benson, L.V., Burdet, J.W., Lund, S.P., Kashgarian, M., and Mensing, S.A., 1997, Nearly synchronous climate change in the Northern Hemisphere during the last glacial termination: Nature, v. 388, no. 6639, p. 263-265.

Benson, L.V., Lund, S., Negrini, R., Linsley, B., and Mladen, Z., 2003, Response of North American Great Basin Lakes to Dansgaard-Oescher oscillations: Quaternary Science Reviews, v. 22, no. 21, p. 2239-2251.

Benson, L.V., Lund, S.P., Burdett, J.W., Kashgarian, M., Rose, T.P., Smoot, J.P., and Schwarz, M., 1998, Correlation of Late-Pleistocene lake-level oscillations in Mono Lake California, with North Atlantic climate events: Quaternary Research, v. 49, no. 1, p. 1-10.

Bischoff, J.L., and Cummins, K., 2001, Wisconsin glaciations of the Sierra Nevada (79,000-15000 yr B.P.) as recorded by rock flour in sediments of Owens Lake, California: Quaternary Research, v. 55, no. 1, p. 14-24.

Blackwelder, E., 1931, Pleistocene glaciation in the Sierra Nevada and Basin and Ranges: Bulletin of the Geological Society of America, v. 42, no. 4, p. 865-922.

Blois, J.L., Williams, J.W., Fitzpatrick, M.C., and Jackson, S.T., 2013, Space can substitute for time in predicting climate-change effects on biodiversity: Proceedings of the National Academy of Sciences, v. 110, no. 23, p. 9374-9379.

Boggs, S., 1995, Grain Size. *in* Principles of Sedimentology and Stratigraphy: New Jersey, Prentice Hall, p.79-93.

Brault, M.-., Mysak, L.A., Matthews, H.D., and Simmons, C.T., 2013, Assessing the impact of late Pleistocene megafaunal extinctions on global vegetation and climate: Climate of the past, v. 9, p. 1761-1771.

Burke, R.M., and Birkland, P., 1979, Reevaluation of multiparameter relative dating techniques and their application to the glacial sequence along the eastern escarpment of the Sierra Nevada, California: Quaternary Research, v. 11, no. 1, p. 21-51.

Bursik, M., 1991, Relative dating of moraines based on landform degradation, Lee Vining Canyon, California: Quaternary Research, v. 35, no. 3, p. 451-455.

Bursik, M., and Gillespie, A.R., 1993, Late Pleistocene glaciation of Mono Basin, California: Quaternary Research, v. 39, no. 1, p. 24-35.

Cannone, N., Diolaiuti, G., Gugliemin, M., and Smiraglia, C., 2008, Accelerating climate change impacts alpine glacier forefield ecosystms in the European Alps: Ecological Applications, v. 18, no. 3, p. 637-648.

Carson, M.A., and Kirkby, M.J., 1972, Hillslope Form and Process: Cambridge, England, Cambridge University Press 3, 475 p.

Clark, P.U., and Bartlein, P.J., 1995, Correlation of late Pleistocene glaciation in the western United States with North Atlantic Heinrich events: Geology, v. 23, no. 6, p. 483-486.

Clark, P.U., Dyke, A.S., Shakun, J.D., et al., 2009, The Last Glacial Maximum: Science, v. 325, no. 5941, p. 710-714.

Culling, W.E.H., 1965, Theory of erosion on soil-covered slopes: The Journal of Geology, v. 73, no. 2, p. 230-254.

Culling, W.E.H., 1960, Analytical theory of erosion: The Journal of Geology, v. 68, no. 3, p. 336-344.

Dansgaard, W., Johnsen, S.J., Clausen, H.B., et al., 1993, Evidence for general instability of past climate from 250-kyr ice-core record: Nature, v. 364, p. 218-220.

Davis, W.M., 1902, Base level, grade, peneplaine: Journal of Geology, v. 10, no. 1, p. 77-111.

Deardorff, D., 2000, Introduction to measurements and error analysis: Chapel Hill, NC, University of North Carolina, Chapel Hill, Department of Physics and Astronomy, 1 p.

Dee, D., and Fasullo, J., Climate Data Guide, 2014, Atmospheric reanalyis data: overview and comparison tables: https://climatedataguide.ucar.edu/climate-data/atmospheric-reanalysis-overview-comparison-tables (10/23/2014).

Deganutti, A., Tecca, P.R., and Genevois, R., 2011, Characterization of friction angles for stability and deposition of granular material: Italian Journal of Engineering Geology and Environment, v. 3, no. B-036, p. 313-318.

ESRI, ESRI Maps and Map Layers, 2014, World Topo Map: http://services.arcgisonline.com/ArcGIS/rest/services/World_Topo_Map/MapServer (November/01/2014).

Field, J.P., Breshears, D.D., Whicker, J.J., and Zou, C.B., 2011, On the ratio of wind- to water-driven sediment transport: conserving soil under global-change-type extreme events: Journal of Soil and Water Conservation, v. 66, no. 2, p. 51-56.

Finlayson, B., 1981, Field measurements of soil creep: Earth Surface Process and Landforms, v. 6, p. 35-48.

Gabet, E.J., Reichman, O.J., and Seabloom, E.W., 2003, The effect of bioturbation on soil processes and sediment transport: Annual Review of Earth and Planetary Science, v. 31, p. 249-273.

Galaasen, E.V., Ninnemann, U.S., Irvali, N., Kleiven, H.F., Rosenthal, Y., Kissel, C., and Hodell, D., 2014, Rapid reductions in North Atlantic deep water during the peak of the last interglacial period: Science, v. 343, no. 6175, p. 1129-1132.

Gamper, M.W., 1983, Controls and rates of movement of solifluction lobes in the eastern Swiss Alps, *in* Proceedings of the Fourth International Conference on Permafrost: Fairbanks, Alaska, Nationa Academy Press, p. 328-333.

Gilbert, G.K., 1909, The convexity of hilltops: The Journal of Geology, v. 17, no. 4, p. 344-350.

Gillespie, A.R., Clark, M.M., and Burk, R.M., 1999, Mountains shaped by ice: Eliot Blackwelder and the alpine glaciations of the Sierra Nevada. *in* Moores, E.M., Sloan, D. and Stout, D.L., eds., Classic Cordilleran Concepts: A View from California, Geological Society of America 338, p.440-452.

Gillespie, A.R., and Zehfuss, P.H., 2004, Glaciations of the Sierra Nevada, California, USA. *in* Ehlers, J. and Gibbard, P.L., eds., Quaternary Glaciations - Extent and Chronology: Amsterdam, Netherlands, Elsevier 2, p.51-62.

Goldner, A., Huber, M., Diffenbaugh, N., and Caballero, R., 2011, Implications of the permanent El Nino teleconnection "blueprint" for past global and North American hydroclimatology: Climate of the past, v. 7, p. 723-743.

Hallet, B., and Putkonen, J., 1994, Surface dating of dynamic landforms: young boulders on aging moraines: Science, v. 265, no. 5174, p. 937-940.

Hanks, T.C., Bucknam, R.C., Lajoie, K.R., and Wallace, R.E., 1984, Modification of wave-cut and faulting-controlled landforms: Journal of Geophysical Research, v. 89, no. B7, p. 5771-5790.

Heritage, G.L., and Large, A.R.G., 2009, Laser Scanning for the Environmental Sciences: UK, Wiley-Blackwell, 278 p.

Heusser, L., 1998, Direct correlation of millenial-scale changes in western North American vegetation and climate with changes in the California Current system over the past ~60 kyr: Paleoceanography, v. 13, no. 3, p. 252-262.

Heusser, L.E., 1995, Pollen stratigraphy and paleoecological interpretation of the 160-k.y. record from Santa Barbara Basin, Hole 893A: Proceedings of the Ocean Drilling Program Scientific Results, v. 146, p. 265-279.

Hill, M., 2006, Geology of the Sierra Nevada: Berkeley, California, University of California Press, 453 p.

Hilley, G.E., and Arrowsmith, J.R., 2008, Geomorphic response to uplift along the Dragon's Back pressure ridge: Geology, v. 36, no. 5, p. 367-370.

Hostetler, S.W., and Benson, L.V., 1990, Paleoclimate implication of the high stand of Lake Lohontan derived from models of evaporation and lake level: Climate Dynamics, v. 4, p. 207-217.

Hostetler, S.W., and Clark, P.U., 1997, Climatic controls of western U.S. glaciers at the last glacial maximum: Quaternary Science Reviews, v. 16, no. 6, p. 505-511.

Jaeger, H.M., and Nagel, S.R., 1992, Physics of the granular state: Science, v. 255, no. 5051, p. 1523-1531.

Jahn, A., 1991, Slow soil movement in Tarfala Valley, Kebnekaise Mountains, Swedish Lapland: Geografiska Annaler. Series A, Physical Geography, v. 73, no. 2, p. 93-107.

James, L.A., Harbor, J., Fabel, D., Dahms, D., and Elmore, D., 2002, Late Pleistocene glaciations in the northwestern Sierra Nevada, California: Quaternary Research, v. 57, no. 3, p. 409-419.

Jimenez-Moreno, G., Anderson, R.S., Despreat, S., et al., 2010, Millenial-scale variability during the last glacial in vegetation records from North America: Quaternary Science Reviews, v. 29, no. 21, p. 2865-2881.

Kirkby, A., and Kirkby, M.J., 1974, Surface wash at the semi-arid break in slope: Zeitschrift fur Geomorphologie N.F., v. 21, no. 2, p. 151-176.

Kirkby, M.J., 1995, A model for variations in gelifluction rates with temperature and topography: implications for global change: Geografiska Annaler. Series A, Physical Geography, v. 77, no. 4, p. 269-279.

Koehler, P.A., and Anderson, S.R., 1995, Thirty thousand years of vegetation changes in the Alabama Hills. Owens Valley, California: Quaternary Research, v. 43, no. 2, p. 238-248.

Leopold, L.B., Emmett, W.W., and Myrick, R.M., 1966, Channel and hillslope processes in a semiarid area New Mexico: erosion and sedimentation in a semiarid environment: 352-G, 193 p.

Li, J., Lowenstein, T.K., Brown, C., Ku, T., and Luo, S., 1996, A 100 ka record of water tables and paleoclimates from salt cores, Death Valley, California: Paleoceangraphy, Paleoclimatology, Paleoecology, v. 123, no. 2, p. 179-203.

Licciardi, J.M., Clark, P.U., Brook, E.J., Elmore, D., and Sharma, P., 2004, Variable responses of western U.S. glaciers during the last deglaciation: Geology, v. 32, no. 1, p. 81-84.

Litwin, R.J., Adam, D.P., Frederiksen, N.O., and Woolfenden, W.B., 1997, An 800,000-year pollen record from Owens Lake, California: Preliminary Analyses. *in* Smith, G.I. and Bischoff, J.L., eds., An 800,000-year Paleoclimate Record from Core OL-92, Owens Lake, Southeast California: Boulder, Colorado, Geological Society of America, p.127-141.

Litwin, R.J., Smoot, J.P., Durika, N.J., and Smith, G.I., 1999, Calibrating Late Quaternary terrestrial climate signals: radiometrically dated pollen evidence from the southern Sierra Nevada, USA: Quaternary Science Reviews, v. 18, no. 10, p. 1151-1171.

Lowenstein, T.K., Li, J., Brown, C., Roberts, S.M., Ku, T., Luo, S., and Yang, W., 1999, 200 k.y. paleoclimate record from Death Valley salt core: Geology, v. 27, no. 1, p. 3-6.

Lowenstein, T.K., Li, J., and Brown, C.B., 1998, Paleotemperatures from fluid inclusions in halite: method verification and 100,000 year paleotemperature record, Death Valley, CA: Chemical Geology, v. 150, no. 3, p. 223-245.

Mackay, J.R., 1981, Active layer slope movement in a continuous permafrost environment, Garry Island, Northwest Territories, Canada: Canadian Journal of Earth Science, v. 18, p. 1666-1680.

Marrero, S., Phillips, F.M., Borchers, B., Lifton, N., Aumer, R., and Balco, G., submitted 2014, Cosmogenic nuclide systematics and the CRONUScalc program.

Martin, Y., 2000, Modelling hillslope evolution: linear and nonlinear transport relations: Geomorphology, v. 34, no. 1, p. 1-21.

Martin, Y., and Church, M., 1997, Diffusion in landscape development models: on the nature of basic transport relations: Earth Surface Process and Landforms, v. 22, no. 3, p. 273-279.

Matsuoka, N., 2001, Solifluction rates, processes and landforms: a global review: Earth Science Reviews, v. 55, p. 107-134.

Matsuoka, N., 1998, Modeling frost creep rates in an alpine environment: Permafrost and Periglacial Processes, v. 9, p. 397-409.

Matsuoka, N., Hirakawa, K., Watanabe, T., and Moriwaki, K., 1997, Monitroring of periglacial slope proceses in the Swiss Alps: the first two years of frost shattering, heave, and creep: Permafrost and Periglacial Processes, v. 8, p. 155-177.

Matsuura, K., and Willmott, C.J., 2012, Terrestrial air temperature: 1900-2010 gridded monthly time series: Newark, DE, Department of Geography, University of Delaware, 1 p.

Matsuura, K., and Willmott, C.J., Earth System Research Laboratory: Physical Sciences Division, 2010, UDel_AirT_Precip data: •http://www.esrl.noaa.gov/psd/thredds/dodsC/Datasets/udel.airt.precip/var.time.stat.nc (5/5/2014).

Mensing, S.A., 2001, Late-Glacial and early Holocene vegetation and climate change near Owens Lake, eastern California: Quaternary Research, v. 55, no. 1, p. 57-65.

Minnich, R.A., 2007, Climate, paleoclimate, and paleovegetation. *in* Barbour, M.G., Keeler-Wolf, T. and Schoenherr, A.S., eds., Terrestrial Vegetation of California, 3rd. ed.: Berkeley, CA, University of California Press, p.43-70.

Molnar, P., 2009, The state of interactions among tectonics, erosion, and climate: a polemic: GSA Today, v. 19, no. 7, p. 44-45.

Molnar, P., and England, P., 1990, Late Cenozoic uplift of mountain ranges and global climate change: chicken or egg?: Nature, v. 346, no. 6279, p. 29-34.

Moores, E.M., Dilek, Y., and Wakabayashi, J., 1999, California terranes. *in* Moores, E.M., Sloan, D. and Stout, D.L., eds., Classic Cordilleran Concepts: Boulder, CO, The Geological Society of America 338, p.227-234.

Moores, E.M., Sloan, D., and Stout, D.L., editors, 1999, Classic Cordilleran Concepts: A View from California: Boulder, CO, The Geological Society of America, 338, 489 p.

Morgan, D., and Putkonen, J., 2012, Moraine degradation rates quantified with cosmogenic be-10 from soil profiles in Bloody Canyon, CA: Geological Society of America Abstracts with Programs, v. 44, no. 7, p. 461.

Nearing, M.A., Pruski, F.F., and O'Neal, M.R., 2004, Expected climate change impacts on soil erosion rates: a review: Journal of Soil and Water Conservation, v. 59, no. 1, p. 43-50.

NOAA, Mono Basin Clearinghouse: Building a Digital Library for Better Resource Management, 2014, NOAA Lee Vining Precipitation since 1989: rainfal xls: http://www.monobasinresearch.org/data/index.php (01/12/2014).

Oehm, B., and Hallet, B., 2005, Rates of soil creep, worldwide: weak climatic controls and potential feedback: Zeitschrift fur Geomorphologie N.F., v. 49, no. 3, p. 353-372.

Owen, L.A., Finkel, R.C., Minnich, R.A., and Perez, A.E., 2003, Extreme southwestern margin of late Quaternary glaciation in North America: timing and controls: Geology, v. 31, no. 8, p. 729-732.

Persico, L.P., Nichols, K.K., and Bierman, P.R., 2005, Tracking painted pebbles: short-term rates of sediment movement on four Mojave Desert piedmont surfaces: Water Resources Research, v. 41, no. W07004, p. 1-15.

Phillips, F.M., Stone, W.D., and Fabryka-Martin, J.T., 2001, An improved approach to calculating low-energy cosmic-ray neutron fluxes near the land/atmosphere interface: Chemical Geology, v. 175, no. 4, p. 689-701.

Phillips, F.M., Zreda, M., Plummer, M.A., Elmore, D., and Clark, D.H., 2009, Glacial geology and chronology of Bishop Creek and vicinity, eastern Sierra Nevada, CA: Geological Society of America Bulletin, v. 121, no. 7, p. 1013-1033.

Phillips, F.M., Zreda, M., Plummer, M.A., Elmore, D., and Clark, D.H., 2009, Glacial geology and chronology of Bishop Creek and vicinity, eastern Sierra Nevada, California: Geological Society of America Bulletin, v. 121, no. 7/8, p. 1013-1033.

Phillips, F.M., Zreda, M.G., Benson, L.V., Plummer, M.A., Elmore, D., and Sharma, P., 1996, Chronology for Fluctuations in Late Pleistocene Sierra Nevada Glaciers and Lakes: Science, v. 274, no. 5288, p. 749-751.

Phillips, F.M., Zreda, M.G., Smith, S.S., Elmore, D., and Kublik, P.W., 1990, Cosmogenic chlorine-36 chronology for glacial deposits at Bloody Canyon, eastern Sierra Nevada: Science, v. 248, no. 4962, p. 1529-1532.

Pickett, S., 1989, Space-for-time substitution as an alternative to long-term studies. *in* Likens, G.E., ed., Long-term studies in ecology, Springer-Verlag 16, p.110-135.

Pierce, K.L., and Colman, S.M., 1986, Effect of height and orientation (microclimate) on geomorphic degradation rates and processes, late-glacial terrace scarps in central Idaho: Geological Society of America Bulletin, v. 97, no. 7, p. 869-885.

Potito, A.P., Poinchu, D.F., MacDonald, G.M., and Moser, K.A., 2006, A late Quaternary chironomid-inferred temperature record from the Sierra Nevada, California, with connections to northeast Pacific sea surface temperatures: Quaternary Research, v. 66, no. 2, p. 356-363.

Price, L.W., 1991, Surface movement on solifluctioh lobes in the Ruby Range, Yukon Territory, Canada - a 20 year study: Arctic and Alpine Research, v. 23, p. 200-205.

Pruski, F.F., and Nearing, M.A., 2002, Climate-induced changes in erosion during the 21st century for eight U.S. locations: Water Resources Research, v. 38, no. 12, p. 1-11.

Putkonen, J., Connolly, J., and Orloff, T., 2008, Landscape evolution degrades the geologic signature of past glaciations: Geomorphology, v. 97, no. 2, p. 208-217.

Putkonen, J., and O'Neal, M., 2006, Degradation of unconsolidated Quaternary landforms in the western North America: Geomorphology, v. 75, no. 4, p. 408-419.

Putkonen, J., Rosales, M., Turpin, N., Morgan, D., Balco, G., and Donaldson, M., 2007, Regolith transport in the Dry Valleys of Antarctica: a keystone in a changing world: 2007-1047, 1 p.

Putkonen, J., and Swansen, T., 2003, Accuracy of cosmogenic ages for moraines: Quaternary Research, v. 59, no. 2, p. 255-261.

Rampino, M.R., Sanders, J.E., Newman, W.S., and Konigsson, L.K., 1987, Climate: History, Periodicity, and Predictability: New York, Van Nostrand Reinold, 588 p.

Reshetytuk, Y., 2009, Terrestrial Laser Scanning: Error Sources, Self-Calibration, and Direct Georeferencing: Saarbrucken, Germany, VDM Verlag, 161 p.

Ritter, D.F., Kochel, C.R., and Miller, J.R., 2011, Process Geomorphology, 5th ed.: Illinois, Waveland Press, 652 p.

Rood, D.H., Burbank, D.W., and Finkel, R.C., 2011, Chronology of glaciations in the Sierra Nevada, California, from 10Be surface exposure dating: Quaternary Science Reviews, v. 30, no. 6, p. 646-661.

Rudberg, s., 1964, Slow mass movement process and slope development in the Norra Storfjaell area, Swedish Lapland: Zeitschrift fur Geomorphologie N.F. Supplement, v. 5, p. 192-203.

Sampson, K.M., and Smith, L.C., 2006, Relative ages of Pleistocene moraines discerned from pebble counts: eastern Sierra Nevada, California: Physical Geography, v. 27, no. 3, p. 223-235.

Schrott, L., Otto J-C, J.G., and Geilhausen, M., 2013, Fundamental classic and modern field techniques in geomorphology: an overview. *in* Shroder, J., Switzer, A.D. and Kennedy, D.M., eds., Methods in Geomorphology: San Diego, CA, Academic Press 14, p.6-21.

Schumm, S.A., 1964, Seasonal variations of erosion rates and processes on hillslopes in western Colorado: Zeitschrift fur Geomorphologie N.F., v. 5, no. 8, p. 215-238.

Selby, M.J., 1993, Hillslope Materials and Processes: Oxford, Oxford University Press, 451 p.

Shackleton, N.J., 2000, Phase relationships between millenial scale events 64,000 to 24,000 years ago: Paleoceanography, v. 15, no. 6, p. 565-569.

Shackleton, N.J., Backman, J., Zimmerman, H., Kent, D.V., Hall, M.A., and Roberts, D.G., 1984, Oxygen isotope calibration of the onset of ice-rafting and history of glaciation in the North Atlantic region: Nature, v. 307, p. 620-623.

Shackleton, N.J., Sanchez-Goni, M.F., Pailler, D., and Lancelot, Y., 2003, Marine isotope substage 5e and the Eemian Interglacial: Global and Planetary Change, v. 36, no. 3, p. 151-155.

Skianis, G.A., Vaiopoulos, D., and Evelpidou, N., 2008, Solution of the linear diffusion equation for modelling erosion processes with a time varying diffusion coefficient: Earth Surface Process and Landforms, v. 33, no. 10, p. 1491-1501.

Smith, D.J., 1992, Long-term rates of contemporary solifluction in the Canadian Rocky Mountains, *in* Proceedings of the 22nd Annual Binghamton Symposium in Geomorphology: Binghamton, UK, Wiley, p. 203-221.

Smith, D.J., 1988, Rates and controls of soil movement on a solifluction slope in the Mount Rae area, Canadian Rocky Mountains: Zeitschrift fur Geomorphologie N.F. Supplement, v. 71, p. 25-44.

Smith, G.I., and Bischoff, J.L., editors, 1997, An 800,000-Year Paleoclimate Record from Core OL-92, Owens Lake, Southeast California: Boulder, Colorado, Geological Society of America, 317, 165 p.

Smith, G.I., and Bischoff, J.L., 1997, Core OL-92 from Owens Lake: project rationale, geologic setting, drilling procedures, and summar. *in* Smith, G.I. and Bischoff, J.L., eds., An 800,000-Year Paleoclimatic Record from Core OL-92: Boulder, CO, Geological Society of America 317, p.1-8.

Smith, G.I., and Bischoff, J.L., 1993, Core OL-92 from Owens Lake, southeast California: 93-683, 1 p.

Street, J.H., Anderson, R.S., and Paytan, A., 2012, An organic geochemical record of Sierra Nevada climate since the LGM from Swamp Lake, Yosemite: Quaternary Science Reviews, v. 40, p. 89-106.

Sundborg, A., 1957, The River Klaralven, a study of fluvial processes: Geografiska Annaler. Series A, Physical Geography, v. 38, p. 125-316.

Tausch, R.J., Wigand, P.E., and Burkhardt, W., 1993, Viewpoint: plant community thresholds, multiple steady states, and multiple successional pathways: legacy of the Quaternary?: Journal of Range Management, v. 46, no. 5, p. 439-447.

Taylor, K.C., Lamorey, G.W., Doyle, G.A., and Alley, R.B., 1993, The 'flickering switch' of late Pleistocene climate change: Nature, v. 361, p. 432-436.

Thackray, G.D., 2008, Varied climatic and topographic influences on late Pleistocene mountain glaciation in the western United States: Journal of Quaternary Science, v. 23, no. 6-7, p. 671-681.

Tricart, J., and Macar, P., 1967, Field methods for the study of slope and fluvial processes: a contribution to the International Hydrological decade: France, Jacque et Dentrond, Besancon, 44 p.

Tucker, G.E., and Hancock, G.R., 2010, Modeling landscape evolution: Earth Surface Process and Landforms, v. 35, no. 1, p. 28-50.

Wells, W.G., and Wohlgemuth, P.M., 1987, Sediment traps for measuring onslope surface sediment movement: PSW-393, 1 p.

Woolfenden, W.B., 2003, A 180,000-year pollen record from Owens Lake, CA: terrestrial vegetation change on orbital scales: Quaternary Research, v. 59, no. 3, p. 430-444.

Woolfenden, W.B., 1996, Sierra Nevada ecosystem project: Final report to Congress, vol. II, Assessments and scientific basis for management options - Quaternary vegetation history, 47 p.

WRCC, Western Regional Climate Center, 2010, Cooperative climatological data summaries: http://www.wrcc.dri.edu/climatedata/climsum/ (06/13/2014).

Zimmerman, S.H., Hemming, S.R., Kent, D.V., and Searle, S.Y., 2006, Revised chronology for late Pleistocene Mono Lake sediments based on paleointensity correlation to the global reference curve: Earth and Planetary Science Letters, v. 252, no. 1, p. 94-106.

Zreda, M.G., Phillips, F.M., and Smith, S.S., 1990, Cosmogenic ^{36}Cl dating of geomorphic surfaces: H90-1, 1 p.